红外光谱物理基础及应用

王楠林

中国科学院物理研究所
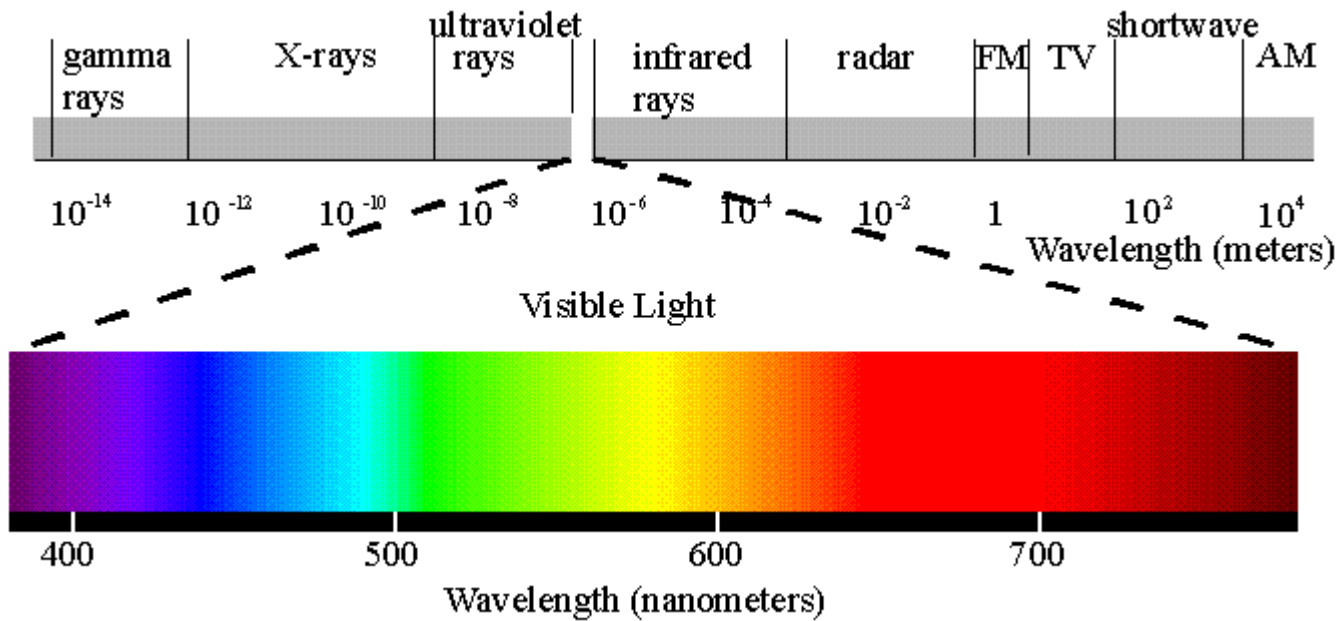
第一讲

- 光谱研究的早期历史

- 固体光学性质基础
  光学常数、Kramers-Kronig变换、带间跃迁、带内跃迁

- 举例（MgTi2O4、CuIr2S4轨道驱动的Peierls相变）
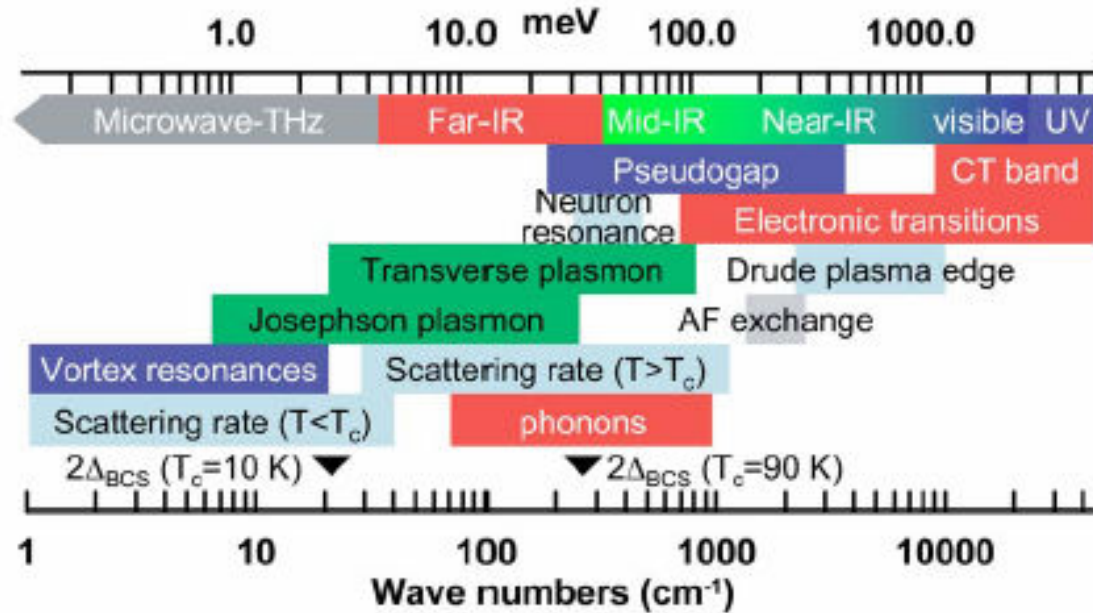
第二讲

- CuxTiSe2的电荷动力学

Light

D. N. Basov, T. Timusk, Rev Mod Phys 2005

能量单位：1 eV = 8065 cm-1 = 11400 K

1.24 eV=10000 cm-1

$\nu = 10000/\lambda$

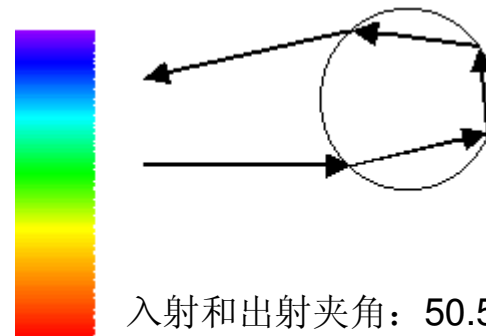(波数 ν: cm-1)　(波长 λ: μm)

Rainbow
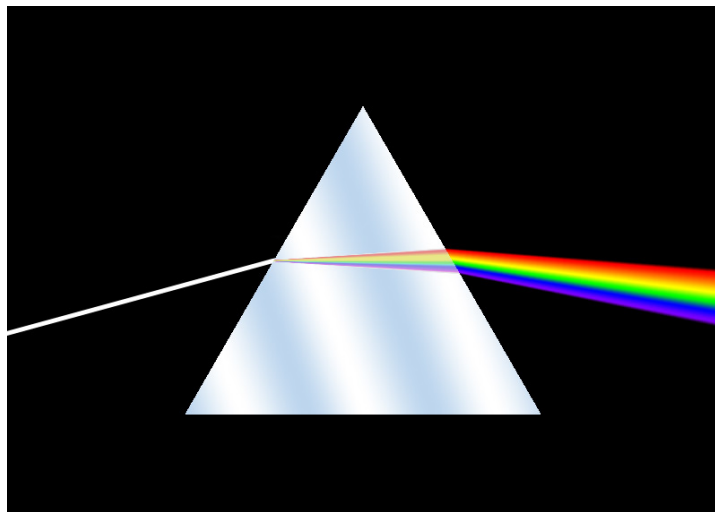

北京

Primary Bow
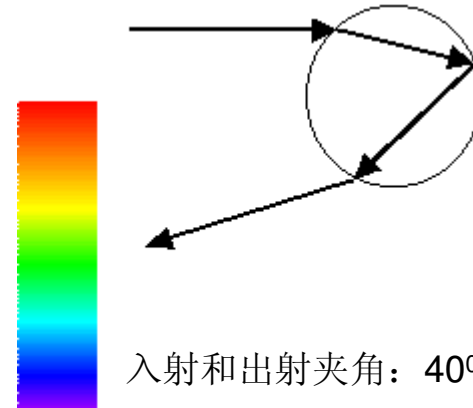
入射和出射夹角：40^0（紫）-42^0（红）

Secondary Bow　　　(reflected twice)

入射和出射夹角：50.5^0（红）-54^0（紫）

1666年Newton用棱镜显示光的色散，确认太阳白光包含不同颜色。Newton 用spectrum这个词描述该现象。

W Herschel (1800) 发现太阳光谱存在于红外波段；J.W. Ritter (1801) 观察到太阳光谱在紫外波段存在。

Newton' s analysis of light was the beginning of the science of spectroscopy.

Discovery of line spectra

Solar spectrum with Fraunhofer's lines
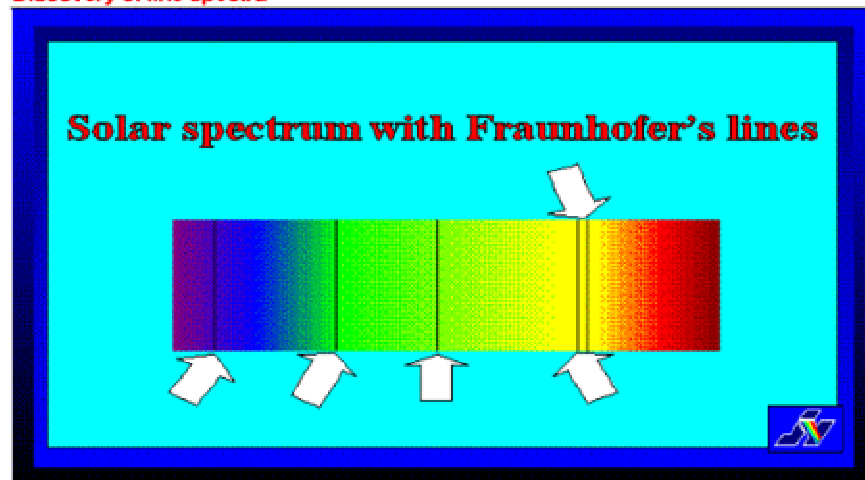
Joseph Fraunhofer(1787-1826) 更细致地研究了太阳光的色散，他发现充分色散的太阳光谱中存在很多暗线（1814），现称为Fraunhofer lines.

T. Young发现光通过狭缝会呈现明暗相间的（干涉）条纹。Fraunhofer 进一步把狭缝数目变成多个，因而发展出透射光栅。透射光栅同样能够把不同波长的光色散开来。利用透射光栅，Fraunhofer能够精确测量太阳光谱中暗线对应的波长。
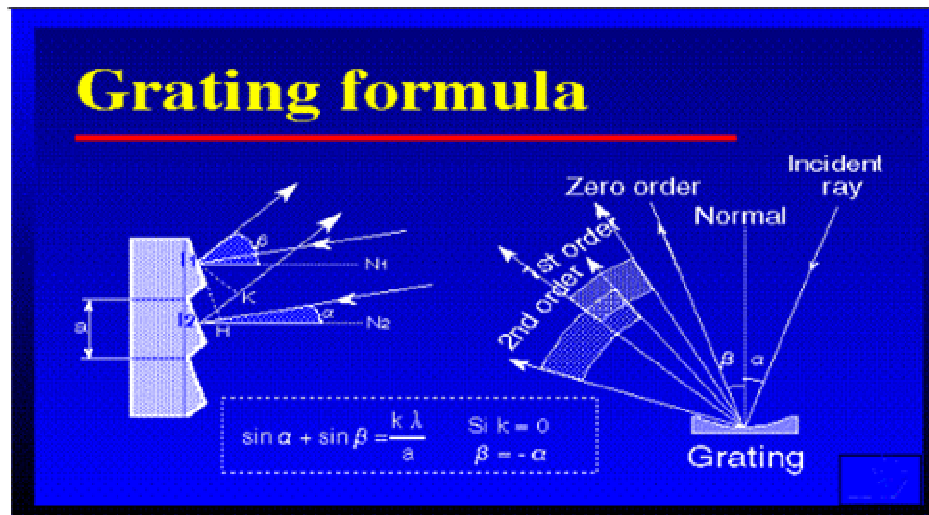
Large holographic gratings

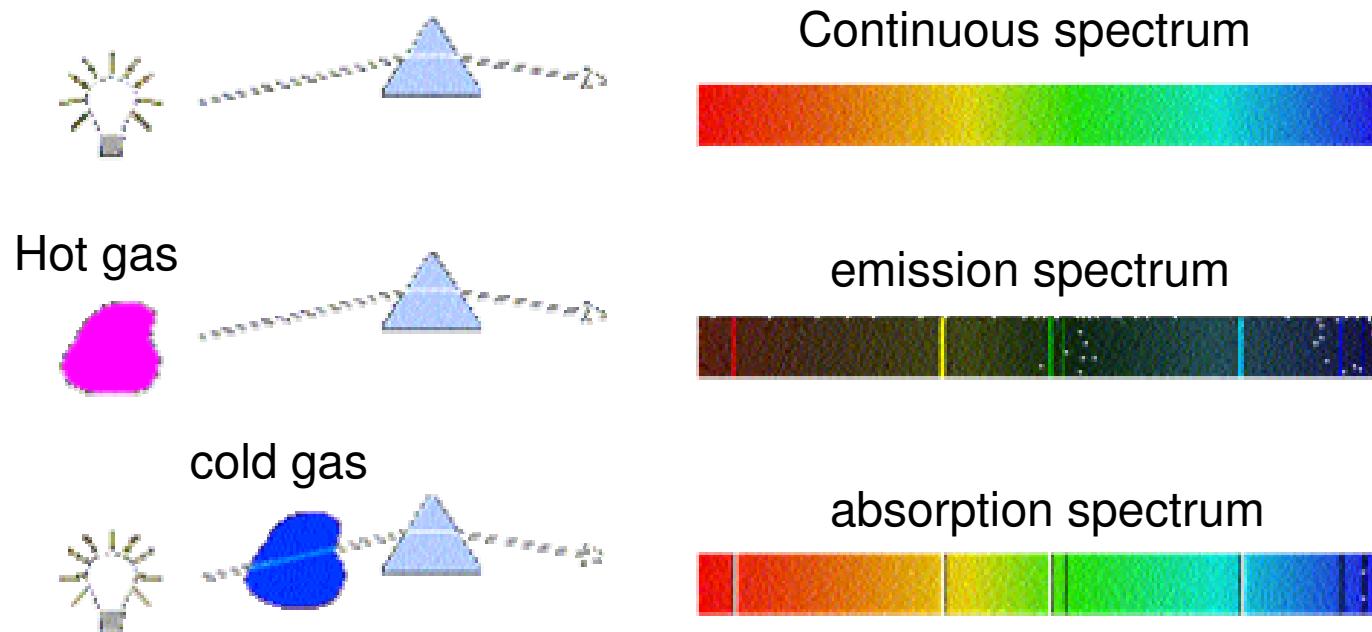但Fraunhofer没有意识到他所观察的谱线具有的重要意义。Fraunhofer去世33年之后，Kirchhoff 认识到同一物质的发射光谱和吸收光谱之间有相当严格的对应关系。某种物质自身发射那些波长的光，它就强烈地吸收那些波长的光。

Continuous spectrum

Hot gas

emission spectrum

cold gas

absorption spectrum

1859 G. Kirchhoff and R. Bunsen：太阳连续光谱中的Fraunhofer 暗线是处于温度较低的太阳表面原子对更加炽热的内核发射的连续光谱进行选择吸收的结果。 把这些吸收线的波长与地球上已知物质发射的原子波长对比，就可知道太阳表面层中包含那些元素。如氢（80％），氦（18％），…

1848年法国物理学家 Foucault首先观察到Na蒸气吸收黄线。这是实验室第一次观察到吸收谱。

白光源

狭缝

NaCl

加热

透镜聚焦
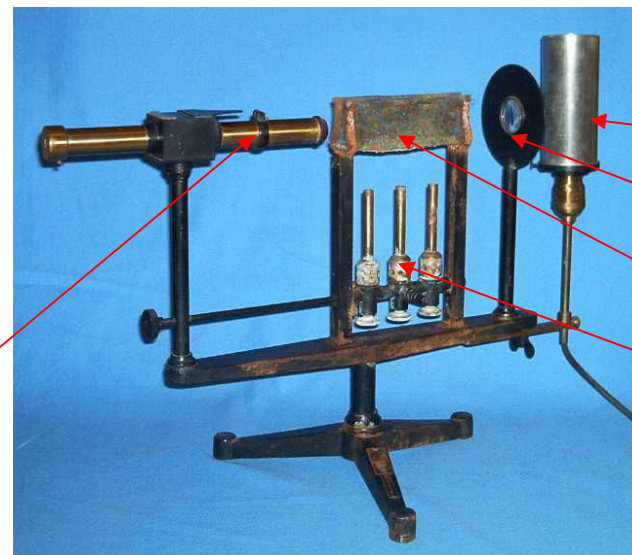
During the latter half of the nineteenth century a tremendous amount of atomic spectral data were collected. Characteristic lines were assigned to each element and their wavelengths were measured precisely. In 1885, J.J. Balmer 发现氢原子的光谱可用下列经验公式表示（称为Balmer series）

$$1/\lambda = R_H(1/2^2 - 1/n^2), n = 3, 4, 5, 6, \ldots$$

后来，又在紫外和红外发现多个谱线序列

赖曼线系　　　$1/\lambda = R_H(1/1^2 - 1/n^2), n = 2, 3, 4, \ldots$　　紫外

帕邢线系　　　$1/\lambda = R_H(1/3^2 - 1/n^2), n = 4, 5, \ldots$　　红外
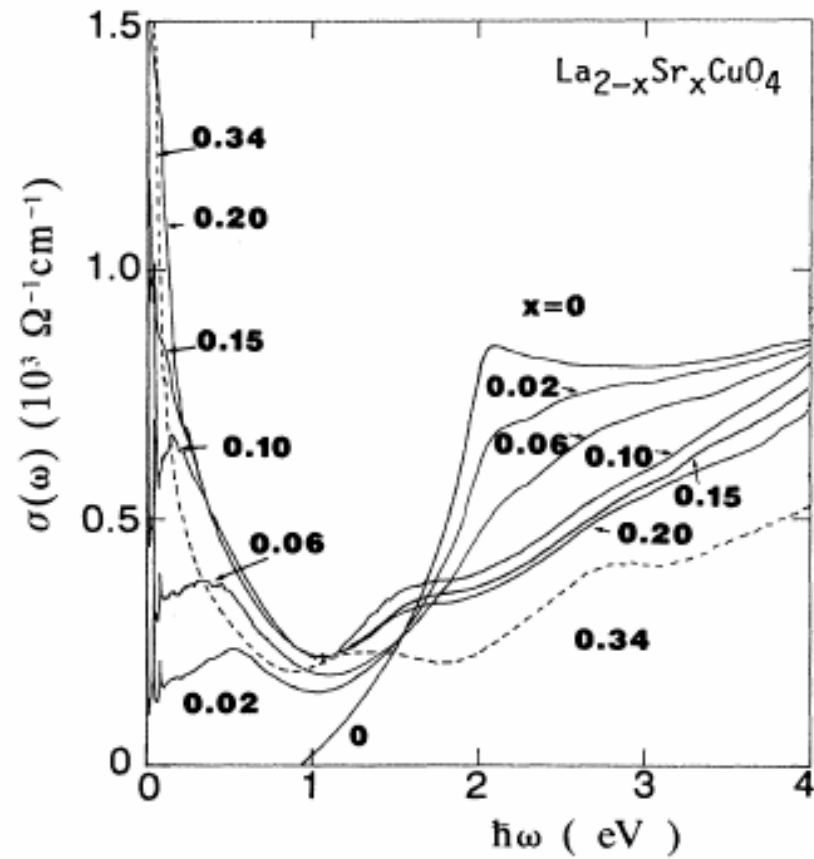
布喇开线系　　$1/\lambda = R_H(1/4^2 - 1/n^2), n = 5, 6, \ldots$　　红外

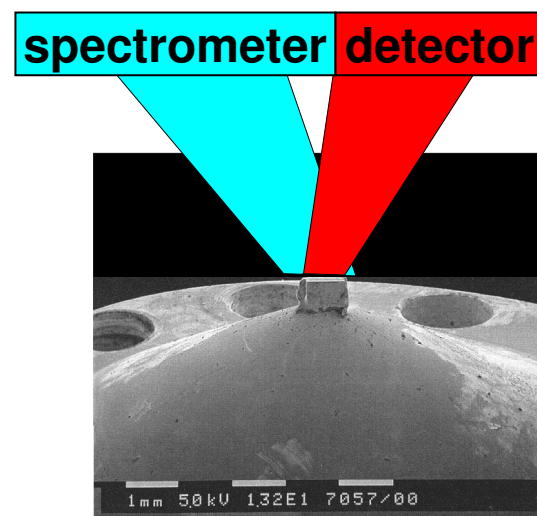一般地　　　　$1/\lambda = R_H(1/m^2 - 1/n^2), n > m$

凝聚态物理关心的光谱：

光电导谱

Optical conductivity

光反射谱测量

- 测量物理量 $R(\omega)$

- 固体物理感兴趣物理量 $\varepsilon(\omega), \sigma(\omega)$
 由$R(\omega)$通过Kramers-Kronig变换得到。

- 提供信息   探测凝聚态物质准粒子激发行为，特别是远红外区的低能激发。

Optical properties of solids

1. Optical constants

2. Kramers-Kronig transformation

3. Interband transition

4. Intraband transition

   - Drude model

   - Non-Drude spectra of strongly correlated electrons

   - Optical spectra of a superconductor

1. Optical constants

Consider an electromagnetic wave in a medium
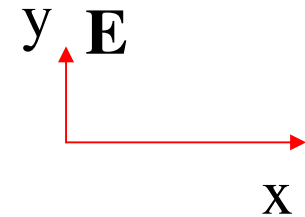
$$E_y = E_0 e^{i(qx - \omega t)} = E_0 e^{i\omega(x/v - t)} = E_0 e^{i\omega(\frac{nx}{c} - t)}$$

where $v \equiv \omega/q = c/n(\omega)$, $n(\omega)$: refractive index

If there exists absorption,

$$E_y = E_0 e^{-\frac{\omega K x}{c}} e^{i\omega(\frac{nx}{c} - t)}$$

K: attenuation factor

Intensity

$$I \propto E_y^2 = E_0^2 e^{-\frac{2\omega K x}{c}}$$

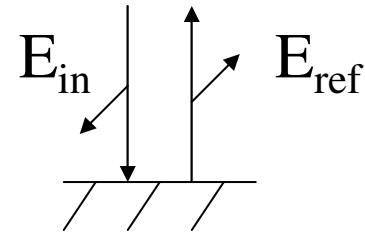Introducing a complex refractive index: $N(\omega) \equiv n(\omega) + iK(\omega)$

$$E_y = E_0 e^{i\omega(\frac{N(\omega)x}{c} - t)}$$

y E

x

Reflectivity

$$\frac{E_{ref}}{E_{in}} \equiv r = r(\omega)e^{i\theta(\omega)}$$

$$= \frac{n + iK - 1}{n + iK + 1} = \sqrt{\frac{(n-1)^2 + K^2}{(n+1)^2 + K^2}}\, e^{i\theta(\omega)}$$

E_{in} \ \ / E_{ref}

$$R = |E_{ref}/E_{in}|^2 = |r(\omega)|^2 = \frac{(n-1)^2 + K^2}{(n+1)^2 + K^2}$$

$$tg\,\theta = \frac{2K}{n^2 + K^2 - 1}$$

$$\boxed{\begin{array}{l} n = \dfrac{1 - R}{1 + R - 2R^{1/2}\cos\theta} \\[2ex] k = \dfrac{-2R^{1/2}\sin\theta}{1 + R - 2R^{1/2}\cos\theta} \end{array}}$$

If n, K are known, we
can get R, θ; vice versa.

Dielectric function
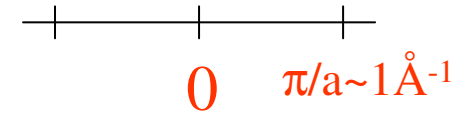
$$D(q, \omega) \equiv \varepsilon(q, \omega) E(q, \omega)$$

$$photon, q \to 0, \varepsilon = \varepsilon(\omega, q \to 0) = \varepsilon(\omega)$$

$$\because \sqrt{\varepsilon(\omega)} = N(\omega)$$

$$\Rightarrow \varepsilon(\omega) \equiv \varepsilon_1(\omega) + i\varepsilon_2(\omega) = (n(\omega) + iK(\omega))^2$$

$$\varepsilon_1(\omega) = n^2(\omega) - K^2(\omega)$$

$$\varepsilon_2(\omega) = 2n(\omega) \cdot K(\omega)$$

0    $\pi/a \sim 1\text{Å}^{-1}$

Infrared
$q = 2\pi/\lambda \sim 10^{-4} \text{ Å}^{-1}$

conductivity

$$\sigma = \sigma_1(\omega) + \sigma_2(\omega)$$

By electrodynamics, $\varepsilon(\omega) = 1 + \dfrac{4\pi i\, \sigma(\omega)}{\omega}$

In a solid, considering the contribution from ions or from high energy electronic excitations

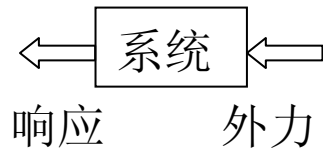$$\varepsilon(\omega) = \varepsilon_\infty + \frac{4\pi i\, \sigma(\omega)}{\omega}$$

Now, we have several pairs of optical constants:

$$
\left\{
\begin{array}{l}
n(\omega),\ K(\omega) \\
R(\omega),\ \theta(\omega) \\
\varepsilon_1(\omega),\ \varepsilon_2(\omega) \\
\sigma_1(\omega),\ \sigma_2(\omega)
\end{array}
\right.
$$

But only $R(\omega)$ can be measured experimentally.

Kramers-Kronig 关系

Kramers-Kronig transformation: 线性无源系统响应函数实部和虚部之间的关系。

响应　　外力

对于一个系统，施加外力，系统会有一响应。响应与外力由响应函数相联系，

例：
$$P(\omega) = \chi(\omega)E(\omega)$$

$\chi(\omega)$ 称为响应函数。

变到时间空间，两边作FT，利用卷积定理

$$P(t) = \int_{-\infty}^{\infty} dt' \, \chi(t - t')E(t')$$

又如：
$$E_r(\omega) = r(\omega)E_i(\omega)$$

$$E_r(t) = \int_{-\infty}^{\infty} dt' \, r(t - t')E_i(t')$$

一般地

$$\chi(\omega) = \alpha(\omega)F(\omega)$$

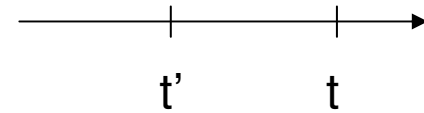$$\chi(t) = \int_{-\infty}^{\infty} dt' \, \alpha(t - t')F(t')$$

ω－空间

t－空间

α(t-t')的实部和虚部关系只依赖与因果率而与具体介质无关

Causality: 先有外力，后有响应。

即当t<t', α(t-t')=0, 因而

相当于取t'=0

$$\alpha(\omega) = \int_{-\infty}^{\infty} \alpha(t) e^{i\omega t} dt = \int_{0}^{\infty} \alpha(t) e^{i\omega t} dt$$

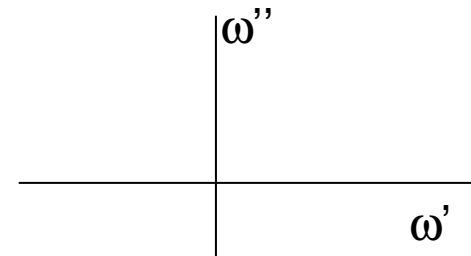
由此因果率，将得到重要结论。

把α(ω)中ω是实轴上定义的函数作解析沿拓到整个复平面，
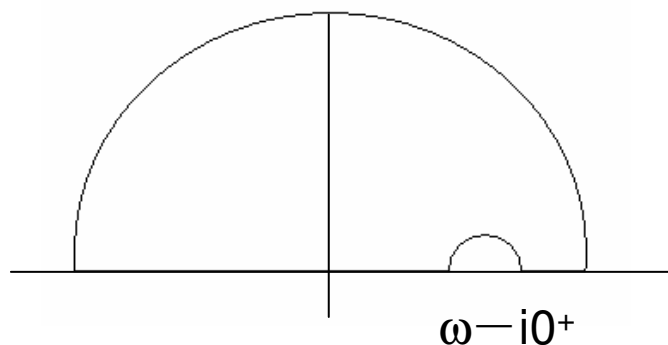
$$\omega \rightarrow \omega = \omega' + i\omega''$$

$$\alpha(\omega) = \int_{0}^{\infty} \alpha(t) e^{i(\omega' + i\omega'')t} dt = \int_{0}^{\infty} \alpha(t) e^{-\omega'' t} e^{i\omega' t} dt$$

$\because t > 0, e^{-\omega'' t}$ 收敛，α(ω)在ω上半复平面解析。

Consider the integral

$$\oint \frac{\alpha(\omega')d\omega'}{\omega'-\omega+i0^+}$$

$\omega - i0^+$

被积函数只在ω−i0+有一阶奇点，所选围道为扣除此奇点的上半复平面，由留数定理，上述积分＝0。

考虑到ω'→∞，α(ω') →0，沿上半圆弧的积分＝0，围道积分变成沿实轴（扣除奇点）的积分

$$\oint \frac{\alpha(\omega')d\omega'}{\omega'-\omega+i0^+} = \int_{-\infty}^{\infty} \frac{\alpha(\omega')d\omega'}{\omega'-\omega+i0^+} = 0$$

α(ω)＝ α₁(ω)+iα₂(ω)
令上式中实、虚部分别
相等即得到K-K关系

$$\because \frac{1}{x \mp i0^+} = \frac{P}{x} \pm i\pi\delta(x) \quad \text{证明稍后}$$

$$\Rightarrow \left| \frac{1}{\pi i} P \int_{-\infty}^{\infty} \frac{\alpha(\omega')d\omega'}{\omega'-\omega} - \alpha(\omega) = 0 \right.$$

$$\alpha_1(\omega) = \frac{1}{\pi} P \int_{-\infty}^{+\infty} \frac{\alpha_2(\omega')d\omega'}{\omega'-\omega}$$

$$\alpha_2(\omega) = \frac{-1}{\pi} P \int_{-\infty}^{+\infty} \frac{\alpha_1(\omega')d\omega'}{\omega'-\omega}$$

现补证：　　$\dfrac{1}{x \mp i0^+} = \dfrac{P}{x} \pm i\pi\delta(x)$

证　$\because \dfrac{1}{x-i\delta} = \dfrac{x+i\delta}{x^2+\delta^2} = \dfrac{x}{x^2+\delta^2} + i\dfrac{\delta}{x^2+\delta^2}$

当δ→0+时，实部　　$\dfrac{x}{x^2+\delta^2} = \dfrac{1}{x}$　for x≠0

而　　$\dfrac{x}{x^2+\delta^2} = 0$　for x=0.　$\Big\}$　因而实部可简记为 $\dfrac{P}{x}$

主值积分　$P\displaystyle\int_{-\infty}^{\infty} \dfrac{f(x)}{x}dx$　相当于挖去了x=0点。

当δ→0+时，虚部　　$\dfrac{\delta}{x^2+\delta^2} = 0$　　　for x≠0

而　　$\dfrac{\delta}{x^2+\delta^2} = \dfrac{1}{\delta} \to \infty$　for x=0.　$\Big\}$　因而虚部满足δ函数定义。

$\therefore \displaystyle\int_{-\infty}^{\infty} \dfrac{\delta}{x^2+\delta^2}dx = \pi$　　$\therefore \dfrac{\delta}{x^2+\delta^2} = \pi\delta(x)$

实、虚部结合：　$\dfrac{1}{x-i0^+} = \dfrac{P}{x} + i\pi\delta(x)$　　　　同样可证 $\dfrac{1}{x+i0^+} = \dfrac{P}{x} - i\pi\delta(x)$

现把K-K关系变成常用形式

$$\because \alpha(\omega) = \int_0^\infty \alpha(t) e^{i\omega t} dt$$

$$\therefore \alpha_1(\omega) = \int_0^\infty \alpha(t) \cos(\omega t) dt \qquad\qquad \alpha_1(\omega) = \alpha_1(-\omega) \qquad\text{偶函数}$$

$$\alpha_2(\omega) = \int_0^\infty \alpha(t) \sin(\omega t) dt \qquad\qquad \alpha_2(\omega) = -\alpha_2(-\omega) \qquad\text{奇函数}$$

$$\alpha_2(\omega) = \frac{-1}{\pi} P \int_{-\infty}^0 \frac{\alpha_1(\omega') d\omega'}{\omega' - \omega} + \frac{-1}{\pi} P \int_0^\infty \frac{\alpha_1(\omega') d\omega'}{\omega' - \omega}$$

用ω'→-ω'
$$= \frac{1}{\pi} P \int_0^\infty \frac{\alpha_1(\omega') d\omega'}{\omega' + \omega} + \frac{-1}{\pi} P \int_0^\infty \frac{\alpha_1(\omega') d\omega'}{\omega' - \omega}$$

$$= \frac{-2\omega}{\pi} P \int_0^\infty \frac{\alpha_1(\omega') d\omega'}{\omega'^2 - \omega^2}$$

考虑到 $\dfrac{1}{\dfrac{\omega' + \omega}{\omega' - \omega}} \dfrac{(\omega' - \omega) d\omega' - (\omega' + \omega) d\omega'}{(\omega' - \omega)^2} = \dfrac{-2\omega d\omega'}{\omega'^2 - \omega^2}$

$$= \frac{-1}{\pi} P \int_0^\infty [d \ln \left| \frac{\omega' + \omega}{\omega' - \omega} \right|] \alpha_1(\omega')$$

$$= \frac{-1}{\pi} P \int_0^\infty \ln \left| \frac{\omega' + \omega}{\omega' - \omega} \right|] \frac{d\alpha_1(\omega')}{d\omega} \qquad\qquad \text{分步积分}$$

同样可证 $\quad \alpha_1(\omega) = \dfrac{2}{\pi} P \displaystyle\int_0^{+\infty} \dfrac{\omega' \alpha_2(\omega')\mathrm{d}\omega'}{\omega'^2 - \omega^2}$

举例: 反射率

$r(\omega) = \sqrt{R(\omega)} e^{i\theta}$

$\Rightarrow \ln r(\omega) = (1/2)\ln R(\omega) + i\theta$
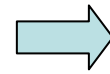
$\Longrightarrow \quad \theta = \dfrac{\omega}{\pi} P \displaystyle\int_0^\infty \dfrac{\ln R(\omega')}{\omega^2 - \omega'^2} d\omega'$

Low- ω extrapolation:

Insulator: R~ constant

Metal: Hagen-Rubens

Superconductor: two-fluids model

High-ω extrapolation:

R~ ω^{-p} (p~4)

介电函数:

$D = E + 4\pi P$

$\Rightarrow 4\pi P = [\varepsilon(\omega) - 1]E$

$\Longrightarrow$

$\begin{cases} \varepsilon_1(\omega) - 1 = \dfrac{2}{\pi} P \displaystyle\int_0^{+\infty} \dfrac{\omega' \varepsilon_2(\omega')\mathrm{d}\omega'}{(\omega')^2 - \omega^2} \\[4mm] \varepsilon_2(\omega) = -\dfrac{2\omega}{\pi} P \displaystyle\int_0^{+\infty} \dfrac{[\varepsilon_1(\omega') - 1]\mathrm{d}\omega'}{(\omega')^2 - \omega^2} \end{cases}$
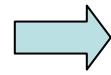
带间电子跃迁

指占据能带（价带）电子吸收光子能量跃迁到准许空能带（导带）。

为简单，考虑直接跃迁，**k'=k**.

初态　　$|v,k>, E_v(k)$

末态　　$|c,k>, E_c(k)$

跃迁条件：　$\hbar\omega = E_c(k) - E_v(k) \equiv E_{cv}(k)$
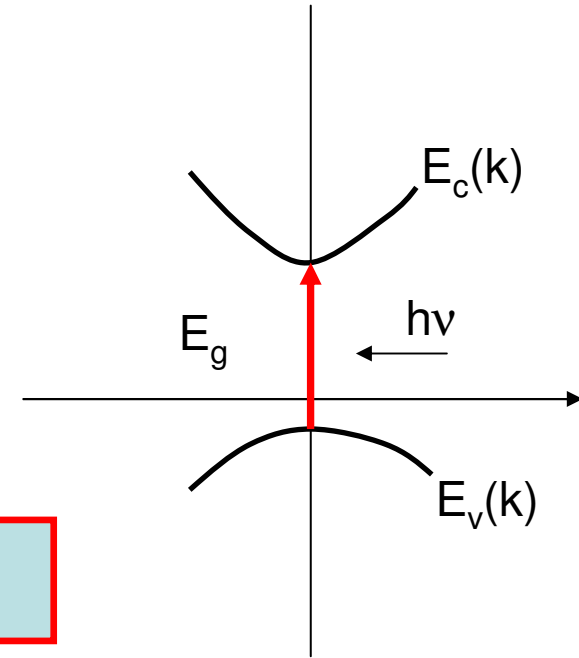
满足上面条件的态越多，吸收越强。

我们下面导出带间电子跃迁的介电函数的虚部（称为Kubo-Greenwood公式），以便与实验测量进行比较，从而对认识能带结构有所帮助。这可从单位体积吸收功率求得，但下面要涉及两个概念：一是van Hove奇点，二是联合态密度。

考虑能量在E—E+ΔE间的能态数目，若ΔZ
表示能态数目，则能态密度定义为 $N(\varepsilon) = \lim \dfrac{\Delta Z}{\Delta E}$
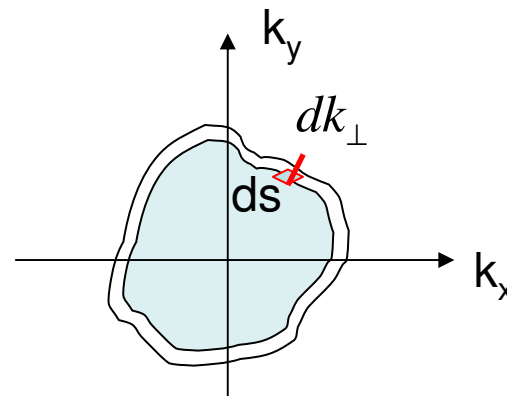
在k空间，由E(k)=const作等能面，那么在E－E +ΔE间的状态数目就是ΔZ。由于状态在k空间是均匀分布，密度为V/(2π)³，

因而ΔZ＝ V/(2π)³•(能量为E—E+ΔE之间的体积)

注意到能量为E—E+ΔE之间的体积可表示为体积元dsdk⊥在面上的积分，

$$\Delta Z = \frac{V}{(2\pi)^3} \int d\vec{k} = \frac{V}{(2\pi)^3} \int ds dk_\perp$$

其中ds为面积元，dk⊥为两等能面之间垂直距离。

$$= \left(\frac{V}{(2\pi)^3} \int \frac{ds}{|\nabla_k E|} \right) \Delta E$$

$\because \Delta E = |\nabla_k E(k)| \cdot dk_\perp$ |∇ₖE|为沿法线方向能量改变率

$$N(E) = \lim \frac{\Delta Z}{\Delta E} = \frac{V}{(2\pi)^3} \int \frac{ds}{|\nabla_k E|}$$

当E(k)已知，就可求出N(E).

例：球形等能面 $\qquad E = \dfrac{(\hbar \vec{k})^2}{2m*}$

$$\nabla_k E(k) = (\frac{\hbar^2 k_x}{m*}, \frac{\hbar^2 k_y}{m*}, \frac{\hbar^2 k_z}{m*})$$

$$\mid \nabla_k E(k) \mid = \frac{\hbar^2}{m*} \sqrt{k_x^2 + k_y^2 + k_z^2} = \frac{\hbar^2 k}{m*} = \frac{\hbar^2}{m*} (\frac{2m*}{\hbar^2})^{1/2} \sqrt{E(k)}$$

$$N(E) = \frac{2V}{(2\pi)^3} \int_0^\pi \int_0^{2\pi} \frac{k^2 \sin\theta \, d\theta \, d\varphi}{(\frac{2\hbar^2}{m*})^{1/2} E^{1/2}} = \frac{V}{2\pi^2} (\frac{2m*}{\hbar^2})^{3/2} E^{1/2} \qquad 为熟知结果$$

考虑自旋

当 $\quad \nabla_k E(k) = 0 \qquad$ 是被积函数奇点 $\equiv$ van Hove singularity

Obviously, the density of states will be high if a band is flat.

联合态密度

$$N(E) = \frac{V}{(2\pi)^3} \int \frac{ds}{|\nabla_k E|}$$

$$\hbar\omega = E_c(k) - E_v(k) \equiv E_{cv}(k)$$ 把上面式中E换成$E_{cv}(k)$

$$\boxed{J(E) = \frac{V}{(2\pi)^3} \int \frac{ds}{|\nabla_k E_{cv}(k)|}}$$
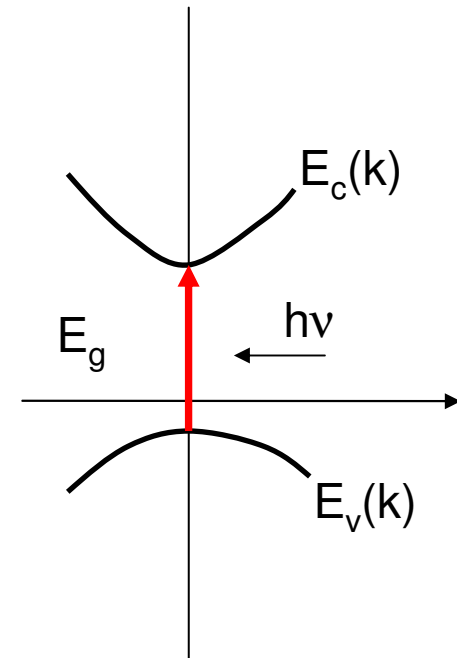
$$E_v = -\frac{\hbar^2}{2m_v{}^*}k^2$$

$$E_c = \frac{\hbar^2}{2m_c{}^*}k^2 + E_g$$

$\Longrightarrow$

$$E_{cv} = \frac{\hbar^2}{2m_c{}^*}k^2 + E_g - \left(-\frac{\hbar^2}{2m_v{}^*}k^2\right)$$

$$= E_g + \frac{\hbar^2}{2}\left(\frac{1}{m_c{}^*} + \frac{1}{m_v{}^*}\right)k^2 = E_g + \frac{\hbar^2}{2\mu}k^2$$

$E_c(k)$

E_g hν

$E_v(k)$

$$\therefore J(E) = \frac{1}{2\pi^2}\left(\frac{2\mu}{\hbar^2}\right)^{3/2}(E - E_g)^{1/2}$$ Kittle书 $J(E) = D_c(E_v + \hbar\omega)D_v(E_v)$ 这种相乘不对

$$\boxed{\text{当} \quad |\nabla_k E_{cv}(k)| = 0 \quad \text{为联合态密度的奇点。}}$$

下面任务是求带间跃迁相应的电导率或介电函数虚部

光波辐照前，体系的 Hamiltonian $\quad H_0 = \dfrac{\vec{p}^2}{2m} + U(r)$

光波照射后（即有电磁场情况）

$$H = \frac{(\vec{p} - \dfrac{e}{c}\vec{A})^2}{2m} + U(r) = \frac{1}{2m}\vec{p}^2 + U(r) - \frac{e}{mc}\vec{A} \cdot \vec{p} = H_0 + H' \qquad 略去 A^2 项$$

这里用到 Coulomb 规范 $\nabla \cdot \mathbf{A} = 0$, $\qquad \because \vec{p} \cdot \vec{A} - \vec{A} \cdot \vec{p} = -i\hbar\nabla \cdot \vec{A}$

注意电场强度 $\quad \vec{E}(t) = -\dfrac{1}{c}\dfrac{\partial \vec{A}(t)}{\partial t} \quad \longrightarrow \quad \boxed{\vec{E} = i\omega\vec{A}/c}$

则在 H' 作用下，每单位时间 |v, k> → |c, k> 跃迁几率

$$W_{v,\vec{k} \to c,\vec{k}} = \frac{2\pi}{\hbar} |<v,\vec{k}\,|\,H'\,|\,c,\vec{k}>|^2\ \delta(E_c(k) - E_v(k) - \hbar\omega)$$

能量守恒条件

取 $\quad \vec{A}(t) = A_0 \vec{e}_s e^{-i\omega t}$

↑
偏振方向

(波矢很小，忽略。只考虑随时间变化，
$\nabla_r \times A(t) = 0$，相当于忽略了磁场影响)

$$W_{v,\vec{k}\to c,\vec{k}} = \frac{2\pi}{\hbar} \mid \frac{e}{mc} A_0 \vec{e}_s \cdot <v,\vec{k}\mid \vec{p}\mid c,\vec{k}>\mid^2 \delta(E_{vc}(k)-\hbar\omega)$$

$$= \frac{2\pi e^2}{\hbar m^2 \omega^2} \mid \vec{p}(E_{vc}(k))\mid^2 \delta(\hbar\omega - E_{vc}(k)) \mid E\mid^2$$

只是与|v, k> → |c, k> 跃迁有关的函数

每单位时间、单位体积|v, k> → |c, k>跃迁几率

$$W_{v\to c} = \frac{2}{V} \sum_k W_{v,\vec{k}\to c,\vec{k}} = 2\int_{BZ} \frac{d^3k}{(2\pi)^3} \cdot \frac{2\pi e^2}{\hbar m^2 \omega^2} \mid \vec{p}(E_{vc}(k))\mid^2 \delta(\hbar\omega - E_{vc}(k)) \mid E\mid^2$$

考虑自旋

对所有满足 $E_{vc}(k) = \hbar\omega$ 的态求和

利用 $\quad 2\int_{BZ} \frac{d^3k}{(2\pi)^3} \delta(\hbar\omega - E_{vc}(k)) = J(\hbar\omega)$

$$W_{v\to c} = \frac{2\pi e^2}{\hbar m^2 \omega^2} J(\hbar\omega) \mid \vec{p}_{vc}(\hbar\omega)\mid^2 \mid E\mid^2$$

即跃迁几率与联合态密度有关

吸收功率＝每单位时间、单位体积吸收光子能量

$$= \hbar\omega W_{v\to c} = \frac{2\pi e^2}{m^2\omega} J(\hbar\omega)\mid \vec{p}_{vc}(\hbar\omega)\mid^2 \mid E\mid^2$$

另一方面，吸收功率＝$\sigma_1 |E|^2 = (1/4\pi)\omega\varepsilon_2(\omega)|E|^2$

$$\varepsilon_2(\omega) = \frac{8\pi^2 e^2}{m^2\omega^2} J(\hbar\omega)\mid \vec{p}_{vc}(\hbar\omega)\mid^2$$

Kubo-Greenwood formula

实验上， $\varepsilon_2(\omega)$由测量反射谱经Kramers-Kronig变换得到，
与此理论计算结果就可进行比较。

联合态密度的奇点 $\nabla_k E_{cv}(\vec{k}) = \nabla_k E_c(\vec{k}) - \nabla_k E_v(\vec{k}) = 0$

(i) $\nabla_k E_c(\vec{k}) = 0$, $\nabla_k E_v(\vec{k}) = 0$,

(ii) $\nabla_k E_c(\vec{k}) = \nabla_k E_v(\vec{k})$

此时， $\vec{v}_c(\vec{k}) = \vec{v}_v(\vec{k})$
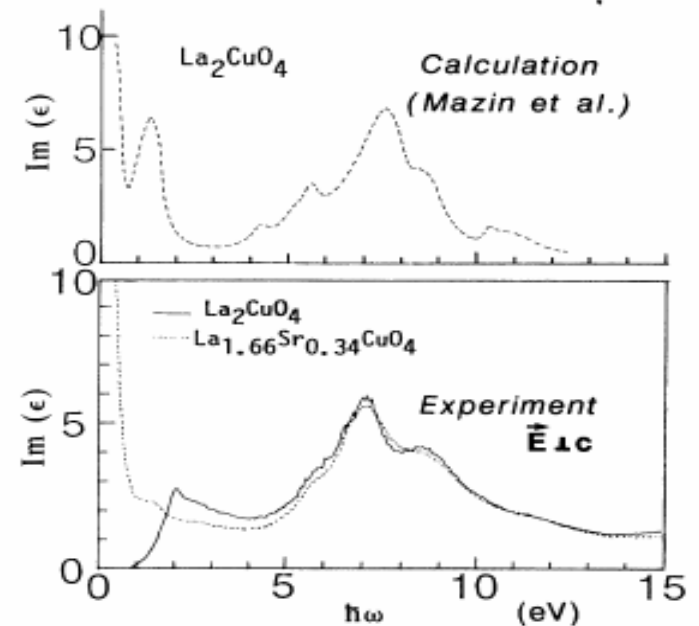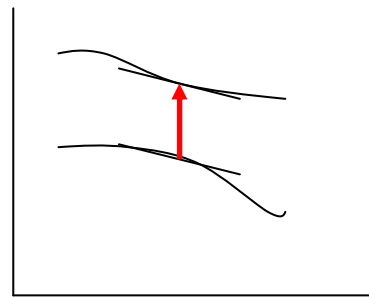
半导体中的光吸收

理想半导体在0K时，价带完全被电子占满，导带是空的。价带电子吸收足够能量的光子后，可激发至导带，而在价带中留下一个空穴，形成电子—空穴对。
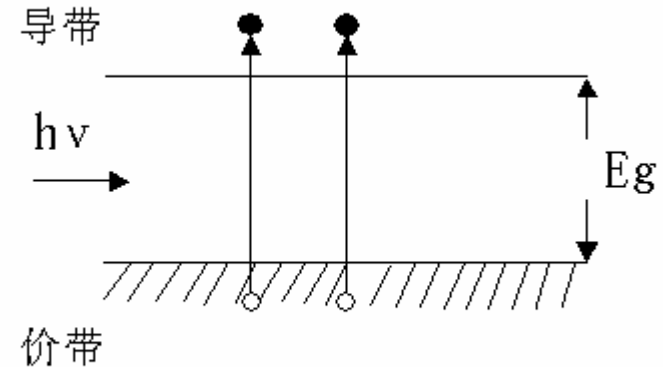
典型半导体

GaAs: Eg= 1.5eV

Si: Eg= 1.12eV

一些半导体的带隙

E_g 和 λ_0 的对应关系
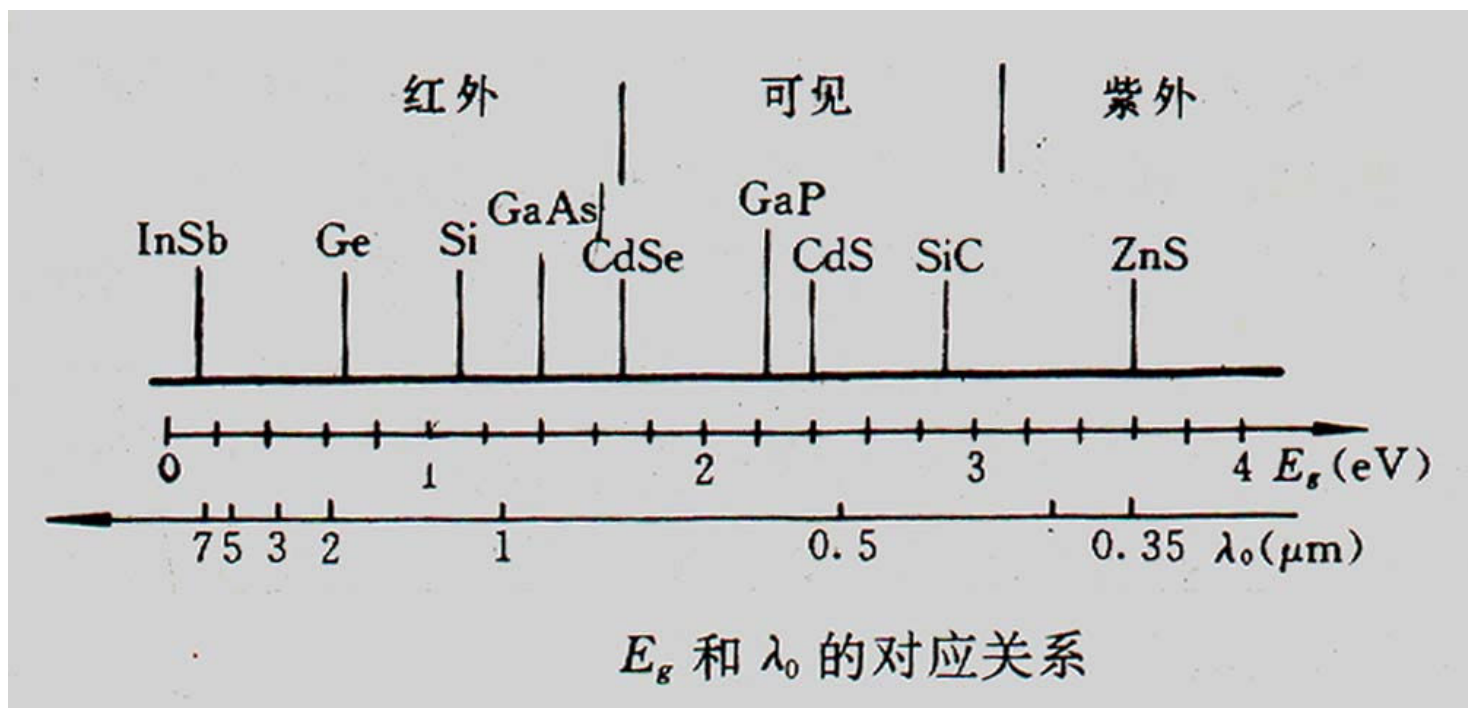
B. 直接跃迁和间接跃迁

电子吸收光子的跃迁过程必须满足能量和动量守恒，由于光子动量几乎为零，电子在跃迁过程中波矢保持不变（在波矢k空间必须位于同一垂线上）➜直接跃迁

电子的直接跃迁

常见半导体GaAs就属于此类：直接带隙半导体
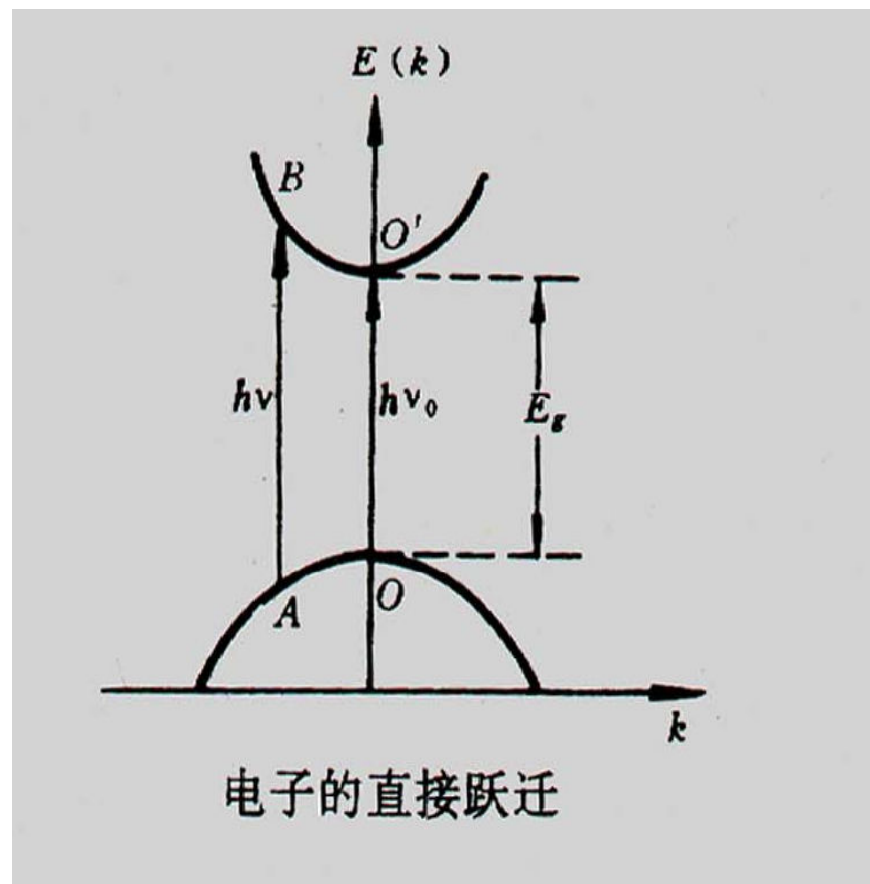
$$\alpha(h\nu) = \begin{cases} A(h\nu - E_g)^{\frac{1}{2}} & h\nu \geq E_g \\ 0 & h\nu < E_g \end{cases}$$

间接跃迁：不是垂直跃迁，为了保证动量守恒，电子不仅吸收光子，同时需要和杂质或晶格交换一定的振动能量，即放出或吸收一个声子。间接跃迁的光吸收系数比直接跃迁小得多。

Si：间接带隙
半导体

直接跃迁和间接跃迁
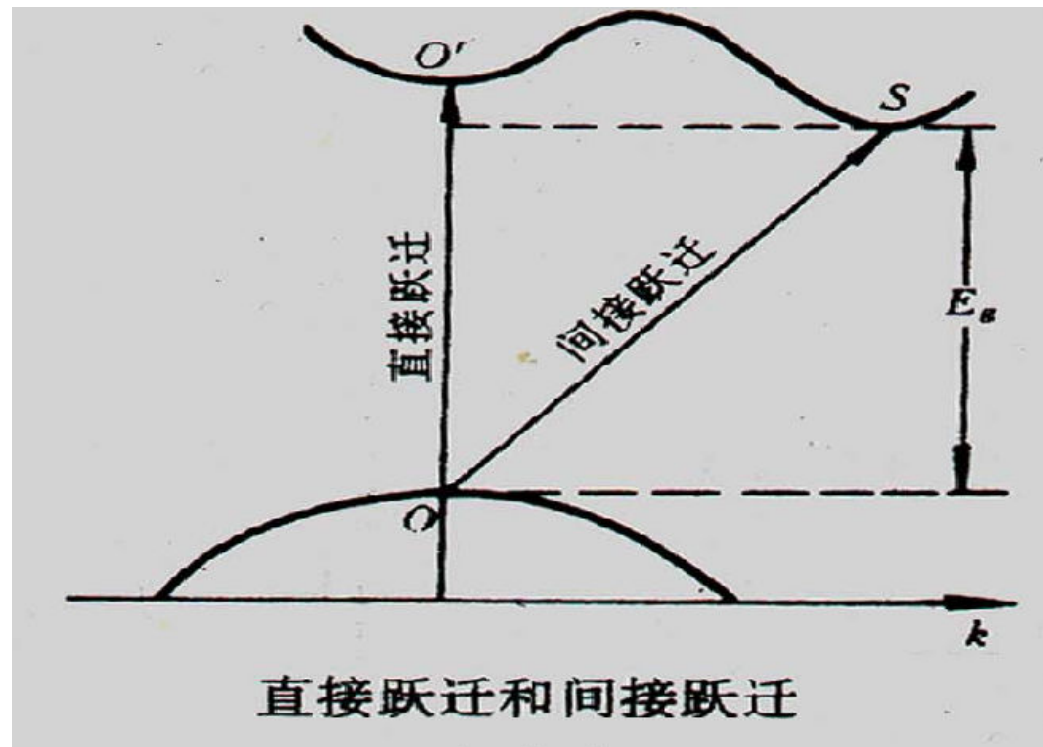
i). 激子吸收：

电子和空穴由于互相静电吸引束缚在一起（电子—空穴对）

激子吸收发生在带隙E_g低能处，束缚能E_b

$$hv = E_g - E_b$$

激子吸收光谱
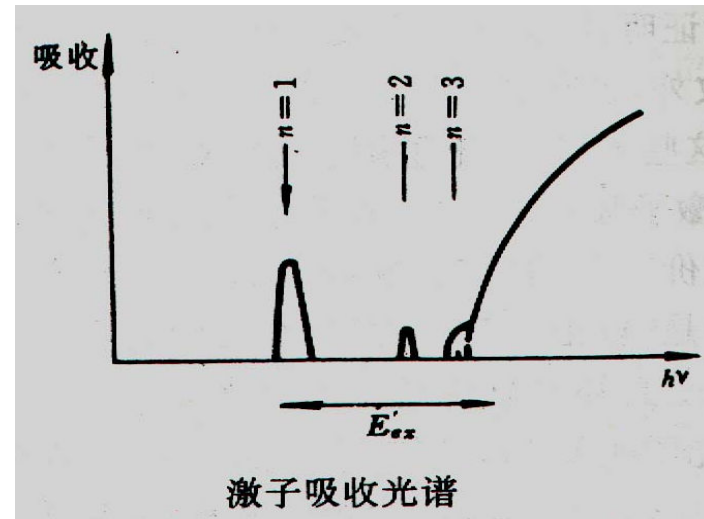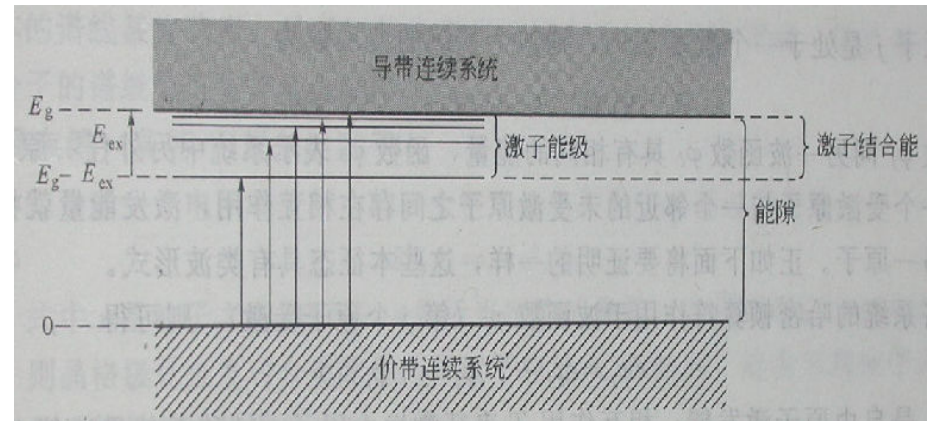
ii). 杂质吸收
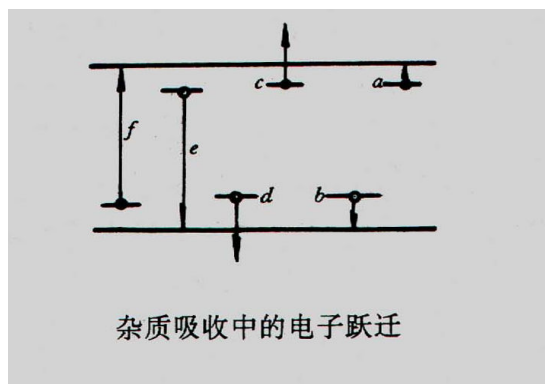
B-doped Diamond   D Wu et al. PRB 06

杂质吸收中的电子跃迁
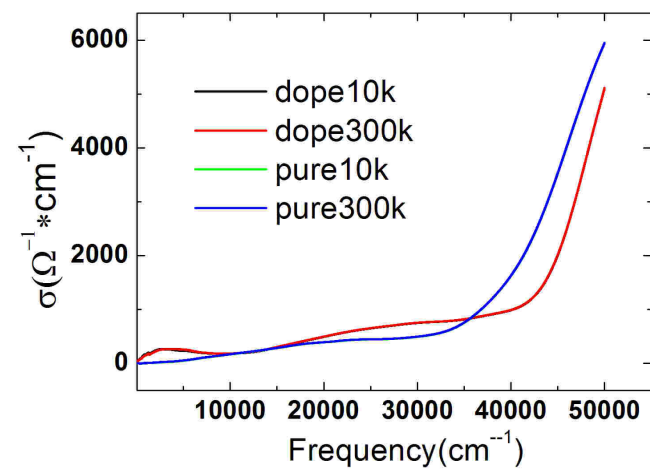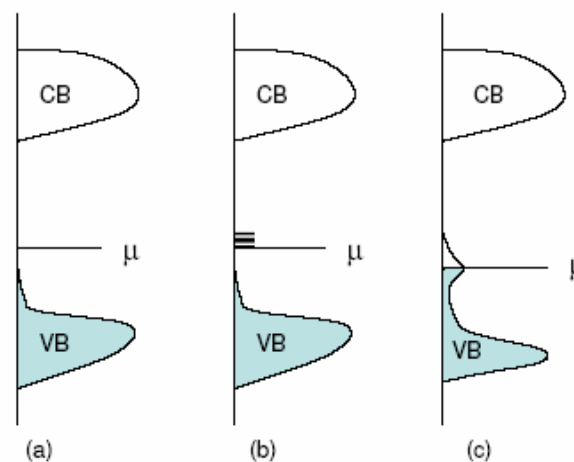
iii). 声子吸收

Drude model

Drude模型是关于自由电子或跨越费米能的能带电子对电场的响应。Drude模型可以由驰豫时间近视下的Boltzman方程导出，也可由更普遍的线性响应理论得到的Kubo方程在局域条件（**q**→0）和驰豫时间近似下得到。如下先用简单的经典图象给出。

$$\sigma(\omega) = \frac{\sigma_0}{1-i\omega\tau}$$

$$\sigma_0 = \frac{ne^2\tau}{m^*} = \frac{\omega_p^2\tau}{4\pi}$$

Paul Drude (1863-1906)

牛顿定律：
$$\frac{d\vec{P}}{dt} + \frac{\vec{P}}{\tau} = -e\vec{E}$$

$$\vec{p}(t) = m^* \vec{v}$$

利用 $\begin{aligned} \vec{E} &= \vec{E}_0 e^{i(\vec{q}\cdot\vec{r} - \omega t)} \\ \vec{P} &= \vec{P}_0 e^{i(\vec{q}\cdot\vec{r} - \omega t)} \end{aligned}$ $\Rightarrow$ $-i\omega\vec{P}(\omega) = -e\vec{E}(\omega) - \frac{1}{\tau}\vec{P}(\omega)$ $\Rightarrow$ $\vec{P}(\omega) = \frac{e}{i\omega - 1/\tau}\vec{E}(\omega)$

由 $\quad \vec{J}(t) = -ne\,\vec{v}(t) = -ne\,\vec{P}(\omega)/m^*$

$$\vec{J}(\omega) = -\frac{ne}{m^*}\vec{P}(\omega) = \frac{ne^2\tau/m^*}{1 - i\omega\tau}\vec{E}(\omega)$$

$\Rightarrow$ $\boxed{\sigma(\omega) = \frac{\sigma_0}{1 - i\omega\tau} = \frac{\omega_D^2}{4\pi}\frac{1}{1/\tau - i\omega}}$ $\qquad \sigma_0 = \frac{ne^2\tau}{m^*} = \frac{\omega_p^2\tau}{4\pi}$

$$\sigma_1(\omega) = \frac{\sigma_0}{1 + \omega^2\tau^2} = \frac{\omega_p^2\tau}{4\pi}\frac{1}{1 + \omega^2\tau^2}$$

$$\sigma_2(\omega) = \frac{\sigma_0\omega\tau}{1 + \omega^2\tau^2} = \frac{\omega_p^2\tau}{4\pi}\frac{\omega\tau}{1 + \omega^2\tau^2}$$
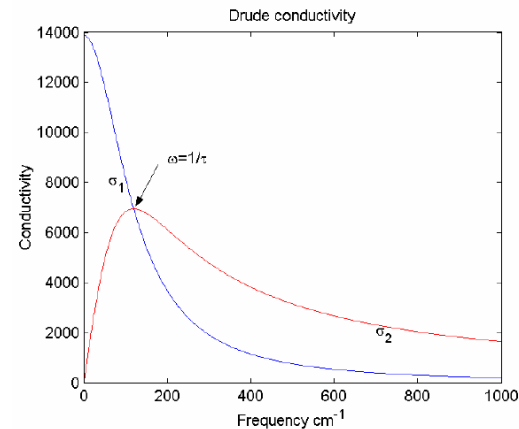
因为 $\varepsilon(\omega) = \varepsilon_1(\omega) + i\varepsilon_2(\omega) = 1 + \dfrac{4\pi i}{\omega}\sigma(\omega)$

固体中 $\varepsilon(\omega) = \varepsilon_\infty + \dfrac{4\pi i}{\omega}\sigma(\omega)$

$$\Rightarrow \quad \varepsilon_1 = \varepsilon_\infty - \frac{\omega_p^{\,2}}{\omega^2 + 1/\tau^2}$$

$$\varepsilon_2 = \frac{4\pi\sigma_1}{\omega} = \frac{\omega_p^{\,2}\tau}{\omega}\frac{1}{1+\omega^2\tau^2}$$

$$\mathrm{Im}\!\left[\frac{1}{-\varepsilon(\omega)}\right] = \frac{\omega_p'^{\,2}\omega/\tau}{(\omega^2 - \omega_p'^{\,2})^2 + \omega^2\tau^{-2}}$$

$$\omega_p' = \omega_p/\sqrt{\varepsilon_\infty}$$

$$\int\limits_0^\infty \sigma_1(\omega)\,d\omega = \frac{\omega_p^2}{8}$$
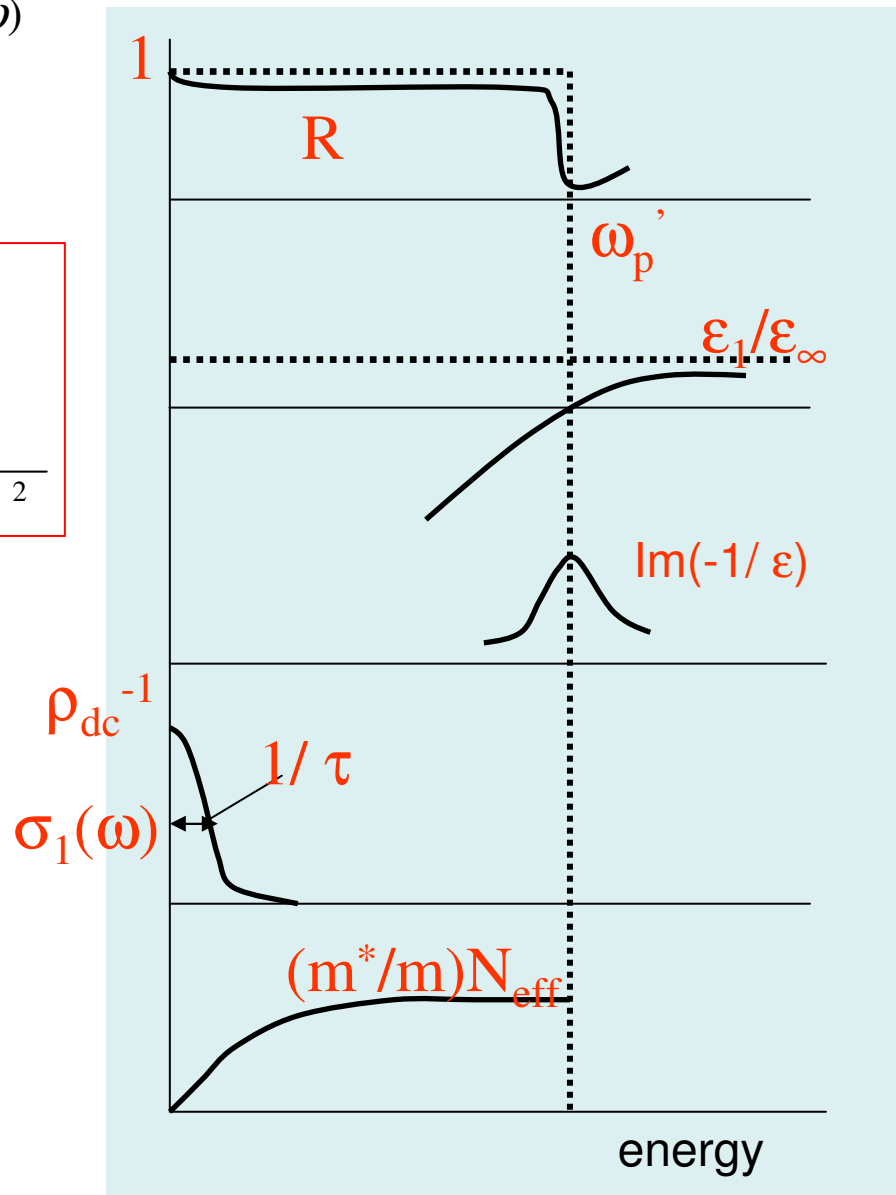
1.Hagen-Rubens regime At low-frequency limit ωτ<<1

$$\begin{cases} \sigma_1(\omega) = \dfrac{\sigma_0}{1+\omega^2\tau^2} = \dfrac{\omega_p^2\tau}{4\pi}\dfrac{1}{1+\omega^2\tau^2} \\ \sigma_2(\omega) = \dfrac{\sigma_0\omega\tau}{1+\omega^2\tau^2} = \dfrac{\omega_p^2\tau}{4\pi}\dfrac{\omega\tau}{1+\omega^2\tau^2} \end{cases} \Rightarrow \begin{cases} \sigma_1(\omega) \approx \sigma_0 \\ \sigma_2(\omega) \approx \sigma_0\omega\tau = \dfrac{\omega_p^2\tau^2}{4\pi}\omega \ll \sigma_1 \end{cases}$$

$$\begin{cases} \varepsilon_1 = \varepsilon_\infty - \dfrac{\omega_p^2}{\omega^2+1/\tau^2} \\ \varepsilon_2 = \dfrac{4\pi\sigma_1}{\omega} = \dfrac{\omega_p^2\tau}{\omega}\dfrac{1}{1+\omega^2\tau^2} \end{cases} \Rightarrow \begin{cases} \varepsilon_1 = \varepsilon_\infty - \dfrac{\tau^2\omega_p^2}{1+\omega^2\tau^2} \approx \varepsilon_\infty - \tau^2\omega_p^2 \\ \varepsilon_2 = \dfrac{\omega_p^2\tau}{\omega}\dfrac{1}{1+\omega^2\tau^2} \approx \dfrac{\omega_p^2\tau}{\omega} = \dfrac{4\pi\sigma_0}{\omega} \gg \varepsilon_1 \end{cases}$$

$$\begin{cases} n = \dfrac{1}{\sqrt{2}}\sqrt{\sqrt{\varepsilon_1^2+\varepsilon_2^2}+\varepsilon_1} \\ k = \dfrac{1}{\sqrt{2}}\sqrt{\sqrt{\varepsilon_1^2+\varepsilon_2^2}-\varepsilon_1} \end{cases} \Rightarrow \quad n = k = \dfrac{1}{\sqrt{2}}\sqrt{\varepsilon_2} = \sqrt{\dfrac{2\pi\sigma_0}{\omega}} \gg 1$$

$$R = \dfrac{(n-1)^2+k^2}{(n+1)^2+k^2} = \dfrac{n^2-2n+1+k^2}{n^2+2n+1+k^2} = \dfrac{1-2/n+1/n^2+k^2/n^2}{1+2/n+1/n^2+k^2/n^2} \approx \dfrac{2-2/n}{2+2/n} \approx 1-2/n = 1-\sqrt{\dfrac{2\omega}{\pi\sigma_0}}$$

2. Relaxation regime $\quad 1/\tau < \omega < \omega_p$

$$\begin{cases} 4\pi\sigma_1(\omega) = \dfrac{\omega_p^2\tau}{1+\omega^2\tau^2} \approx \dfrac{\omega_p^2}{\omega^2\tau} \\[4mm] 4\pi\sigma_2(\omega) = \dfrac{\omega\omega_p^2\tau^2}{1+\omega^2\tau^2} \approx \dfrac{\omega_p^2}{\omega} \end{cases} \qquad \begin{cases} \varepsilon_1 = \varepsilon_\infty - \dfrac{\omega_p^2}{\omega^2} \\[4mm] \varepsilon_2 = \dfrac{\omega_p^2}{\omega^3\tau} \end{cases} \qquad \begin{cases} n \approx \dfrac{\omega_p}{2\tau\omega} \\[4mm] k \approx \dfrac{\omega_p}{\omega} \end{cases}$$
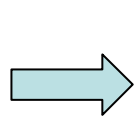
$\Longrightarrow \quad \boxed{R \simeq 1 - \dfrac{2}{\omega_p\tau}} \quad$ a constant if τ is constant, otherwise $1\text{-}R \propto 1/\tau$

3. Ultraviolet transparency regime $\quad \omega \gg \omega_p$

$\varepsilon_1 \to \varepsilon_\infty \quad$ (ε_1 crosses zero at $\omega = \omega_p/\sqrt{\varepsilon_\infty}$) $\quad \boxed{R \to 0}$

Plot of Drude Model spectra

$$\sigma(\omega) = \frac{\omega_D^2}{4\pi} \frac{1}{1/\tau - i\omega}$$

$\varepsilon_\infty \sim 1,\ 1/\tau \equiv \Gamma$

$\Gamma = 0.02\text{eV}$

$4\pi N e^2 / m = \omega_p^2 = 30$

Drude conductivity
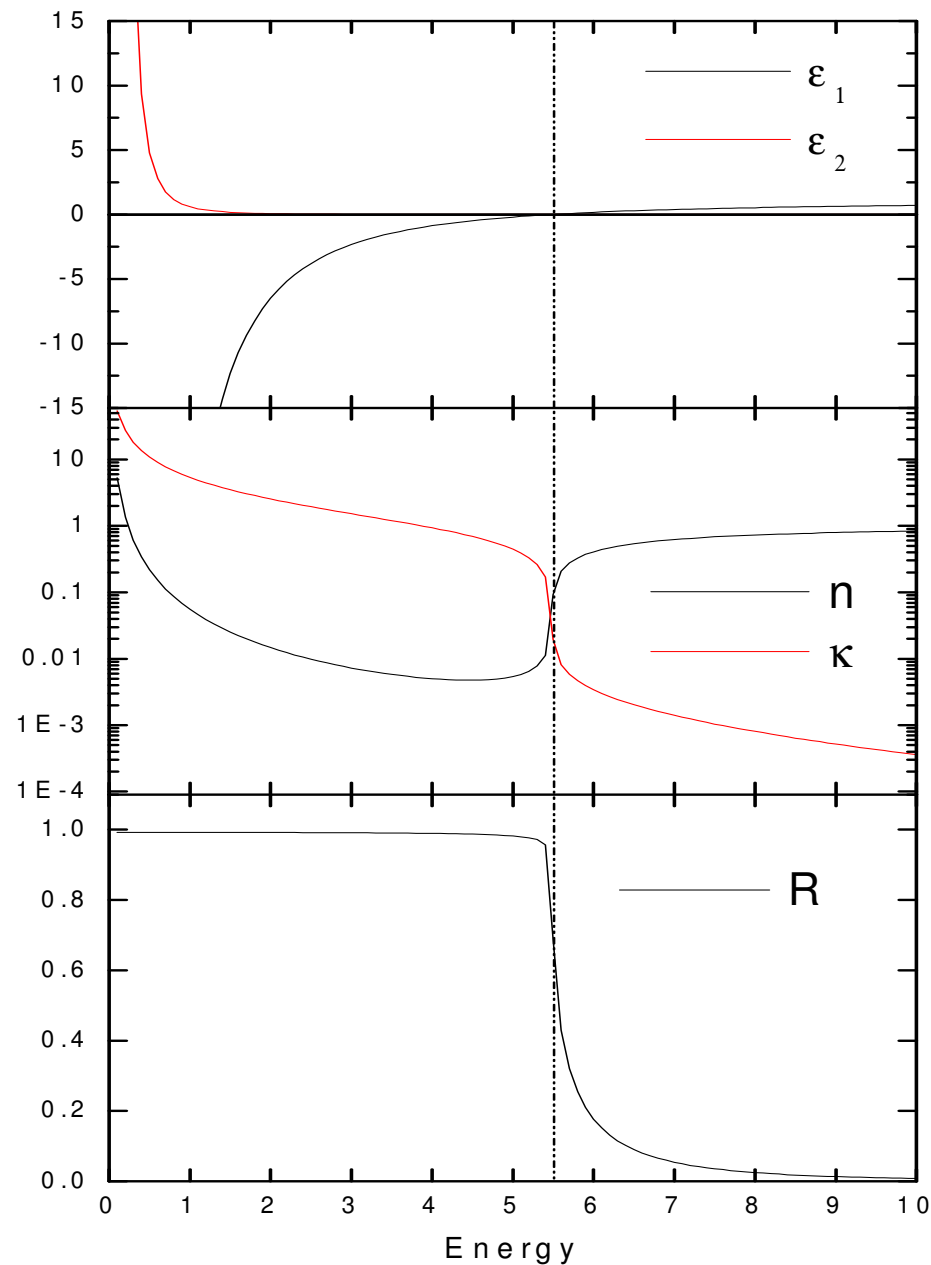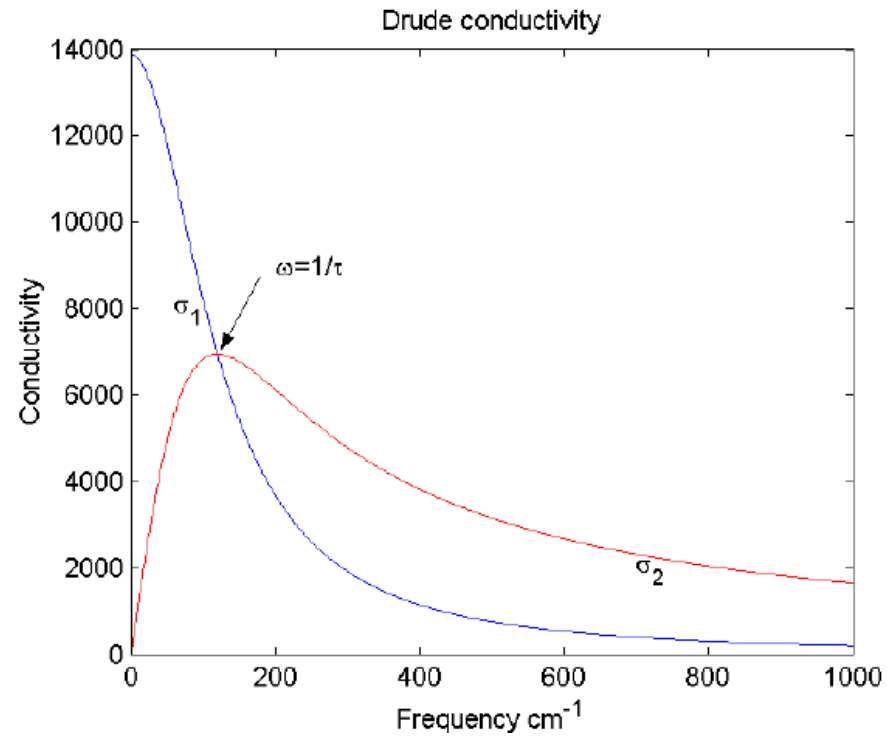
注：Intraband transition要求particle-hole
激发必须通过杂质或Boson mode的参与
帮助，以满足动量守恒。

$\varepsilon = \varepsilon(k)$

E_F
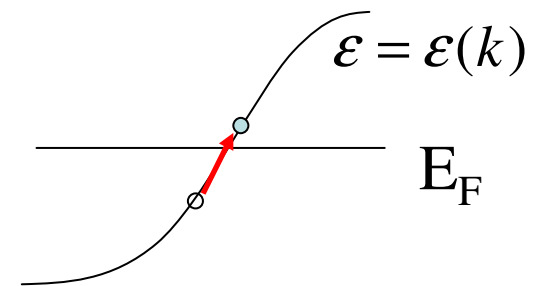
Absorption processes

Infrared light <u>cannot</u> be absorbed by electron-hole pair creation

(The impurities or boson modes are needed to transfer the momemtum of particle-hole excitations. This is called impurities or boson-assisted absorptions.)

$\nu = ck$

ε_k

$\Delta \omega$

Δk

k
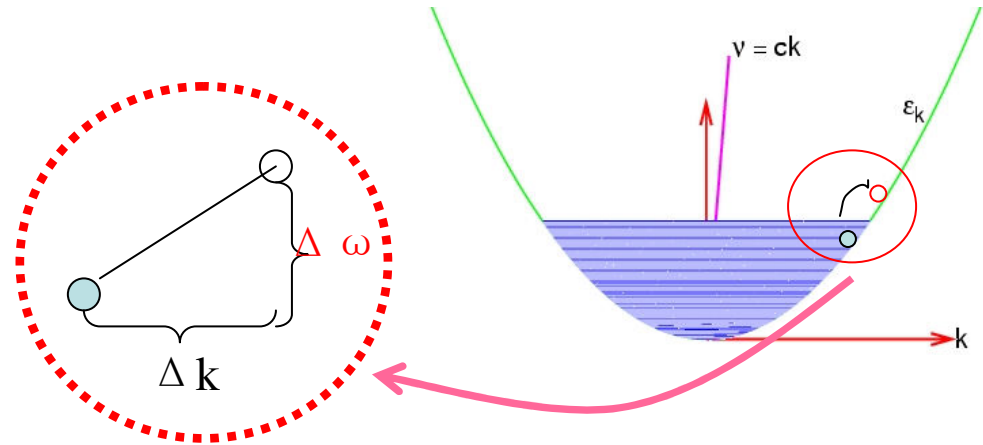
(a) Impurity-assisted absorption

e^- k,E X k',E

(q=0, ν)
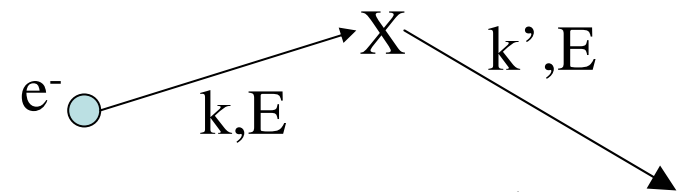
(b) boson-assisted absorption

e^- k,E q, ω_q

k',E'
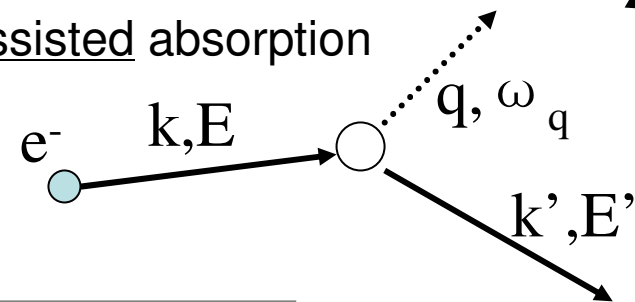
Holstein process, if phonons are involved.

$$\frac{\partial f}{\partial t} + \vec{v}_k \bullet \nabla_r f + \dot{\vec{k}} \bullet \nabla_k f = (\frac{\partial f}{\partial t})_{coll}$$

其中：$f = f(\mathbf{k}, \mathbf{r}, t)$ 是电子分布函数；

对电子在k空间运动，$\dot{\vec{k}} = \frac{\partial \vec{k}}{\partial t} = -\frac{e}{\hbar}(\vec{E} + \frac{1}{c}\vec{v}_k \times \vec{H}) = -\frac{e}{\hbar}\vec{E}$

不考虑磁场

偏离平衡态很小，$f = f_0 + f_1$

$$f_0 = \frac{1}{1 + \exp[(\varepsilon_k - \varepsilon_F)/k_B T]}$$

驰豫时间近似，$(\frac{\partial f}{\partial t})_{coll} = \frac{f - f_0}{\tau} = -\frac{f_1}{\tau}$

另外，$\frac{\partial f}{\partial k} = \frac{\partial f}{\partial \varepsilon}\frac{\partial \varepsilon}{\partial k}$, $\vec{v}_k = \hbar^{-1}\nabla_k \varepsilon(\vec{k})$

$$-\frac{\partial f^1}{\partial t} = \vec{v}_k \bullet \nabla_r f_1 - e\vec{E} \bullet \vec{v}_k \frac{\partial f^0}{\partial \varepsilon} + \frac{f^1}{\tau}$$

假定分布函数随时间空间变化， $f^1 \propto \exp[i(\vec{q} \cdot \vec{r} - \omega t)]$

作FT：
$$f^1 = \frac{-e\vec{E}(\vec{q}, \omega) \cdot \vec{v}_k (-\frac{\partial f^0}{\partial \varepsilon})\tau}{1 - i\omega\tau + i\vec{v}_k \cdot \vec{q}\tau}$$

电流密度： $\vec{J}(q, \omega) = -\frac{2e^2}{(2\pi)^3} \int f^1 \vec{v}_k d\vec{k} = \frac{2e^2}{(2\pi)^3} \int d\vec{k} \frac{\tau\vec{E}(\vec{q}, \omega) \cdot \vec{v}_k (-\frac{\partial f^0}{\partial \varepsilon})}{1 - i\omega\tau + i\vec{v}_k \cdot \vec{q}\tau} \vec{v}_k$

$$\hat{\sigma}(q, \omega) = \frac{2e^2}{(2\pi)^3} \int d\vec{k} \frac{\tau\vec{v}_k \vec{v}_k (-\frac{\partial f^0}{\partial \varepsilon})}{1 - i\omega\tau + i\vec{v}_k \cdot \vec{q}\tau}$$

考虑到 $\lim_{T \to 0}(-\frac{\partial f^0}{\partial \varepsilon}) = \delta(\varepsilon - \varepsilon_F),$

$$d\vec{k} = dS dk_\perp = dS \frac{d\varepsilon}{|\nabla_k \varepsilon|} = \frac{dS}{\hbar v_k} d\varepsilon$$

$$\hat{\sigma}(\vec{q},\omega) = \frac{2e^2}{(2\pi)^3} \int\!\!\int \frac{\tau\vec{v}_k\vec{v}_k}{1-i\omega\tau+i\vec{v}_k\cdot\vec{q}\tau}\left(-\frac{\partial f^0}{\partial\varepsilon}\right)\frac{dS}{\hbar v_k}d\varepsilon$$

$$= \frac{2e^2}{(2\pi)^3}\int_{\varepsilon=\varepsilon_F} \frac{\tau\vec{v}_k\vec{v}_k}{1-i\omega\tau+i\vec{v}_k\cdot\vec{q}\tau}\frac{dS_F}{\hbar v_k}$$

在局域极限下q→0

$$\hat{\sigma}(q,\omega) = -\frac{e^2}{4\pi^3\hbar}\int \frac{\tau\vec{v}_k\vec{v}_k}{v_k}\frac{dS_F}{1-i\omega\tau} = \sigma_{dc}\frac{1}{1-i\omega\tau}$$

电导率更普遍形式－Kubo公式

光波辐照前，体系的Hamiltonian $\quad H_0 = \frac{1}{2m}\sum_{i=1}^{N}\vec{p}_i^2 + \sum_{i=1}^{N}V_i(\vec{r}_i) + \frac{1}{2}\sum_{i,j=1}\frac{e^2}{|\vec{r}_i - \vec{r}_j|}$

光波照射后（即有电磁场情况）

$$H = \frac{1}{2m}\sum_{i=1}^{N}[\vec{p}_i - \frac{e}{c}\vec{A}(\vec{r}_i)]^2 + \sum_{i=1}^{N}V_i(\vec{r}_i) + \frac{1}{2}\sum_{i,j=1}\frac{e^2}{|\vec{r}_i - \vec{r}_j|} = H_0 + H' \quad \text{略去A²项}$$

其中 $\quad H' = -\frac{e}{2mc}\sum_{i=1}^{N}[\vec{p}_i \cdot \vec{A}(\vec{r}_i) + \vec{A}(\vec{r}_i) \cdot \vec{p}_i] = -\frac{e}{mc}\sum_{i=1}^{N}\vec{p}_i \cdot \vec{A}(\vec{r}_i)$

这里用到Coulomb规范$\nabla \cdot \mathbf{A} = 0$

引入电流密度算子 $\quad \vec{J}(\vec{r}) = \frac{e}{2m}\sum_{i=1}^{N}[\vec{p}_i\delta(\vec{r} - \vec{r}_i) + \delta(\vec{r} - \vec{r}_i)\vec{p}_i]$

则 $\quad H' = -\frac{1}{c}\int d\vec{r}\vec{J}(\vec{r}) \cdot \vec{A}(\vec{r},t) \quad$ 在动量空间 $\quad H' = -\frac{1}{c}\vec{J}(\vec{q}) \cdot \vec{A}(\vec{q})$

则在H'作用下，每单位时间 |s> → |s'>跃迁几率

$$W_{s \to s'} = \frac{2\pi}{\hbar^2} |< s | H' | s' >|^2 \ \delta[\omega - (\omega_{s'} - \omega_s)]$$

$$= \frac{2\pi}{\hbar^2 c^2} < s' | \vec{J}(\vec{q}) | s > < s | \vec{J}^*(\vec{q}) | s' > | \vec{A}(\vec{q}) |^2 \ \delta[\omega - (\omega_{s'} - \omega_s)]$$

$$W = \sum_{s,s'} W_{s \to s'} = \frac{2\pi}{\hbar^2 c^2} \sum_{s,s'} < s' | \vec{J}(\vec{q}) | s > < s | \vec{J}^*(\vec{q}) | s' > | \vec{A}(\vec{q}) |^2 \ \delta[\omega - (\omega_{s'} - \omega_s)]$$

利用 $\quad \delta(\omega) = \frac{1}{2\pi} \int \exp(-i\omega t) dt$

$$W = \frac{1}{\hbar^2 c^2} \sum_{s,s'} \int dt \exp(-i\omega t) < s' | \vec{J}(\vec{q}) | s > < s | \exp(-i\omega_s t) \vec{J}^*(\vec{q}) \exp(-i\omega_s t) | s' > | \vec{A}(\vec{q}) |^2$$

在Schrodinger表象，J(q)和J*(q)是不含时的，

变到Heisenberg表象，
$$\vec{J}(\vec{q}, t) = e^{iH_0 t/\hbar} \vec{J}(\vec{q}) e^{-iH_0 t/\hbar}$$

$$\vec{J}^*(\vec{q}, t) = e^{-iH_0 t/\hbar} \vec{J}^*(\vec{q}) e^{iH_0 t/\hbar}$$

另 $\quad \sum_{s'} | s' > < s' | = 1$

吸收功率＝每单位时间、单位体积吸收光子能量

利用

$$\boxed{\vec{E} = i\omega\vec{A}/c}$$

$$P = \hbar\omega W = |\vec{A}(\vec{q})|^2 \frac{\omega}{\hbar c^2} \sum_s \int dt < s \,|\, \vec{J}(\vec{q},0)\vec{J}^*(\vec{q},t) \,|\, s > \exp(-i\omega t)$$

$$= |\vec{E}(\vec{q})|^2 \frac{1}{\hbar\omega} \sum_s \int dt < s \,|\, \vec{J}(\vec{q},0)\vec{J}^*(\vec{q},t) \,|\, s > \exp(-i\omega t)$$

$$\Longrightarrow \quad \boxed{\sigma(\mathbf{q},\omega) = \frac{1}{\hbar\omega} \sum_s \int dt \left\langle s \,|\, \mathbf{J}(\mathbf{q},0)\mathbf{J}^*(\mathbf{q},t) \,|\, s \right\rangle \exp\{-i\omega t\}}$$

The **Kubo** formula for the **q** and ω depenent conductivity

现假定（i） a constant correlation time τ for all states

$$\vec{J}(\vec{q},t) = \vec{J}(\vec{q},0)\exp(-t/\tau)$$

$$\vec{J}(\vec{r}) = \frac{e}{2m}\sum_{i=1}^{N}[\vec{p}_i\delta(\vec{r}-\vec{r}_i) + \delta(\vec{r}-\vec{r}_i)\vec{p}_i]$$

并利用 $\quad \vec{J}(\vec{q}) = \int \vec{J}(\vec{r})\exp(-i\vec{q}\cdot\vec{r})d\vec{r} = -\frac{e}{m}\sum_j \vec{p}_j$

（ii） only zero wavevector is considered (local limit)，$\exp(i\vec{q}\cdot\vec{r}) \approx 1$

$$\Longrightarrow \quad \sigma(\omega) = \frac{e^2}{m^2\hbar\omega}\int dt \exp\{-i\omega t - |t|\tau\}\sum_{s,s',j}|\langle s'|\mathbf{P_j}|s\rangle|^2$$

引入 $\quad 2\sum_{s,s',j}\dfrac{|\langle s'|\mathbf{P_j}|s\rangle|^2}{m\hbar\omega_{s's}} = f_{s's}$ $\qquad$ the osillator strength

$$\sigma(\omega) = \frac{e^2\tau}{m}\frac{f_{s's}}{1-i\omega\tau} \xrightarrow{\;f_{s's}=N\;} \sigma(\omega) = \frac{Ne^2\tau}{m}\frac{1}{1-i\omega\tau}$$

Simple metal
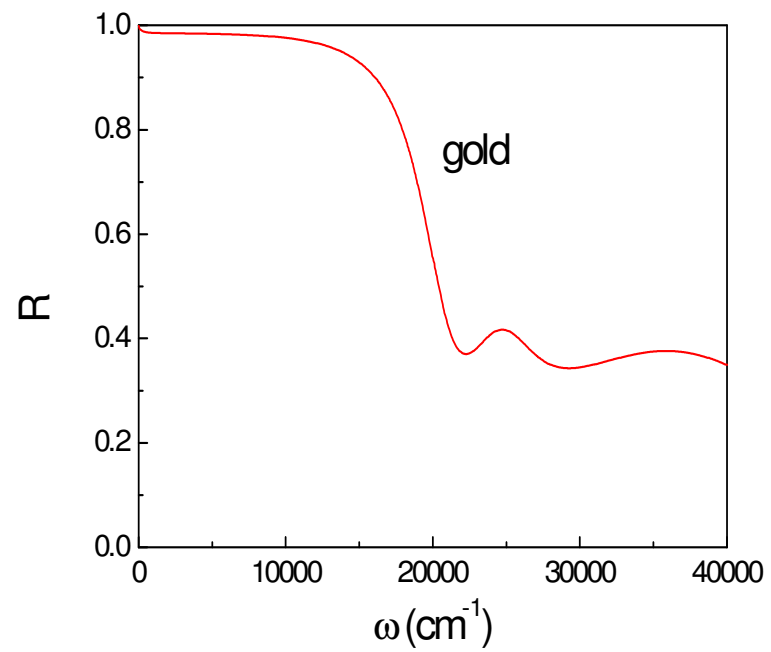
High-T$_c$ cuprates
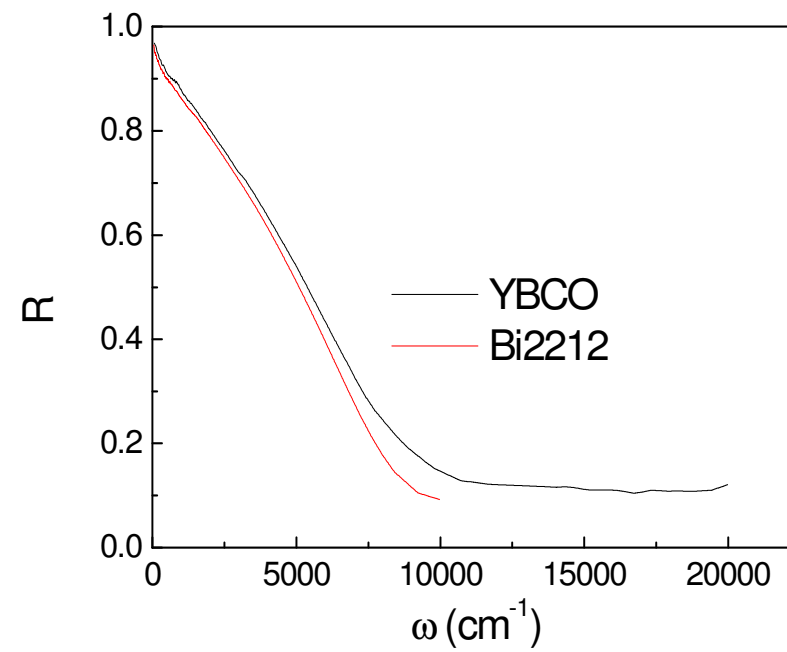
Non-Drude spectra of strongly correlated electrons

General feature: a sharp peak at $\omega=0$

+ a long tail extending to high energies

For example: cuprates

Two possible interpretations
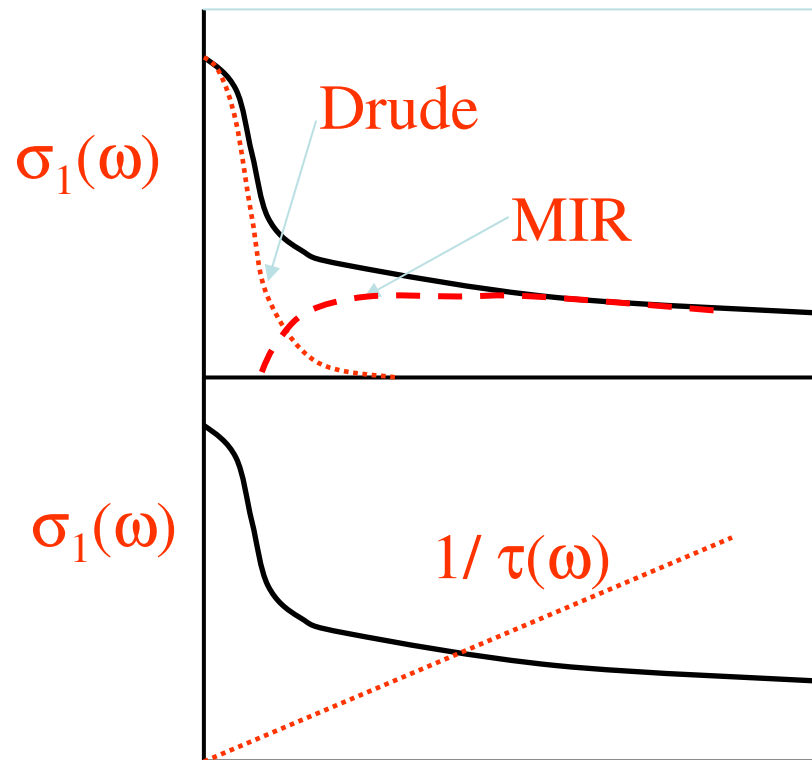
（1） **Drude Model** $\sigma(\omega) = \dfrac{\omega_p^2}{4\pi} \dfrac{1}{1/\tau - i\omega}$

Extended Drude Model

Let $M(\omega,T) = 1/\tau(\omega,T) - i\omega\lambda(\omega,T)$

$1/\tau(\omega,T)$: Frequency dependent scattering rate

λ: Mass enhancement $m^* = m(1+\lambda)$

$$\sigma(\omega,T) = \frac{\omega_p^2}{4\pi} \frac{1}{M(\omega,T) - i\omega}$$

$$= \frac{\omega_p^2}{4\pi} \frac{1}{1/\tau(\omega,T) - i\omega[1 + \lambda(\omega,T)]}$$

$$= \frac{1}{4\pi} \frac{\omega_p^{*2}}{1/\tau^*(\omega,T) - i\omega}$$

$\Longrightarrow$

$1/\tau(\omega,T) = (\omega_p^2/4\pi)\mathrm{Re}(1/\sigma(\omega))$

$1+\lambda(\omega) = (\omega_p^2/4\pi\omega)\mathrm{Im}(1/\sigma(\omega))$

e.g. Marginal Fermi Liquid model:

$$M(\omega,T) = 1/\tau(\omega,T) - i\omega\lambda(\omega,T)$$

$$= g^2 N^2(0)\left(\frac{\pi}{2}x + i\omega\ln\frac{x}{\omega_c} \right)$$

Where x=max(|ω|,T),

or x=(ω²+α(πT)²)^{1/2}

Extended Drude Model

$$\sigma(\omega, T) = \frac{\omega_p^2}{4\pi} \frac{1}{(\gamma(\omega, T) - i\omega)}$$

According to Little and Varma,

$$\gamma(\omega) = -2i\Sigma^{op}$$

$$= -2i[\Sigma_1(\omega) + i\Sigma_2(\omega)]$$

称为光学自能

与上面$1/\tau(\omega)$和m*/m之间的联系

$$\gamma_1(\omega) = 1/\tau(\omega) = 2\Sigma_2$$

$$\gamma_2(\omega) = \omega(1 - m^*/m) = -2\Sigma_1$$
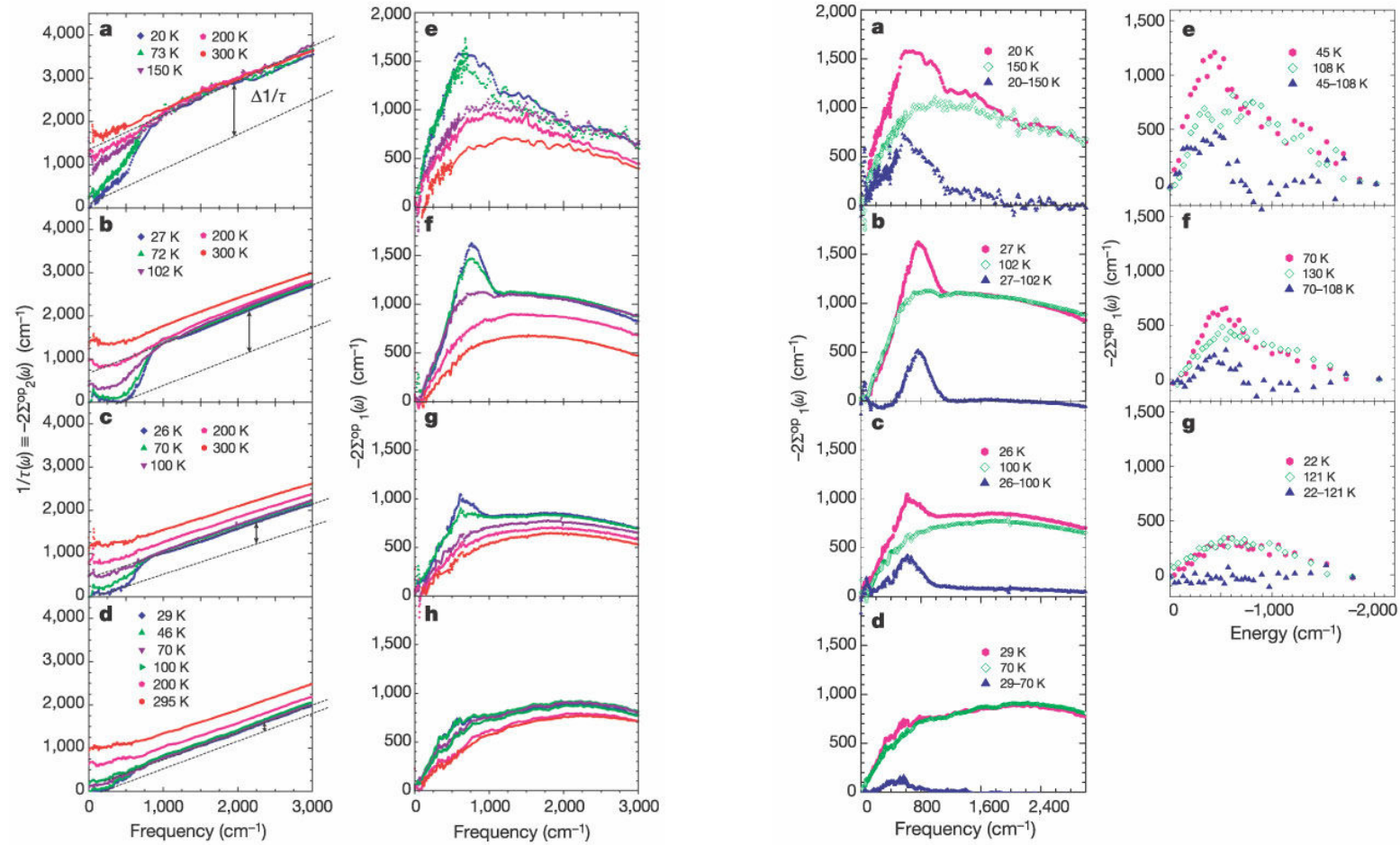
Hwang, Timusk, Gu,
Nature 427, 714 (2004)

(2) Two component picture

Drude component   +   mid-IR component

Sharp peak at $\omega = 0$ Long tail at high energies

Free carriers weakly coupled
with boson excitations

Bound carriers strongly
coupled with phonons, etc.
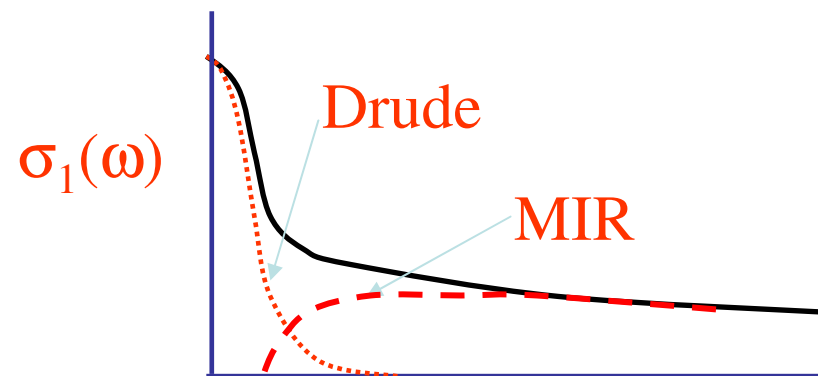
Optical spectra of a superconductor

T=0, London electrodynamics gives

$$\sigma = \frac{1}{8}\omega_{ps}^2 \delta(\omega) + i\omega_{ps}^2/4\pi\omega \;\Rightarrow\; \frac{1}{\lambda_L^2} = \frac{8}{c^2}\int_0^\infty (\sigma_1^n - \sigma_1^s)d\omega \quad \text{or} \quad \frac{1}{\lambda_L^2} = \frac{4\pi}{c^2}\omega\sigma_2(\omega)$$

dirty limit: $\xi > l \;\Longleftrightarrow\; 2\Delta < \Gamma$

Absorption starts at **2Δ**.

clean limit: $\xi < l \;\Longleftrightarrow\; 2\Delta > \Gamma$

Absorption starts at **2Δ+Ω**.

$\sigma_1(\omega)$

ω

1
R

ω

2Δ
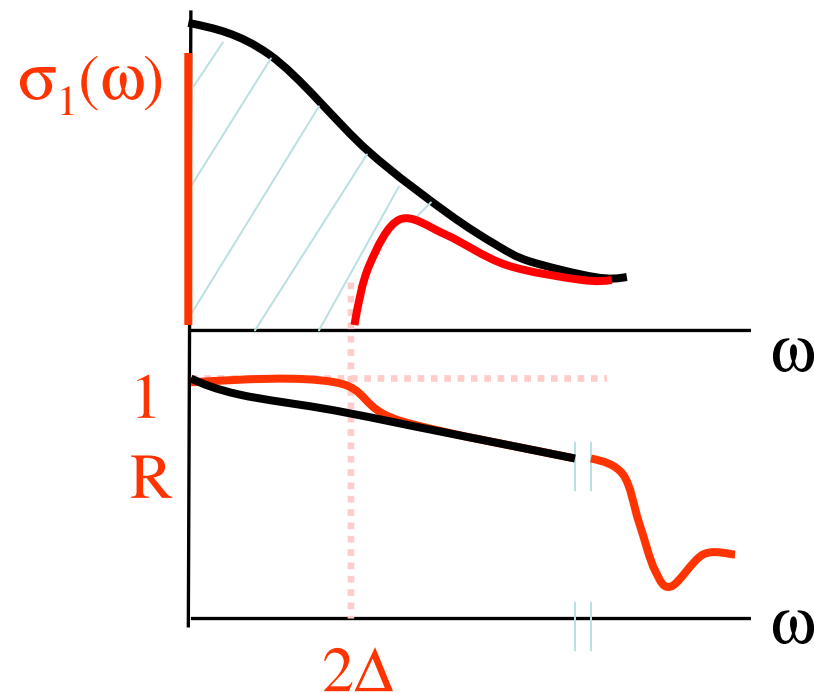
$\because$ pippard coherence length $\xi = v_F/\pi\Delta$, $\Gamma = 1/\tau = v_F/l$

Optical study of CuIr2S4 and MgTi2O4: support for orbital-Peierls transitions

- Metal-insulator transitions in CuIr2S4 and MgTi2O4
- Orbital Peierls transition scenario by Khomskii
- Optical data---evidence for orbital Peierls transitions

For 1D system, Fermi surface instability often drives a system into a symmetry-breaking insulating state. Such instability is not expected to develop in a 3D system.

Peierls (Metal-insulator) transition may occur in some dimension-reduction systems

CuIr2S4

CuIr2S4

CuIr2Se4
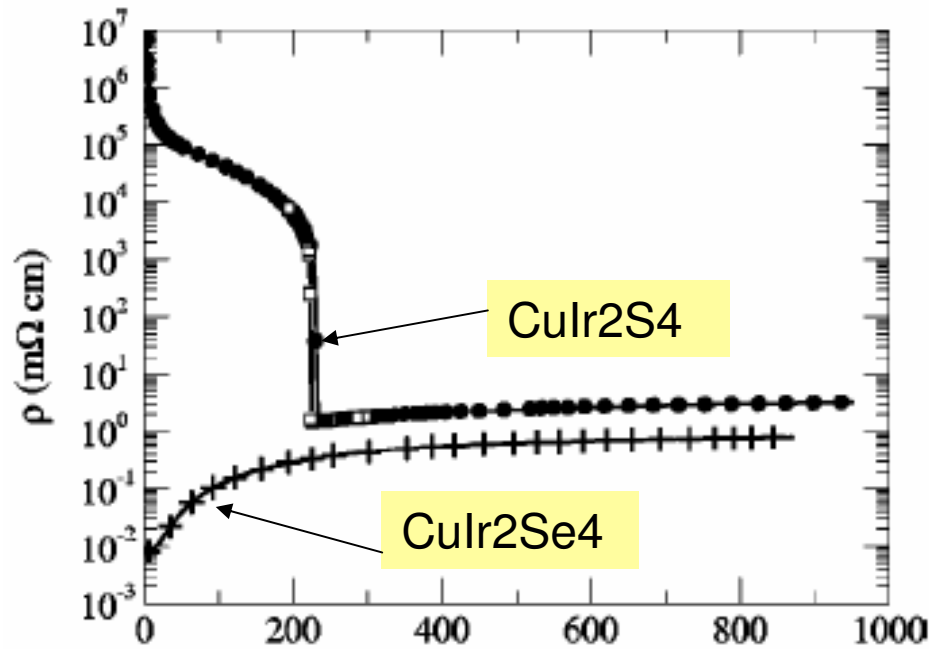
Metal-Insulator
transition at ~230K

Discovered in 1994 by S.
Nagata et al.

A: $x=0.0$
B: $x=0.1$
C: $x=0.2$
D: $x=0.225$
E: $x=0.25$
F: $x=0.3$
G: $x=0.4$
H: $x=0.5$
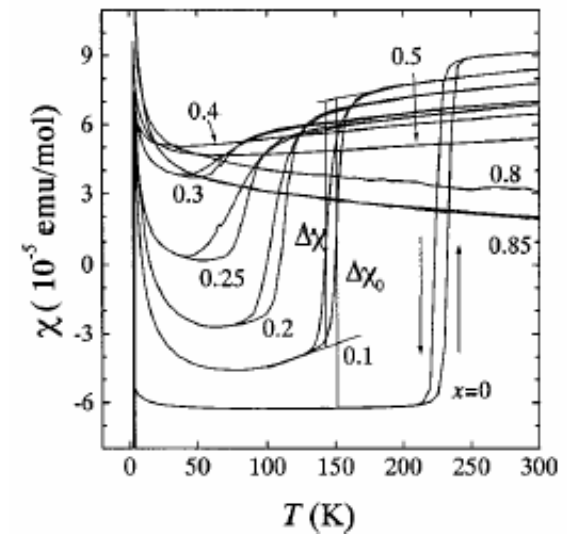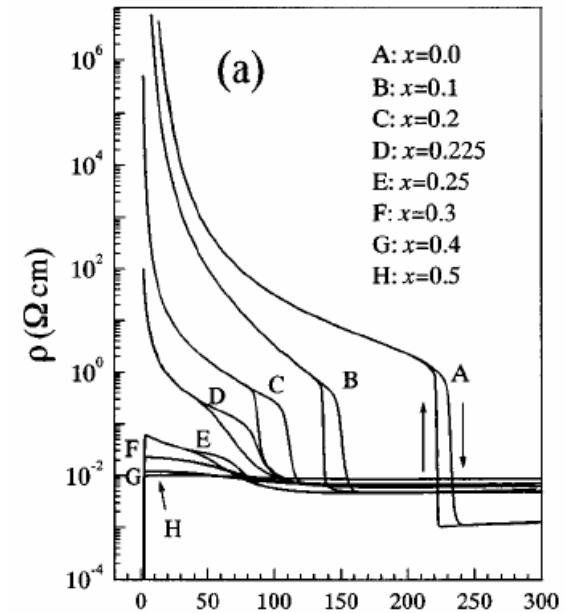
Zn substitution,

G. H. Cao, et al. PRB 64, 214514 (2001)

Structure feature

$A_{tet}[B_2]_{oct}S_4$
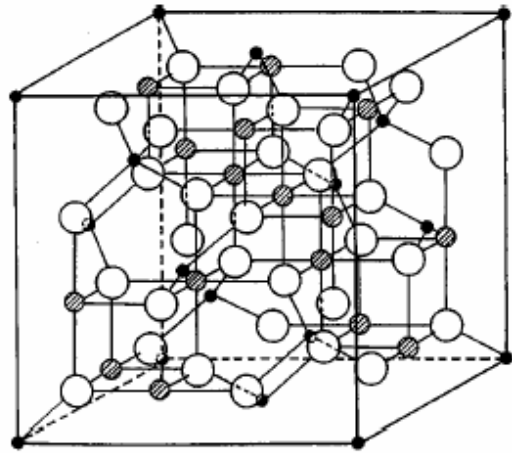
cubic

A site
tetrahedra

B site
octahedra

A site cation has fully filled orbital (e.g. Cu^{1+}, Mg^{2+});

the physical properties are determined by the B site cations.
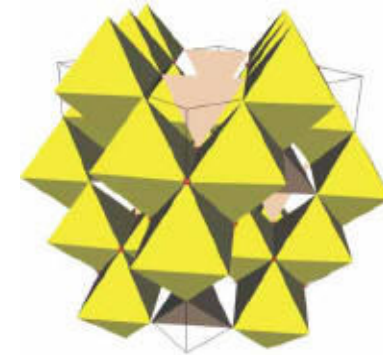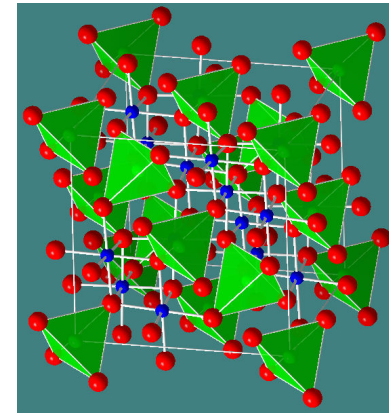
B-site only, pyrochlore lattice
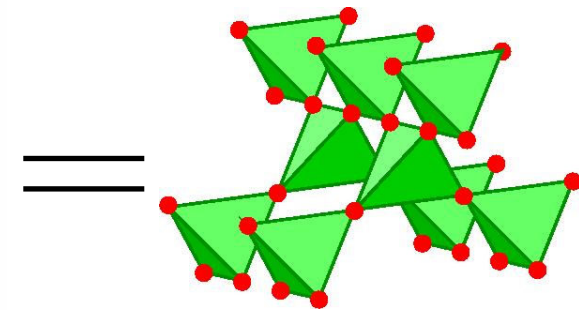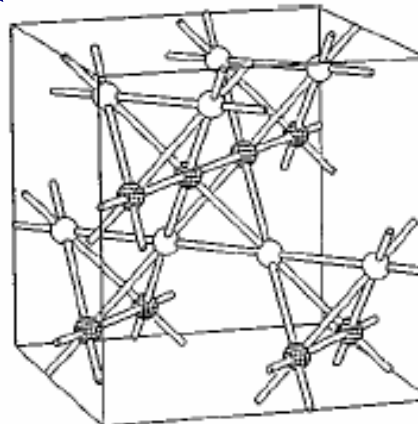
6 chains by three orbitals

Formation of isomorphic Ir 3+ and Ir 4+ octamers and spin dimerization in CuIr2S4

P G Radaelli, et al.,
NATURE 416, 155 (2002)

Low-T structure

$Cu^{+I}Ir^{3+}Ir^{4+}S_4^{2-}$
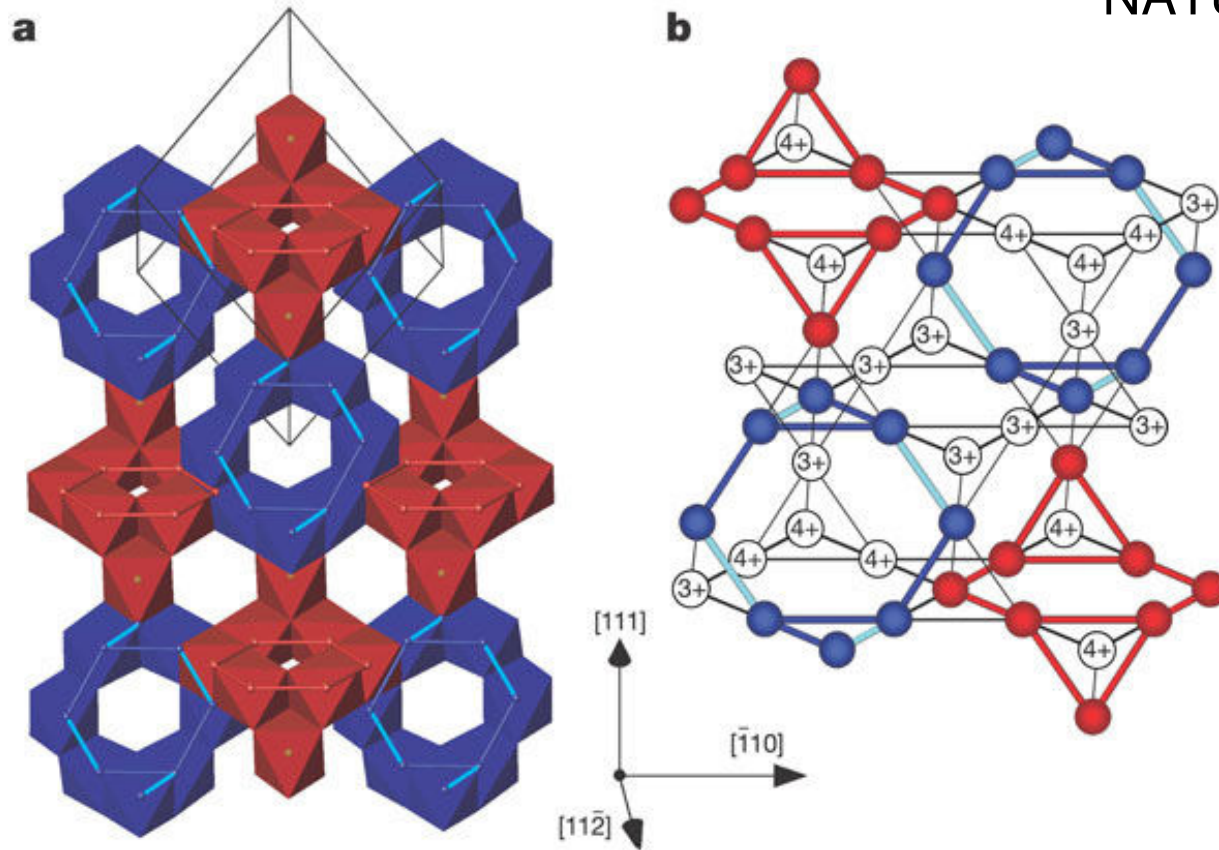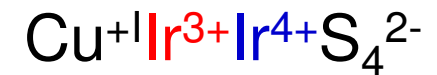
Ir: $5d^7 6s^2$

Ir3+ is nonmagnetic ($t_{2g}^6 e_g^0$, s=0)

Ir4+ has a local moment ($t_{2g}^5 e_g^0$, s=1/2)   (for low spin state)

Observation of Phase Transition from Metal to Spin-Singlet Insulator in MgTi$_2$O$_4$ with $S = 1/2$ Pyrochlore Lattice

Masahiko ISOBE and Yutaka UEDA[*]

JPSJ 2002
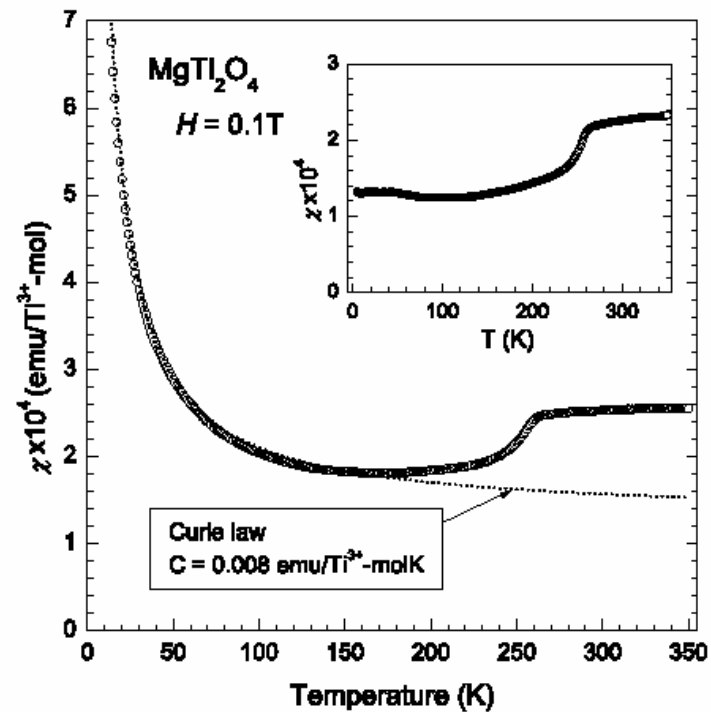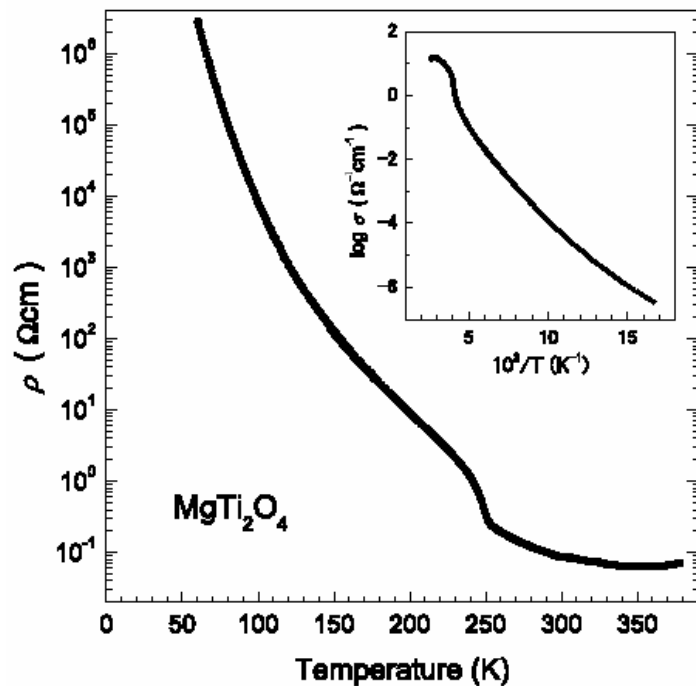
Spin Singlet Formation in $MgTi_2O_4$: Evidence of a Helical Dimerization Pattern

M. Schmidt,[1,2] W. Ratcliff II,[3] P. G. Radaelli,[1,4] K. Refson,[1] N. M. Harrison,[5,6] and S. W. Cheong[3]

Low-T structure

Ti: $3d^2 4s^2$

Ti^{3+}, $3d^1$, s=1/2

(dimerized)

The red: the shortest bond

The purple: the longest bond

The blue: the intermediate bond
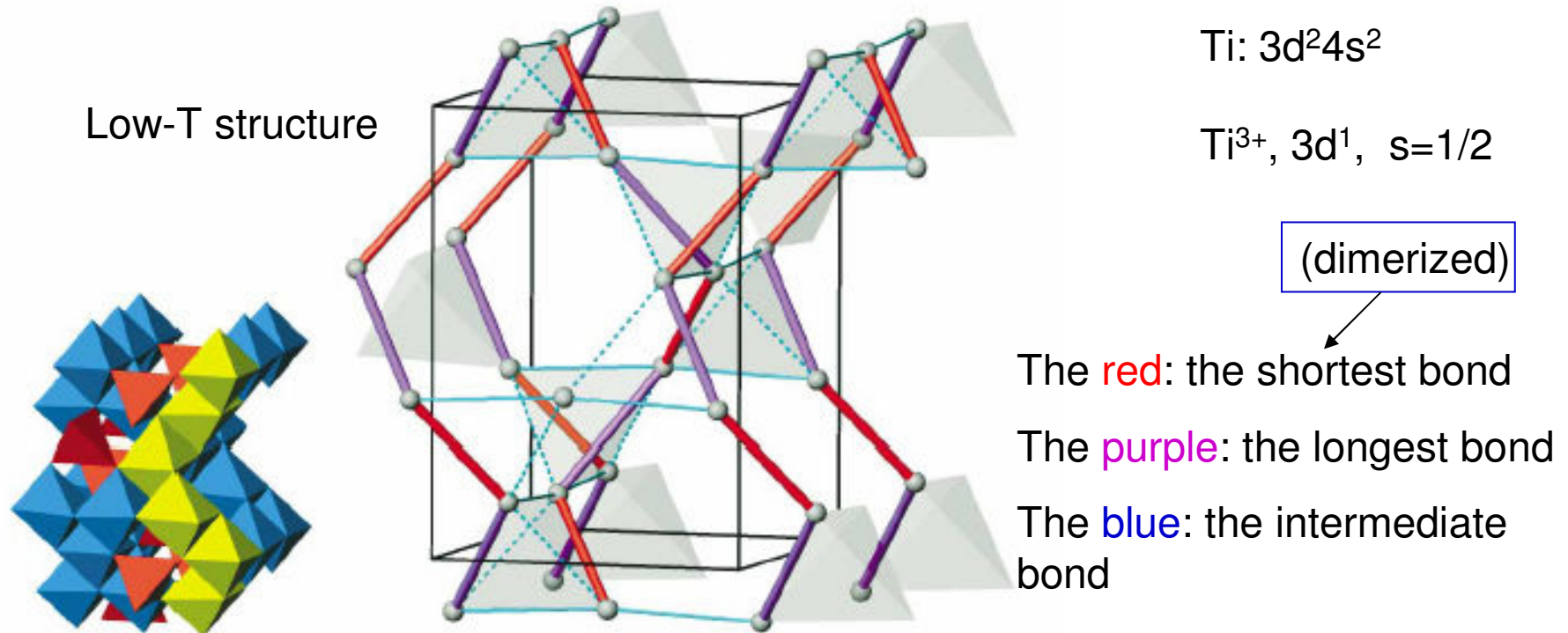
d Orbitals

e$_g$
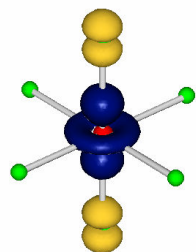
$3z^2$-r^2
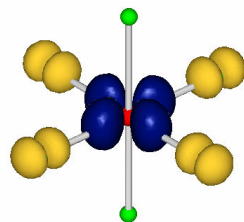
x^2-y^2

t$_{2g}$

xy

yz

zx

八面体沿c方向

伸长   压缩

e$_g$

d orbitals

t$_{2g}$

xy   yz,zx

yz,zx   xy

五重简并   正八面体晶场
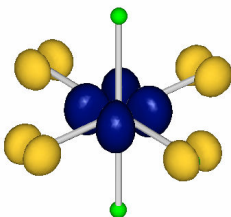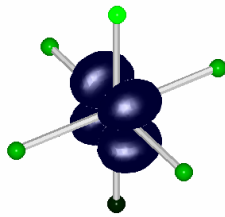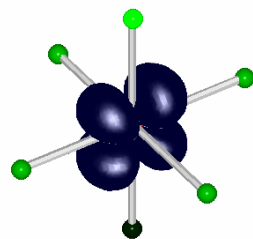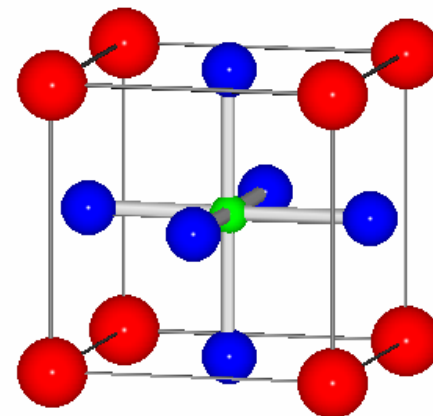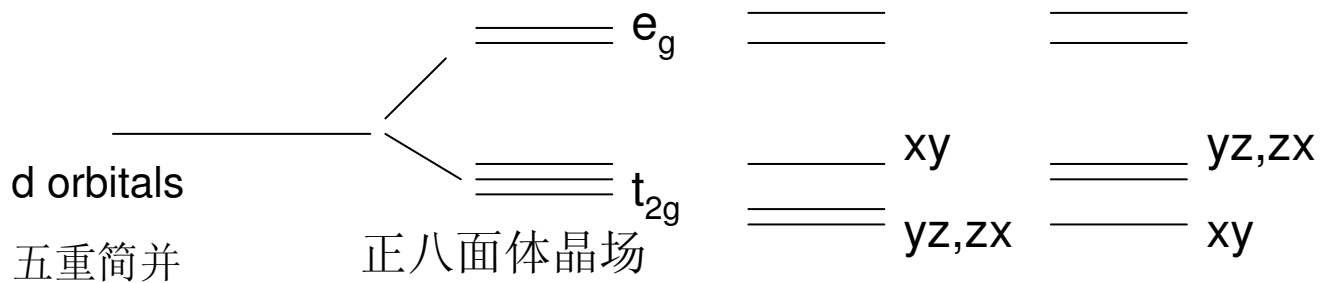
Below T$_{MIT}$

Orbitally Induced Peierls State in Spinels

D. I. Khomskii[1,2] and T. Mizokawa[3]

Ir3+: t$_{2g}^{6}$e$_{g}^{0}$, s=0
Ir4+: t$_{2g}^{5}$e$_{g}^{0}$, s=1/2
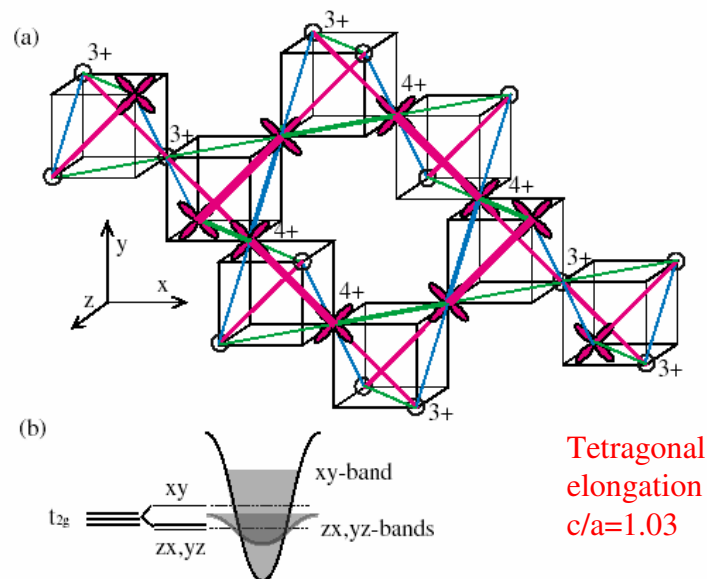
Ti^{3+}: 3d^{1}, s=1/2

Tetragonal
elongation
c/a=1.03

Tetragonal
compression

FIG. 2 (color).   (a) Charge and orbital ordering in CuIr$_2$S$_4$.
Octamer is shown by thick lines. Short singlet bonds are in-
dicated by double lines. (b) Schematic electronic structure of
CuIr$_2$S$_4$.
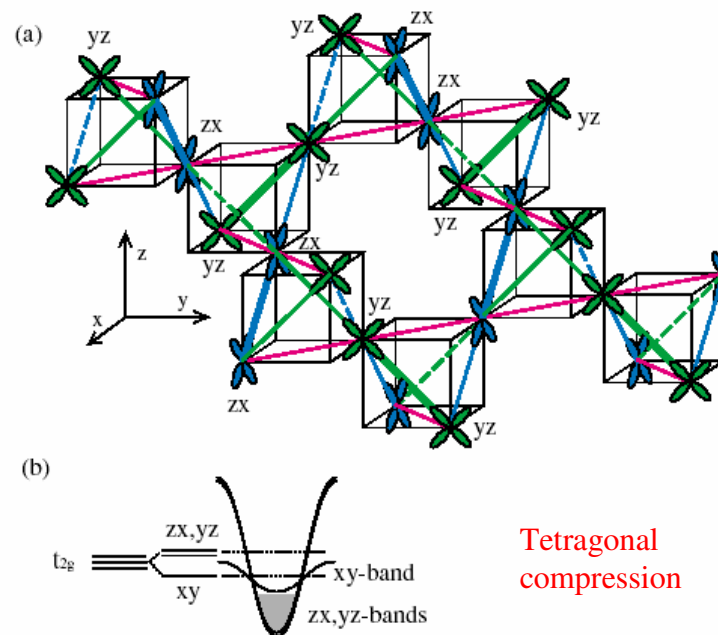
FIG. 3 (color).   (a) Orbital ordering in MgTi$_2$O$_4$. Short singlet
bonds are shown by double, intermediate–single, and long–
dashed lines. yz orbitals are shown in green and zx orbitals in
blue. (b) Schematic electronic structure of MgTi$_2$O$_4$. Note
different orientation of coordinate axes as compared with
Figs. 1 and 2.

tetramerization

Electrons arranged in chains formed by respective orbitals!!

Room temperature spectra
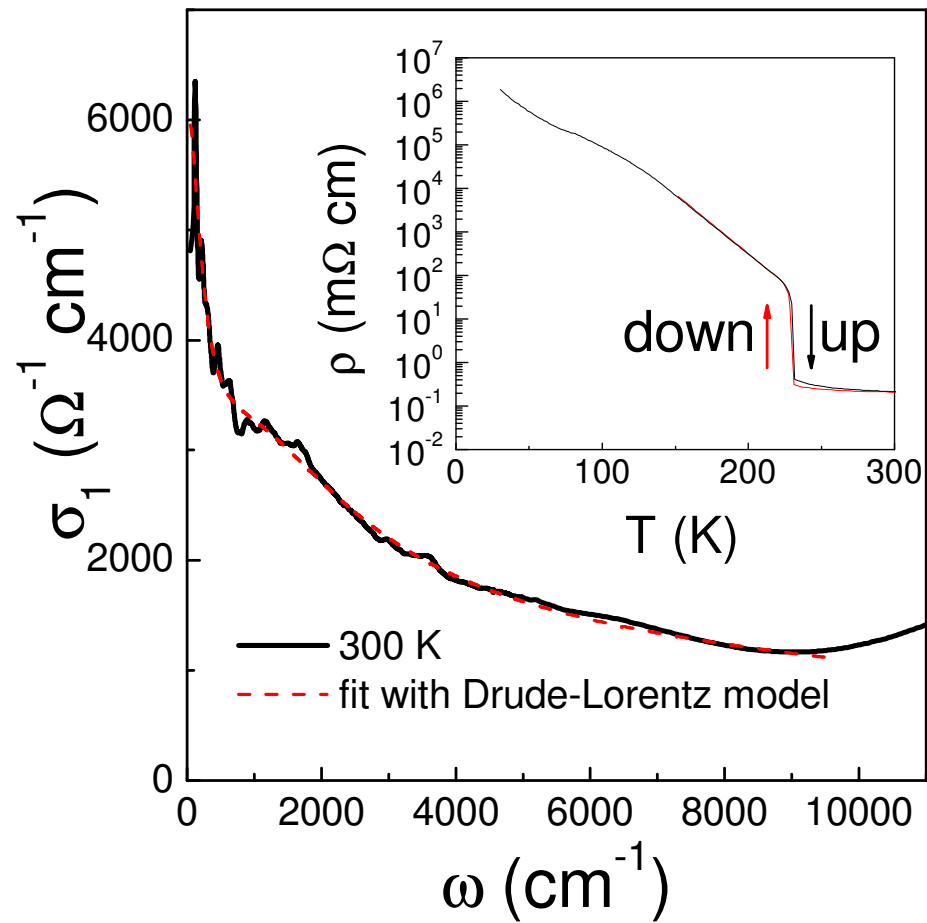
CuIr2S4

◆ Drude like response at low frequency

Temperature-dependent spectra
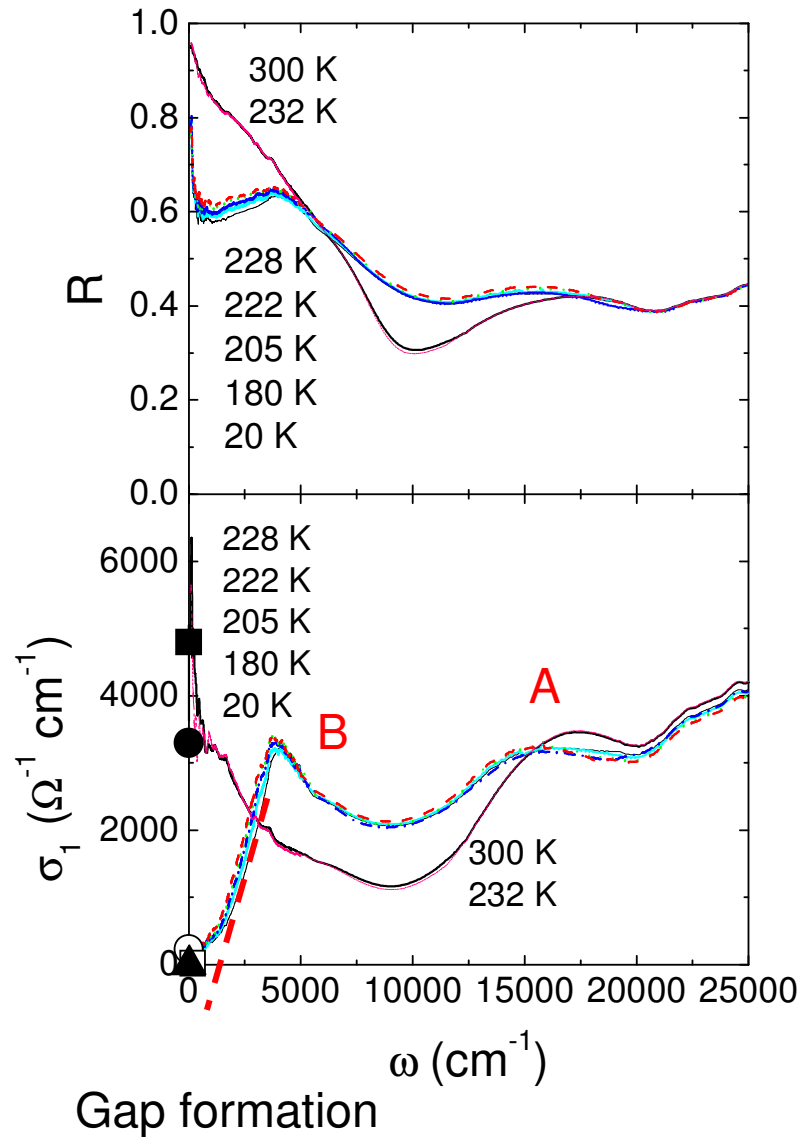
B: new peak emerged only below T_{MI};

A is present also at high temperatures.

N. L. Wang et al PRB (2004)
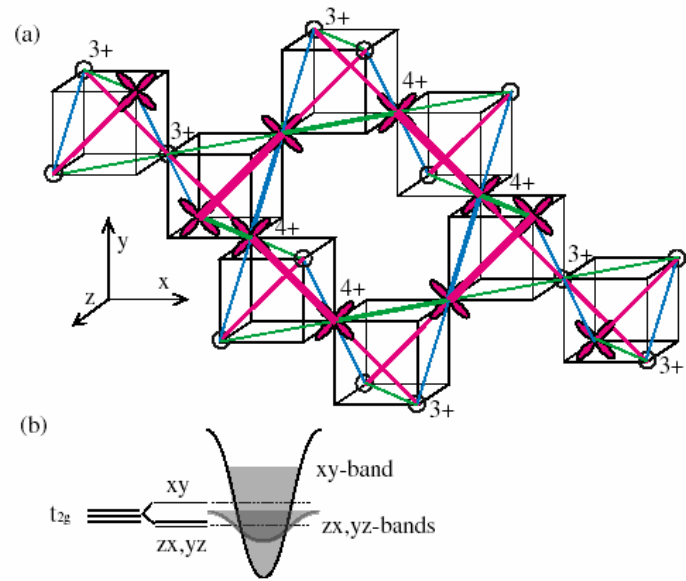
FIG. 2 (color). (a) Charge and orbital ordering in $CuIr_2S_4$. Octamer is shown by thick lines. Short singlet bonds are indicated by double lines. (b) Schematic electronic structure of $CuIr_2S_4$.

yz, zx bands fully occupied

xy orbital band splitted
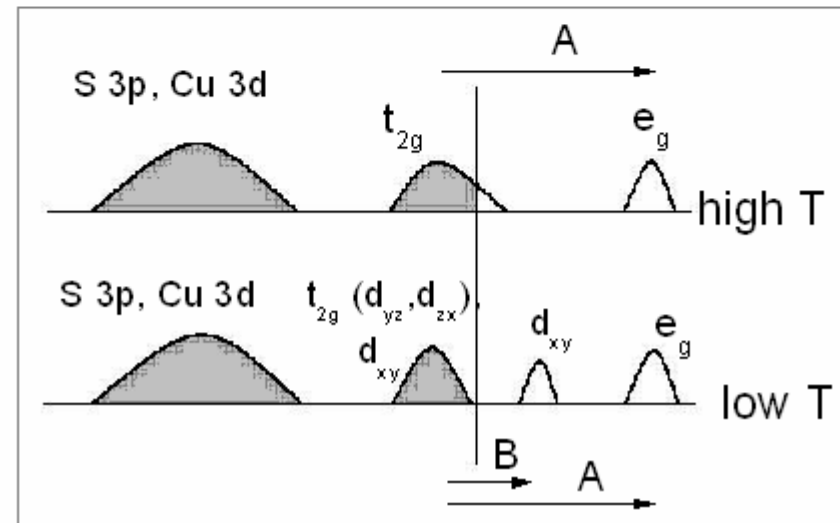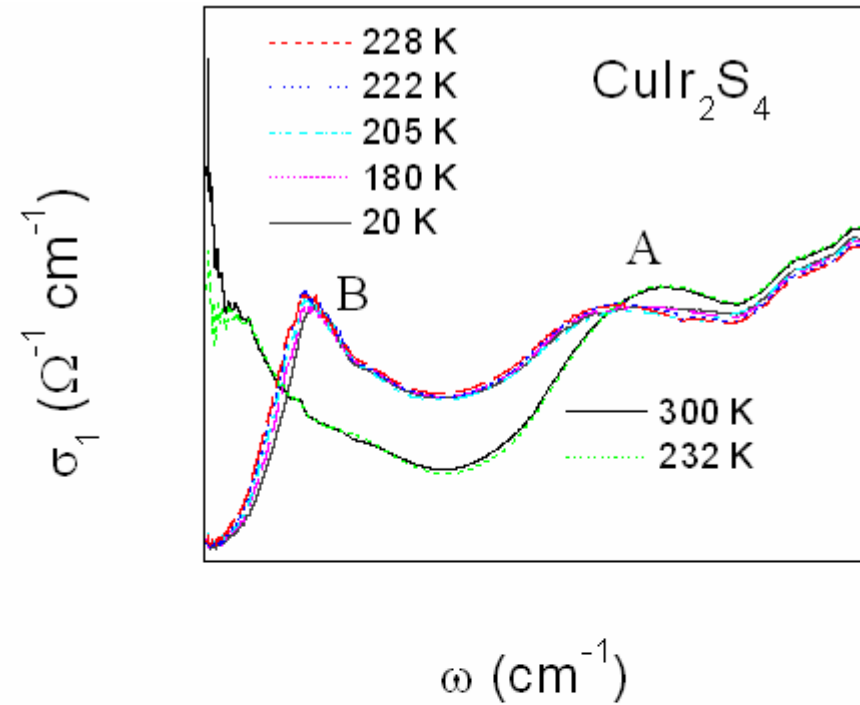
MgTi2O4
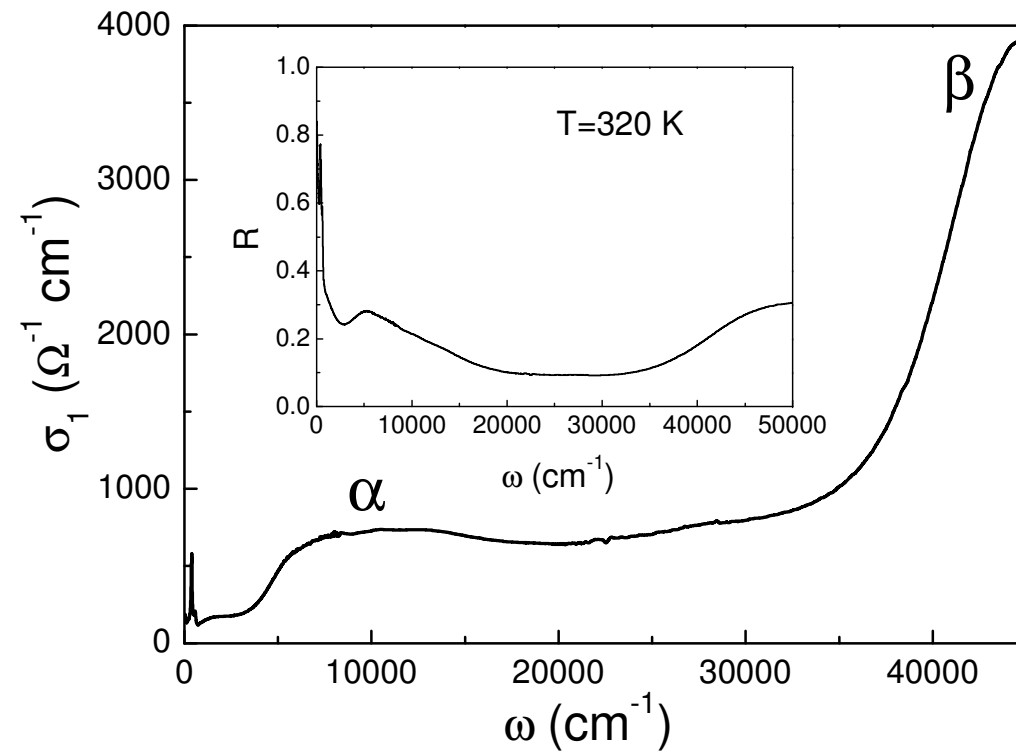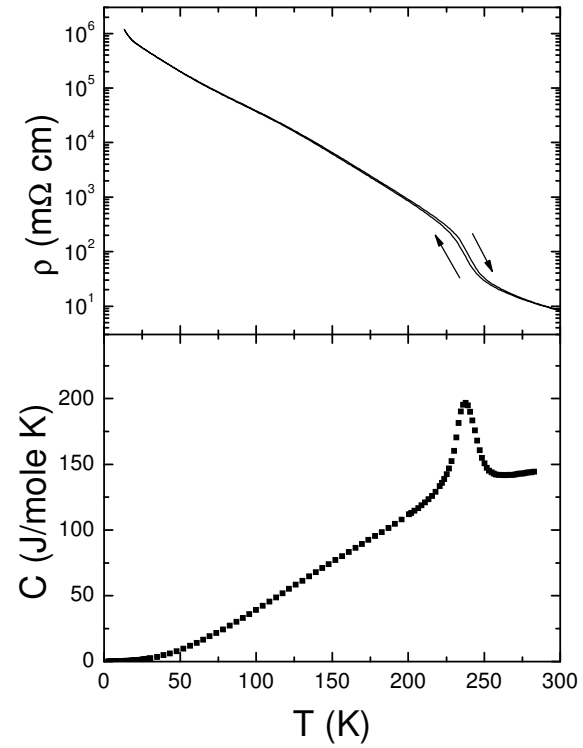
Four directions: [0,1,1], [0,1,-1], [1,0,1], and [1,0,-1]
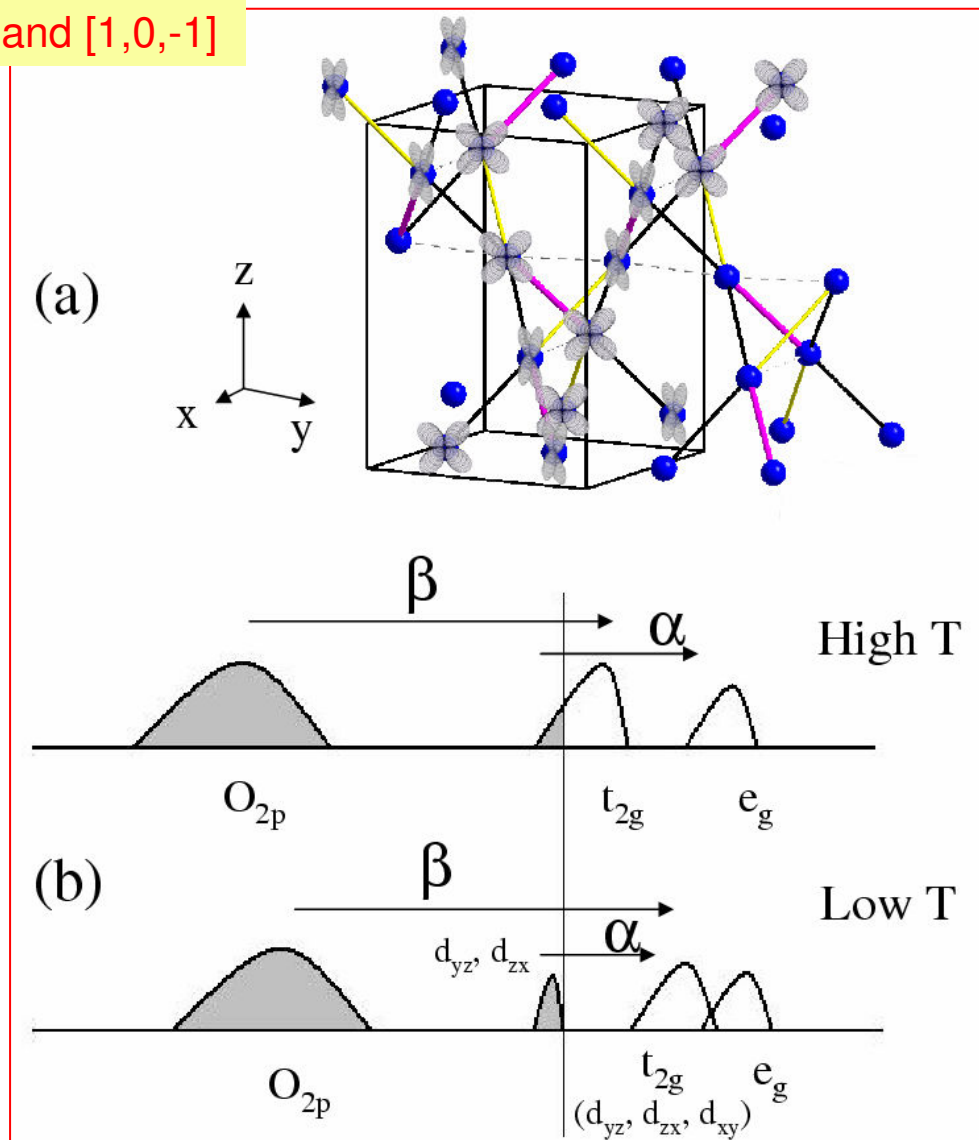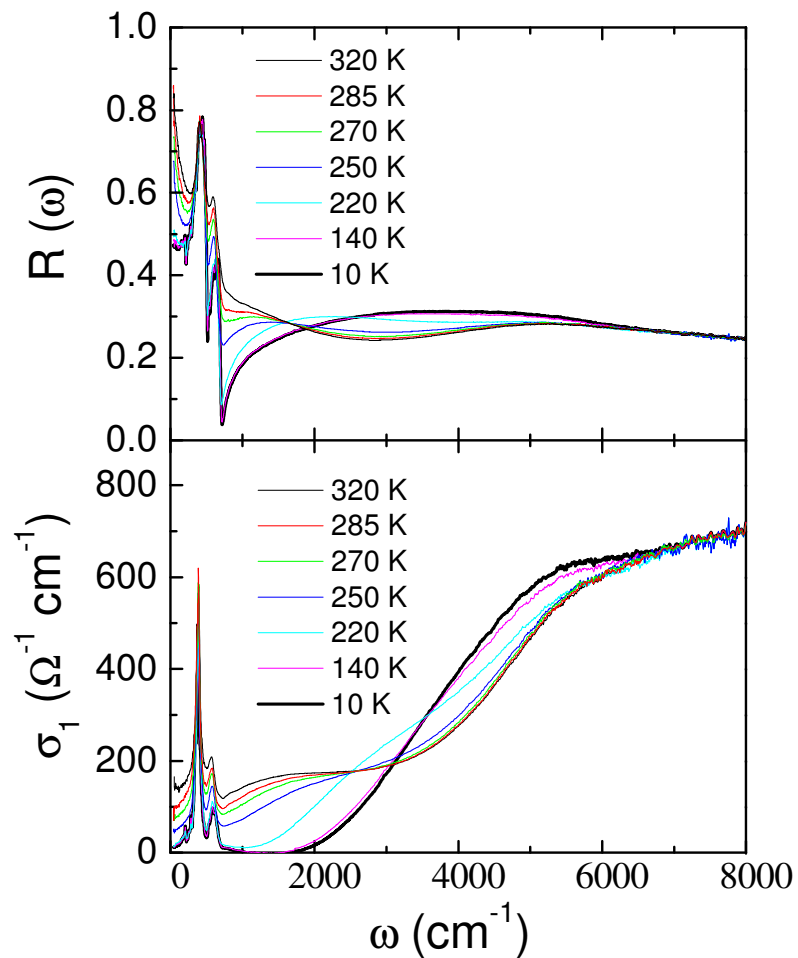
xy orbital (band) empty,

J. Zhou et al, PRB 2006

yz, zx orbitals (bands) quarterly filled, and splitted at low T

TRANSITION METAL OXIDES

Travels in one dimension

The discovery that electrons in $Tl_2Ru_2O_7$ lose their three-dimensional nature at low temperatures and arrange in chains, opens up a new direction in research into transition metal oxides.

JEROEN VAN DEN BRINK

is at the Instituut-Lorentz for Theoretical Physics, Leiden University, 2300 RA Leiden, The Netherlands.

e-mail: brink@lorentz.leidenuniv.nl

The world of transition metal oxides is full of surprises and intriguing effects, ranging from large changes of resistance in the presence of a magnetic field (the colossal magnetoresistance), to high-temperature superconductivity. In this issue, Seongsu Lee and co-workers uncover yet another revelation[1]. A detailed investigation of the crystallographic, magnetic and electronic properties of the ruthenium oxide $Tl_2Ru_2O_7$ indicates that at temperatures below 120 K the electrons reorganize and effectively change their dimensionality — they go one-dimensional.

At elevated temperatures, $Tl_2Ru_2O_7$ seems to be an unassuming three-dimensional conductor, much like, for instance, iron. But there are startling changes in electronic and magnetic properties when $Tl_2Ru_2O_7$ is cooled down. Below the critical temperature, the electrical resistivity suddenly increases by two orders of magnitude: the metal freezes into an insulator. By combining neutron scattering experiments with
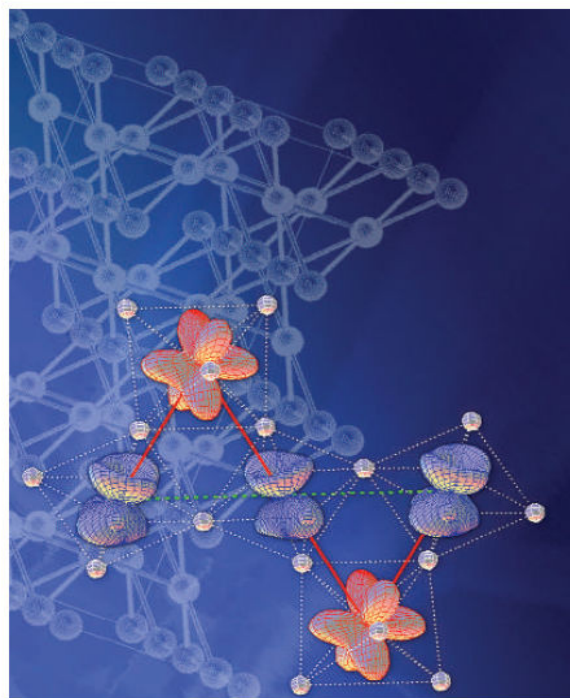
Figure 1 Orbital ordering in $Tl_2Ru_2O_7$. Driven by orbital degrees of freedom, electrons in the three-dimensional crystal (background) self-organize into one-dimensional chains (foreground).

SEONGSU LEE AND JE-GEUN PARK

Nature Materials (issue of June, 2006)

Spin gap in $Tl_2Ru_2O_7$ and the possible formation of Haldane chains in three-dimensional crystals

SEONGSU LEE[1], J.-G. PARK[1,2]*, D. T. ADROJA[3], D. KHOMSKII[4], S. STRELTSOV[5], K. A. McEWEN[6], H. SAKAI[7], K. YOSHIMURA[7], V. I. ANISIMOV[5], D. MORI[8], R. KANNO[8] AND R. IBBERSON[3]

$t_{2g}^3 \uparrow t_{2g}^1 \downarrow$
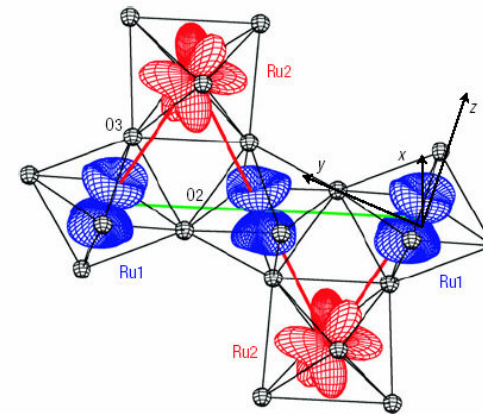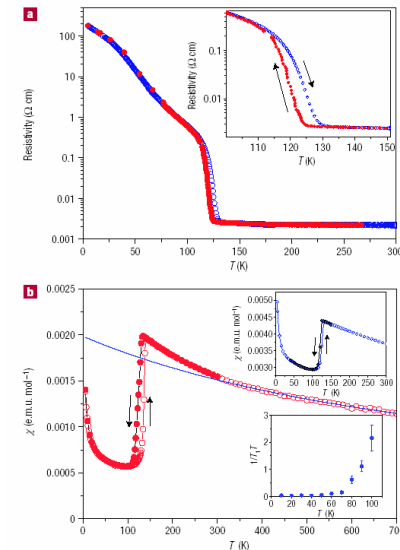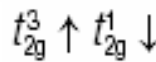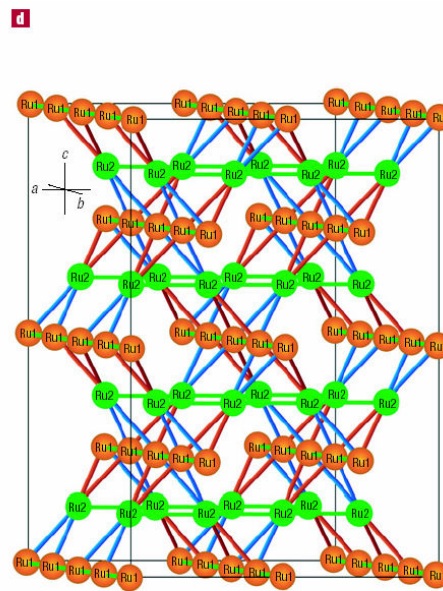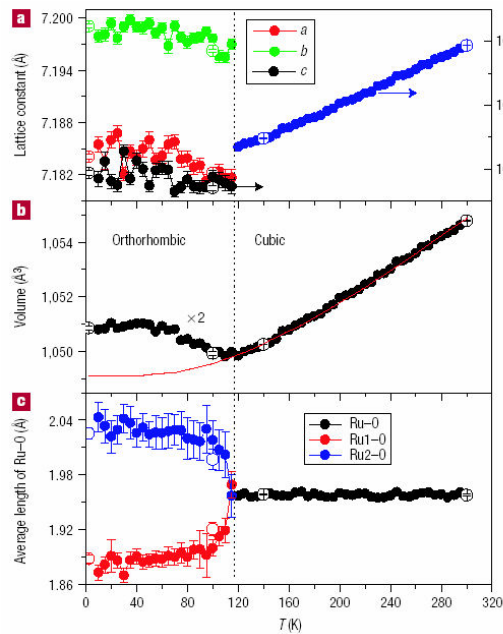
Neutron experiment: spin gap ~ 11 meV

Below T_{MI}, Ru1 and Ru2 ions exist

both Ru1 and Ru2 as low-spin Ru^{4+} with $S = 1$

Zig-zap 1D Haldane chain with s=1

Universality in one dimensional orbital wave ordering in spinel and related compounds: an experimental perspective

M. Croft, V. Kiryukhin, Y. Horibe, and S-W. Cheong

Rutgers Center for Emergent Materials and Department of Physics and Astronomy, Rutgers University, Piscataway, NJ 08854

Brookhaven National Laboratory, Upton, NY 11973
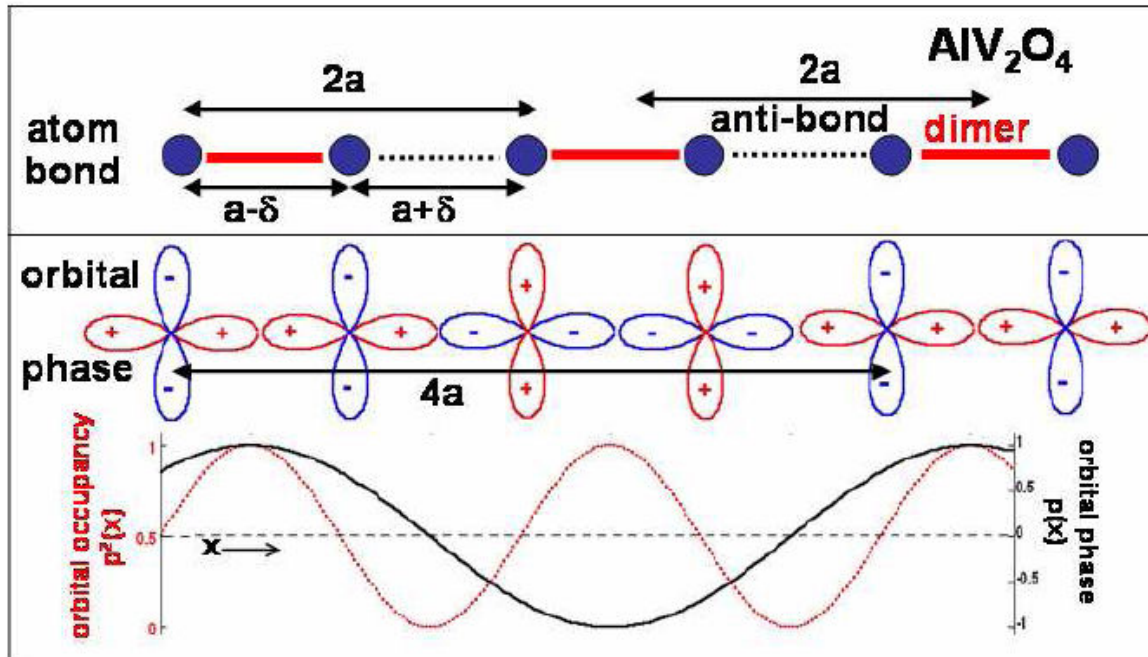
Verwey transition in Fe3O4
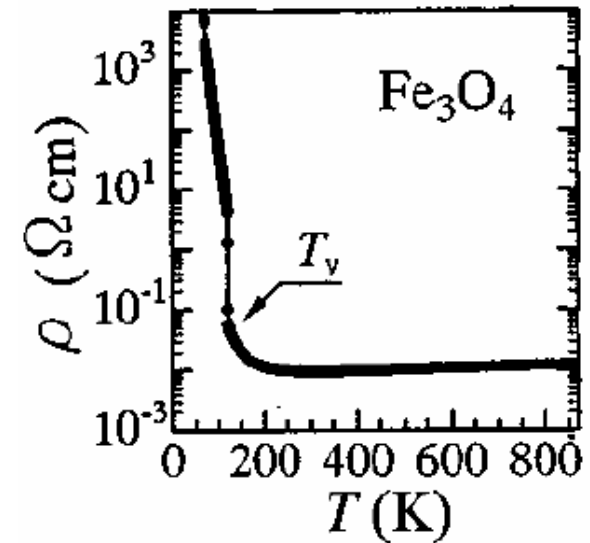
Metal-insulator Transition in a Pyrochlore-type Ruthenium oxide, $Hg_2Ru_2O_7$

Ayako Yamamoto[1, 2, *], Peter A. Sharma[1], Yoshihiko Okamoto[1, 2], Aiko Nakao[1],

Hiroko Aruga Katori[1, 2], Seiji Niitaka[1, 2], Daisuke Hashizume[1], and Hidenori Takagi[1, 2, 3]
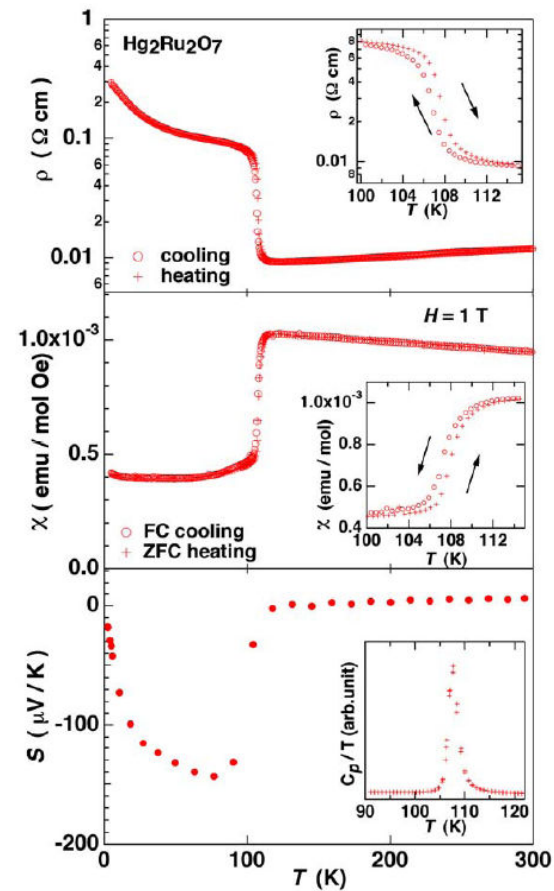
应用举例:高温超导体
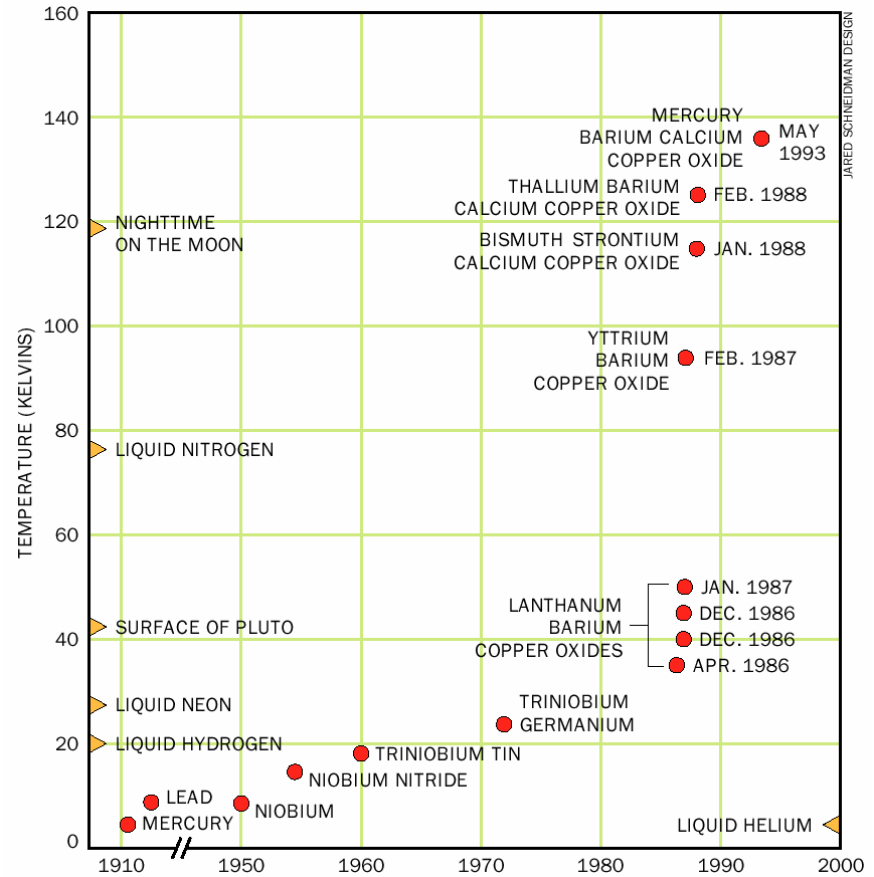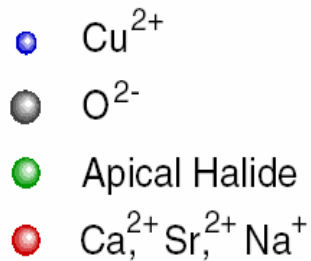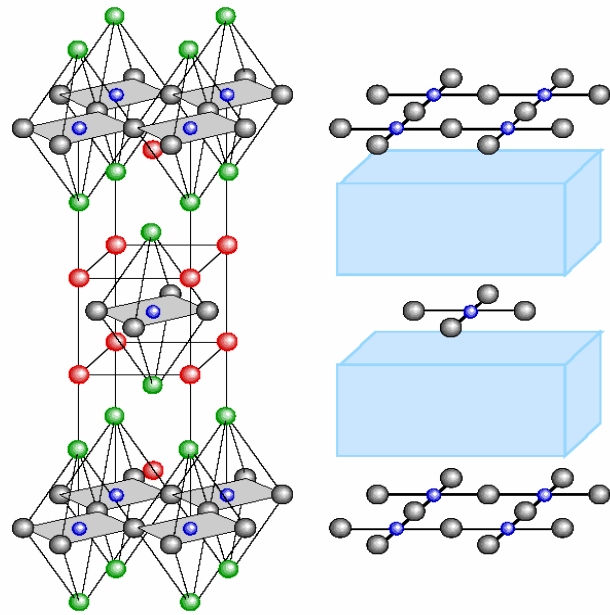
Structure of high-Tc cuprates

YBa$_2$Cu$_3$O$_{7-\delta}$

Bi$_2$Sr$_2$CuO$_{6+\delta}$
Bi2201, T$_{c,max}$=34 K

Bi$_2$Sr$_2$CaCu$_2$O$_{8+\delta}$
Bi2212, T$_{c,max}$=95 K

Bi$_2$Sr$_2$Ca$_2$Cu$_3$O$_{10+\delta}$
Bi2223, T$_{c,max}$=110 K

Superconductivity

Real space

Reciprocal space

CuO$_2$ plane

a

O

Cu

$2\pi/a$

magnetic structure

Parent compound

$(\pi/a, \pi/a)$

$\sqrt{2}\pi/a$
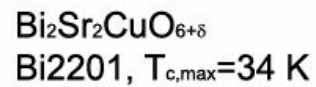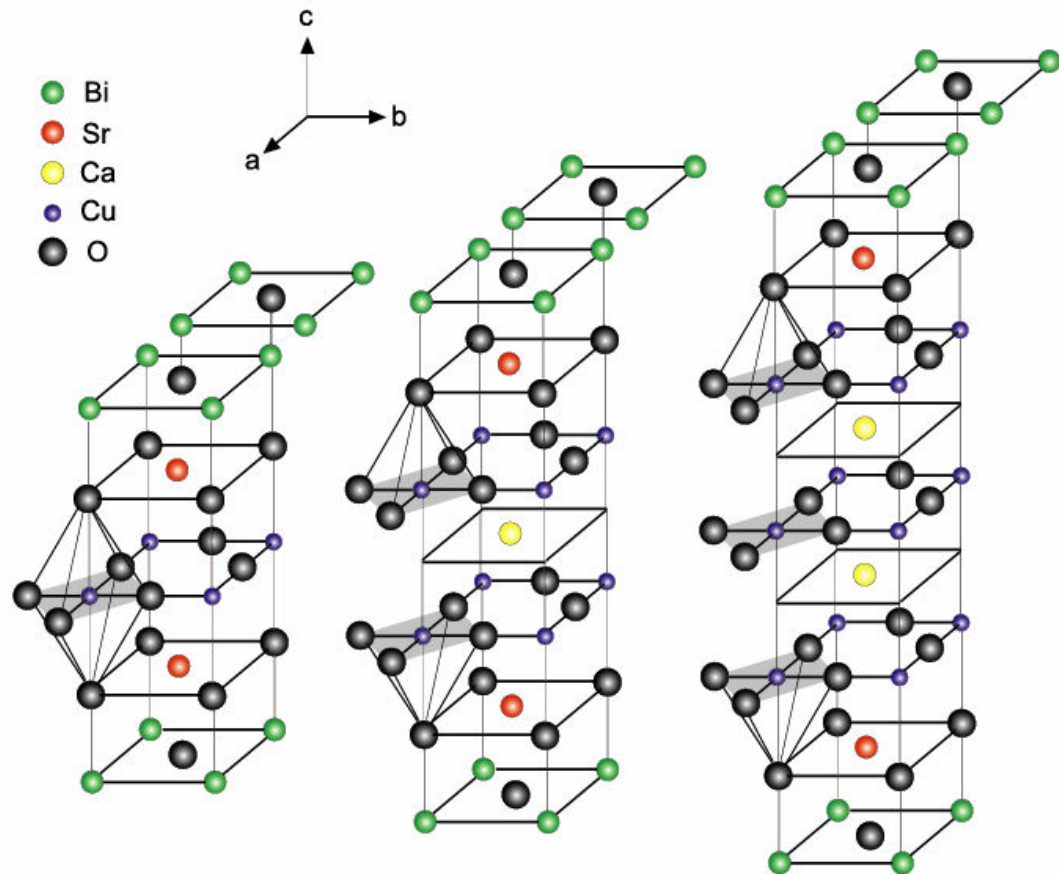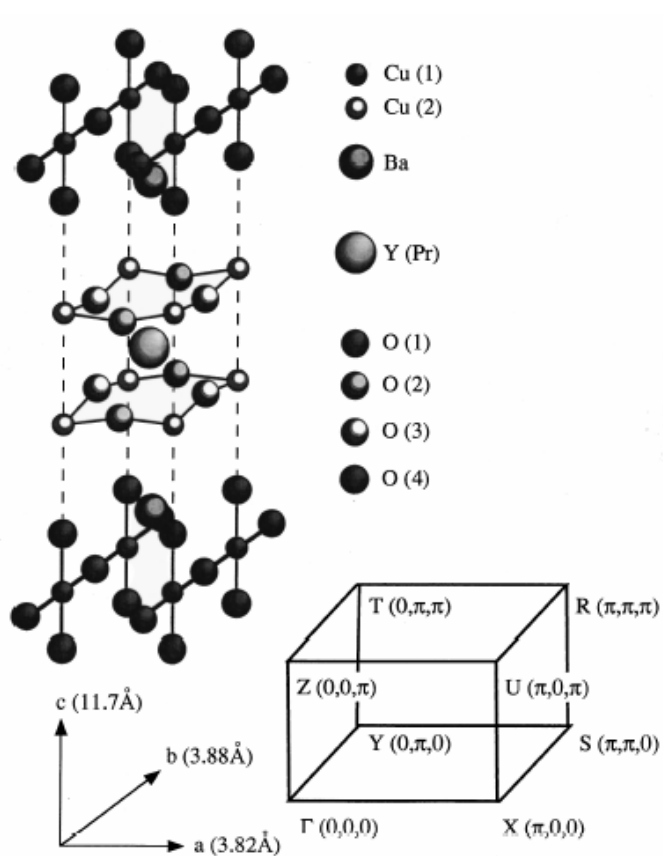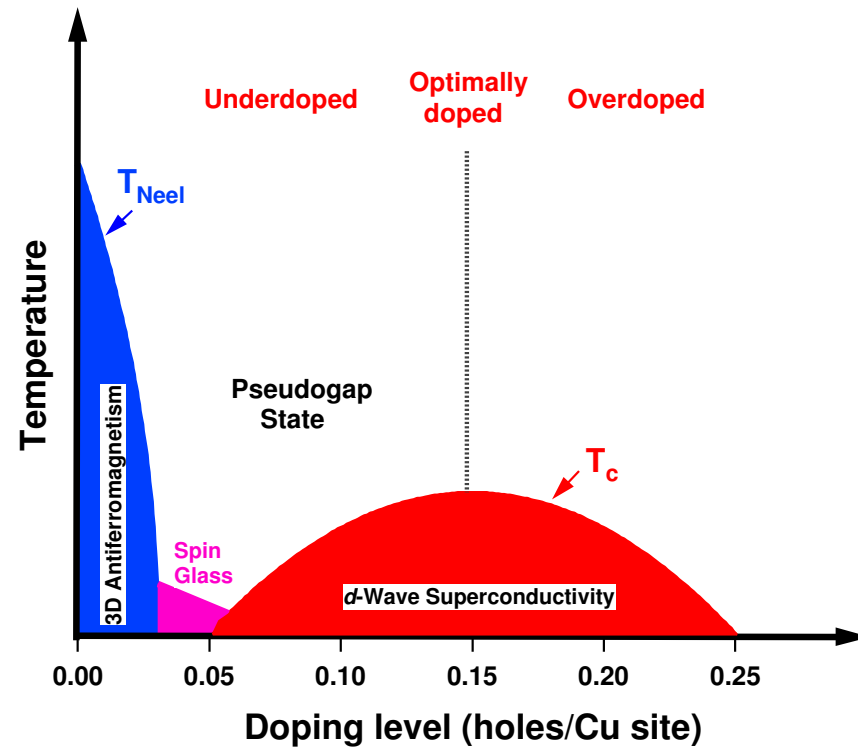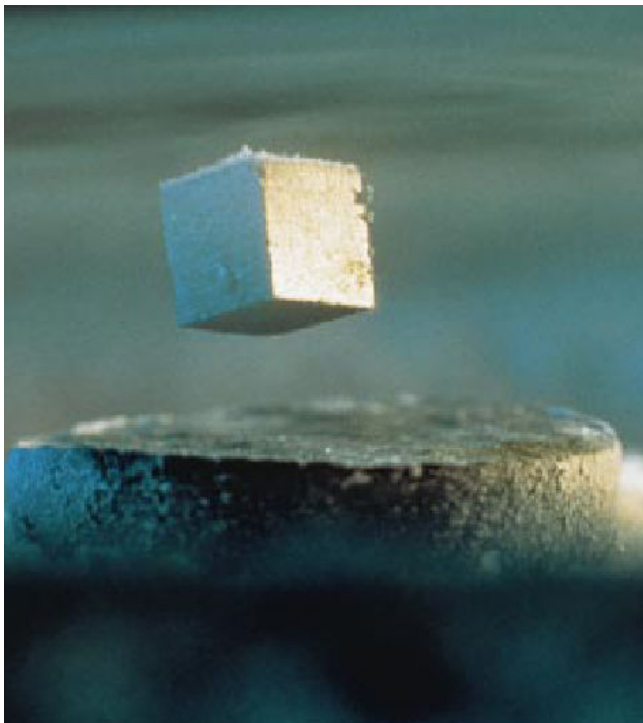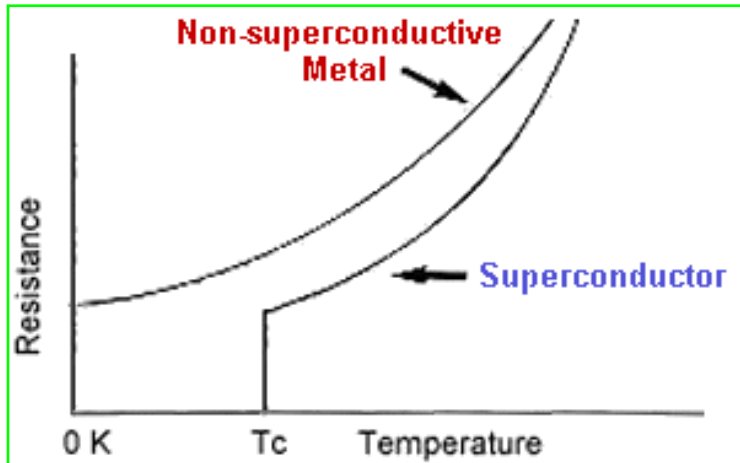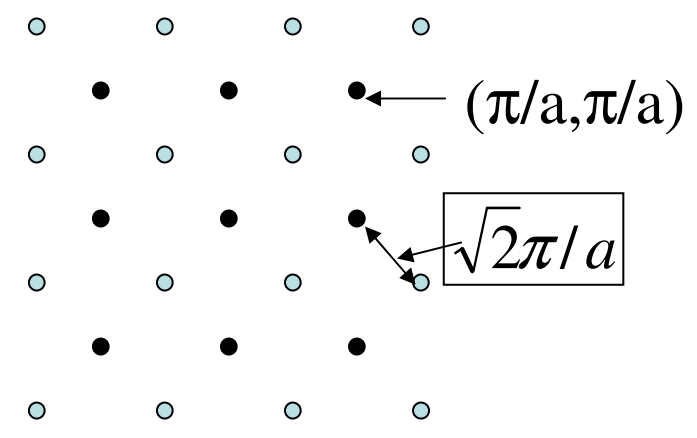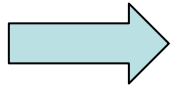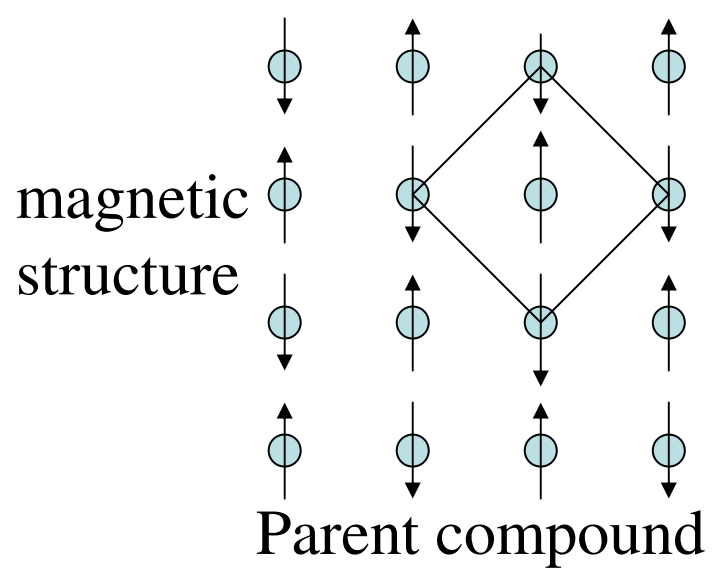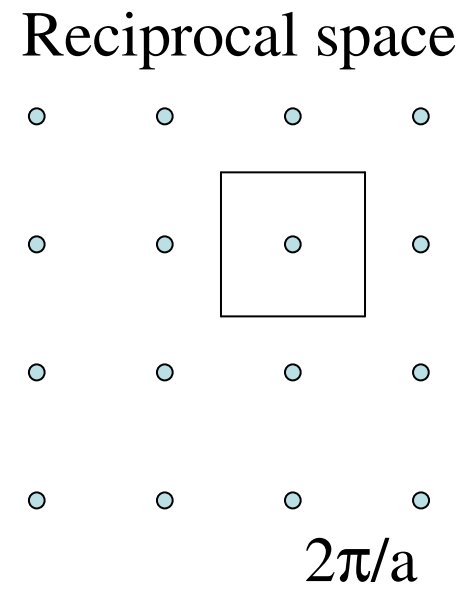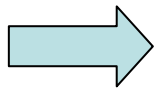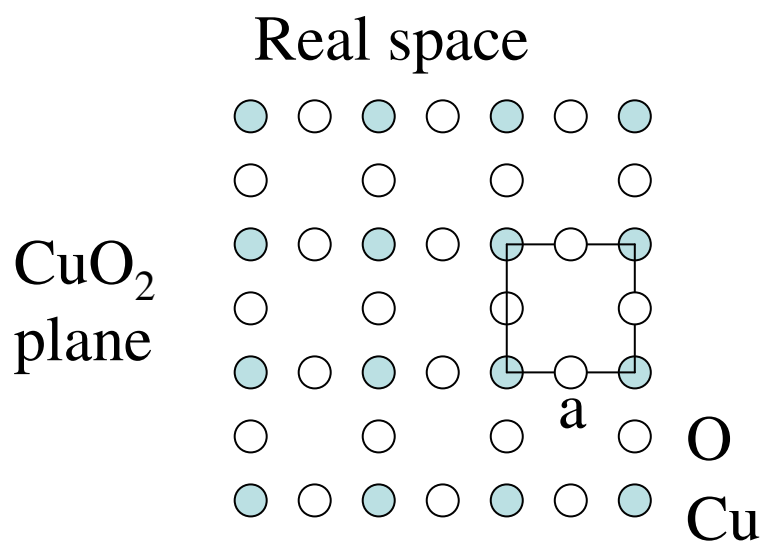
Neutron scattering provides a lot information about spin excitations:

- 3D Bragg peaks at (π, π) for parent compound (Long range order),

- Incommensurate peaks away from the (π, π) point in doped compounds——spin fluctuation,

- **∼40 meV resonance at (π, π) below T_c.**
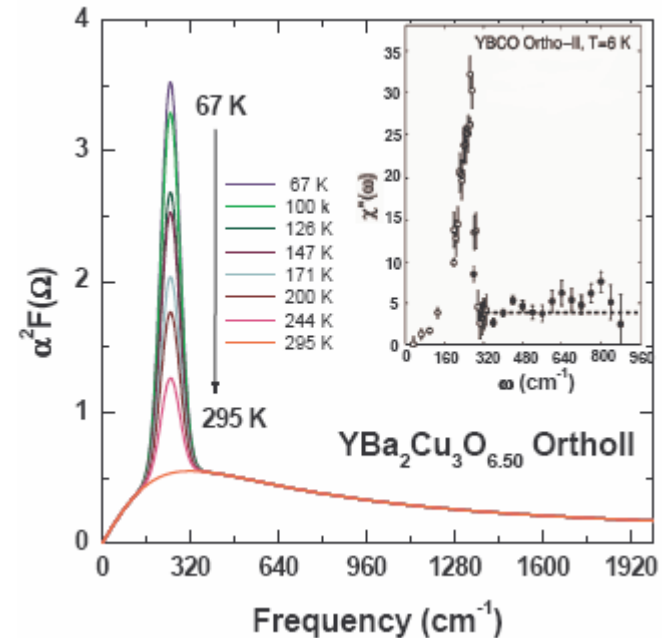
x=0
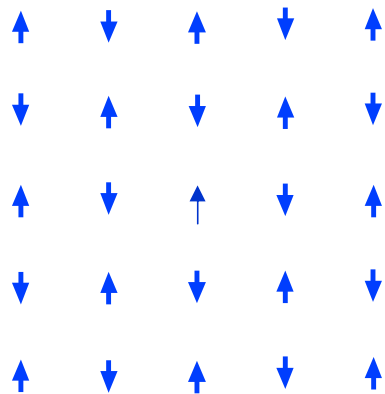
without strong el-el

with strong el-el

LHB **(LHB)** UHB

μ

Δ

U
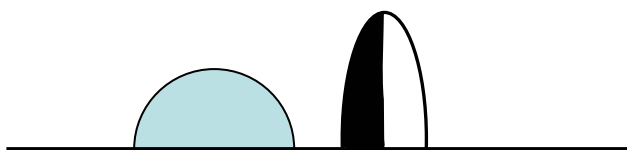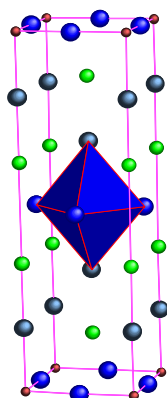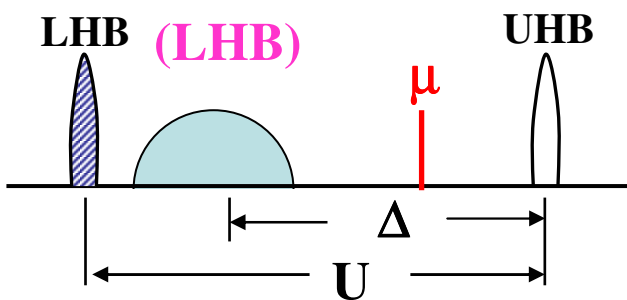
CuO$_2$
(La,Sr)O
(La,Sr)O
CuO$_2$
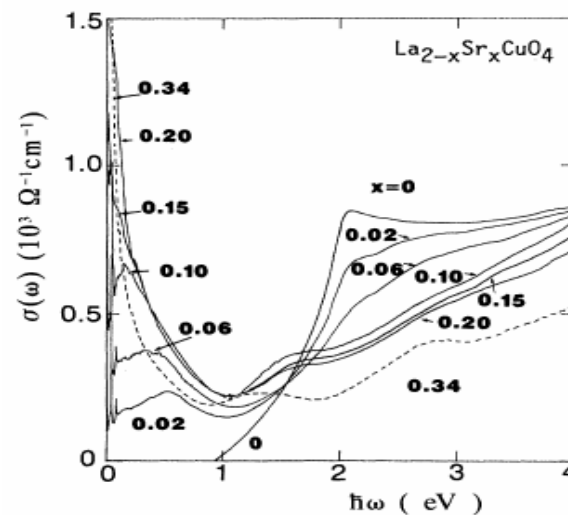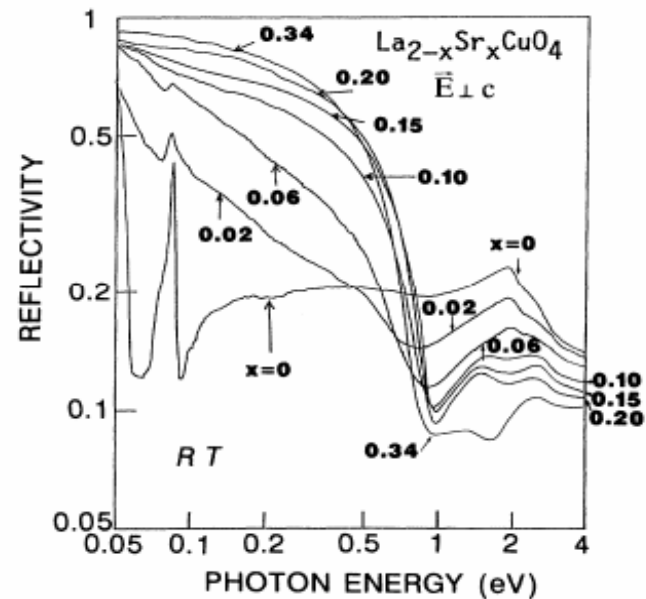
S. Uchida et al.,
PRB43, 7942
(91)

Mott-Hubbard U~8 eV

Gap~1.5-2 eV → Charge transfer insulator for x=0.

Doping →隙间态

掺杂

(a)   (b)   (c)   (d)   (e)

$La_{2-x}Sr_xCuO_4$

$N_{eff}^*(\omega)$

0.20
0.15
0.10

0.27
0.34

0.06
0.02
x=0

$\hbar\omega$ (eV)

AF   SC   NM

$La_{2-x}Sr_xCuO_4$

N_{eff}^* at 1.5eV

$N_{eff}^*=x$

N_D

$R_H>0$ $R_H<0$

X
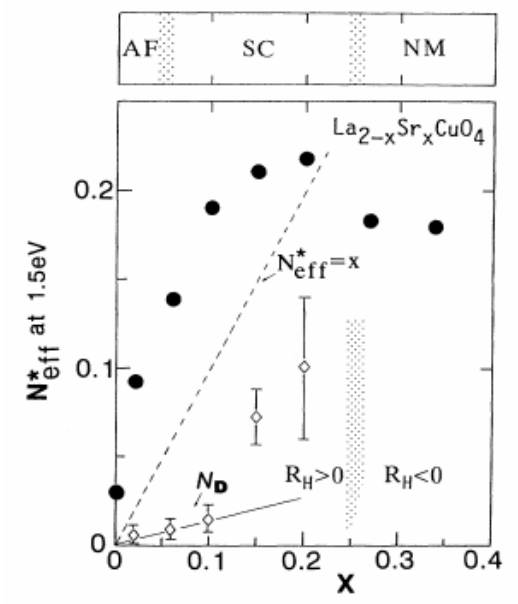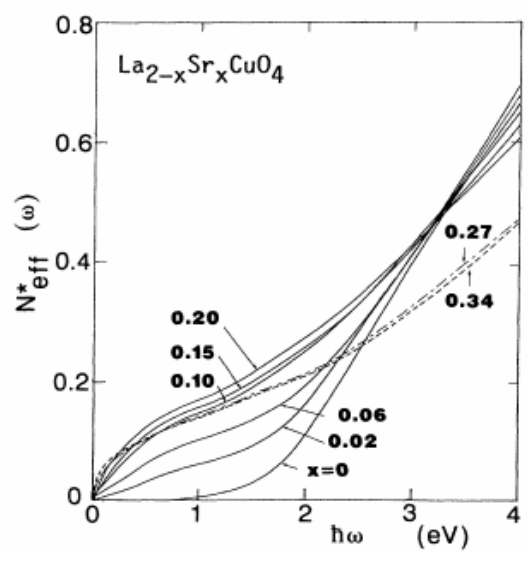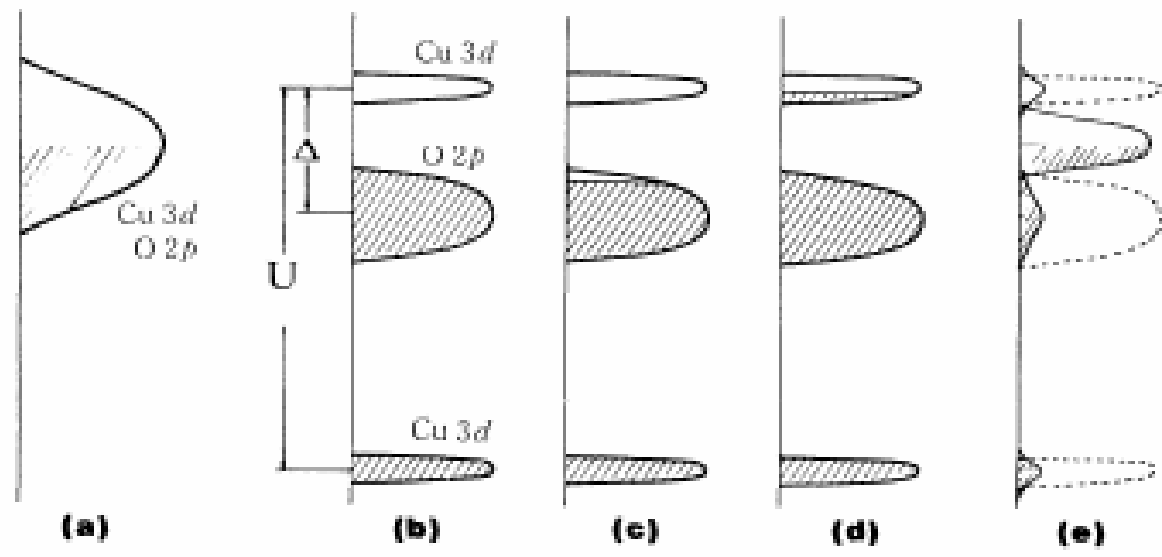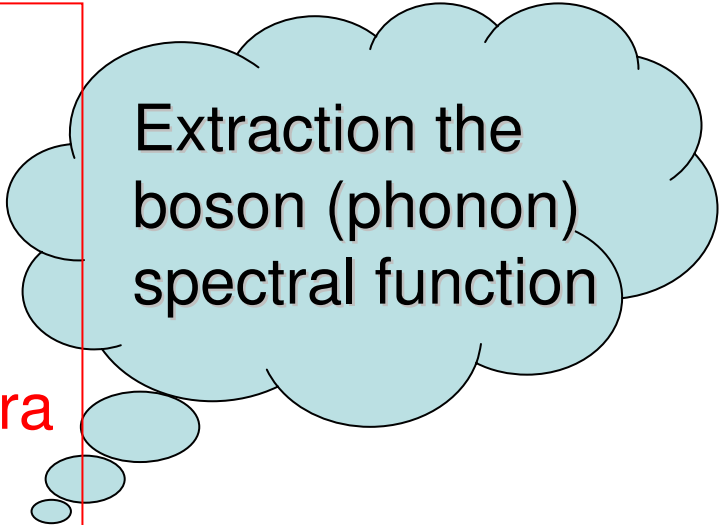
Mode coupling effect in infrared spectra of high-T_c cuprates

- Mode coupling effect in ARPES and tunneling

- Mode coupling effect in IR spectra of conventional superconductor

- Feature in IR spectra of high-Tc superconductors

Extraction the boson (phonon) spectral function

$$\Delta = |V| \frac{1}{N} \sum_k \frac{\Delta}{2E_k}$$ Tc equation

$$\frac{2\Delta}{k_B T_c} = 3.53$$ **Universality** $$\frac{\Delta C}{\gamma T_c} = 1.43$$

Eliashberg Theory

Extension of BCS formalism to include dynamical electron-phonon interaction

$$\Delta(k, \omega) = \mathcal{F}[V_{k,k'}(\omega, \omega')] \longleftarrow$$ A function of the interaction

Question: Can we invert the theory to extract the potential uniquely from a knowledge of $\Delta(k,\omega)$?

I. Giaever, H.R. Hart, Jr., and K. Megerle, PRB 126, 941 (1962)
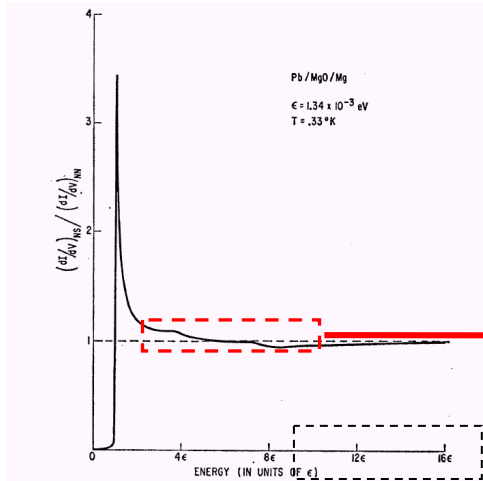
FIG. 10. The relative conductance of a Pb-MgO-Mg sandwich plotted against energy. At higher energies there are definite divergences from the BCS density of states as can be seen from the bumps in the experimental curve. Note that the crossover point corresponds in energy to the Debye temperature.

data Pb

BCS
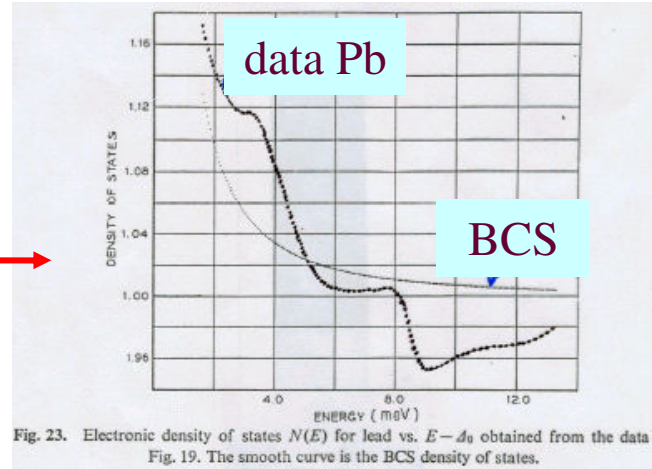
Fig. 23. Electronic density of states $N(E)$ for lead vs. $E - \Delta_0$ obtained from the data of Fig. 19. The smooth curve is the BCS density of states.

McMillan and Rowell, Superconductivity, ed. By R.D. Parks (1969)

requires Eliashberg theory:

- phonon dynamics (retardation) taken into account $[\alpha^2 F(\Omega)]$

- gap is a function of frequency $\Delta(\omega) = \mathcal{F}[\{\alpha^2 F(\Omega)\}, \mu^*]$

- density of states is modified: $\dfrac{dI}{dV} \propto N(\omega) = N(\epsilon_F) \mathrm{Re}\{\dfrac{\omega}{\sqrt{\omega^2 - \Delta^2(\omega)}}\}$

$\alpha^2 F(\omega)$

$\alpha^2 F$

$F(\omega)$
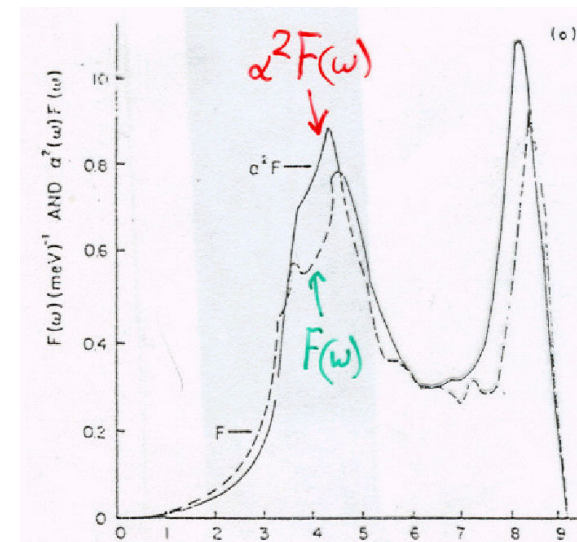
Phonon structure in the tunneling conductance of $Bi_2Sr_2CaCu_2O_8$

D. Shimada, Y. Shiina, A. Mottate, Y. Ohyagi, and N. Tsuda*

Department of Applied Physics, Science University of Tokyo, 1-3 Kagurazaka, Shinjuku-ku, Tokyo 162, Japan

(Received 17 March 1995)

Clear phonon structures were observed in the tunneling conductance of a $Bi_2Sr_2CaCu_2O_8$-GaAs junction. The spectral function of the electron-phonon interaction gives a value of 87.3 K for the critical temperature and 22.2 mcV for half a gap. There is no particularly large phonon structure, and the high T_c cannot be attributed to a particular phonon mode in the electron-phonon mechanism. The gap edge structure is sharp, and an s-wave state is probable. However, if the angular distribution of the tunneling current is highly anisotropic we cannot definitely exclude a d-wave state.
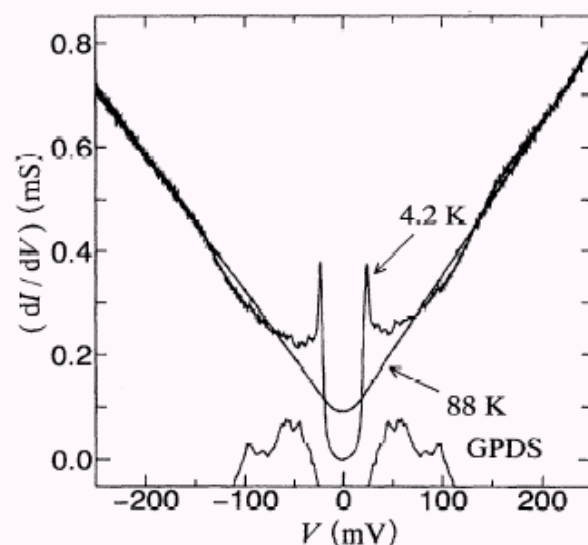
FIG. 2. The normalization procedure was illustrated. The subtracted conductances at 4.2 and 88 K were plotted together with the GPDS of Bi2212 (Ref. 10). These subtracted conductances were normalized. See the text.

FIG. 4. Spectral functions obtained by Vedeneev *et al.* (Ref. 3), Gonnelli *et al.* (Ref. 4), Miyakawa *et al.* (Ref. 5), and the present result are compared with GDPS and the atomic vibrations (Ref. 10). O1; O in the CuO_2 plane, O2; apical O, O3; O in the Bi-O planes.

Fig. 2 together with the generalized phonon density of states (GPDS) obtained by Renker *et al.*[10] The ratio of the depleted area to the accumulated area in the normalized dI/dV is 0.85 at negative bias and 0.61 at positive bias, indicating some

Tunneling spectroscopy of $Bi_2Sr_2CaCu_2O_{8+\delta}$: Eliashberg analysis of the spectral dip feature

J. F. Zasadzinski,[1,2] L. Coffey,[1] P. Romano,[3] and Z. Yusof[2]

[1]*Physics Division, Illinois Institute of Technology, Chicago, Illinois 60616, USA*
[2]*High Energy Physics Division, Argonne National Laboratory, Argonne, Illinois 60439, USA*
[3]*INFM and Facolta di Scienze, Universita del Sannio, Via Port'Arsa 11, I-82100 Benevento, Italy*
(Received 2 September 2003; published 14 November 2003)

Eliashberg strong-coupling theory, extended to a *d*-wave symmetric gap function, is used to fit quantitatively a published tunneling spectrum of $Bi_2Sr_2CaCu_2O_{8+\delta}$ near optimal doping. The shape, location, and strength of the high-bias spectral dip feature is adequately reproduced using a single-peak $\alpha^2F(\omega)$ centered at 36.5 meV. $\alpha^2F(\omega)$ also self-consistently determines the measured gap value $\Delta = 32$ meV. Possible origins of the bosonic spectrum that give rise to high-T_C superconductivity are discussed.
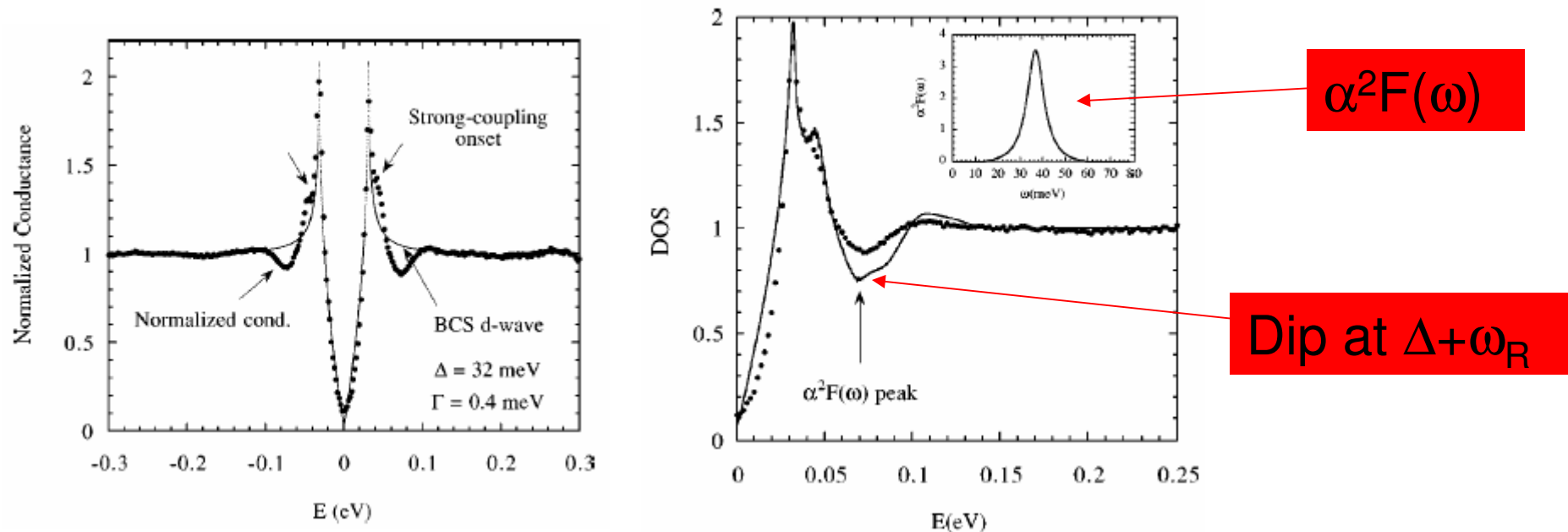
Angle-Resolved Photoemission Spectroscopy (*ARPES*)
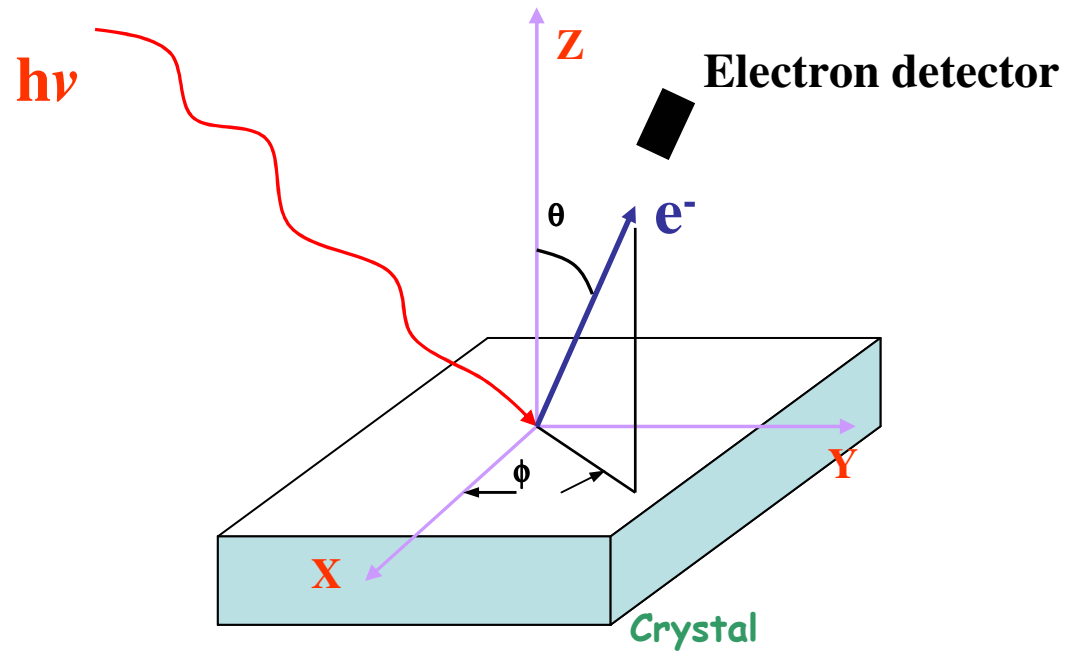
Energy Conservation: $E_B = h\nu - E_{kin} - \Phi$

Momentum Conservation: $K_{\parallel} = k_{\parallel} + G_{\parallel}$

ARPES –Band Mapping and Fermi Surface
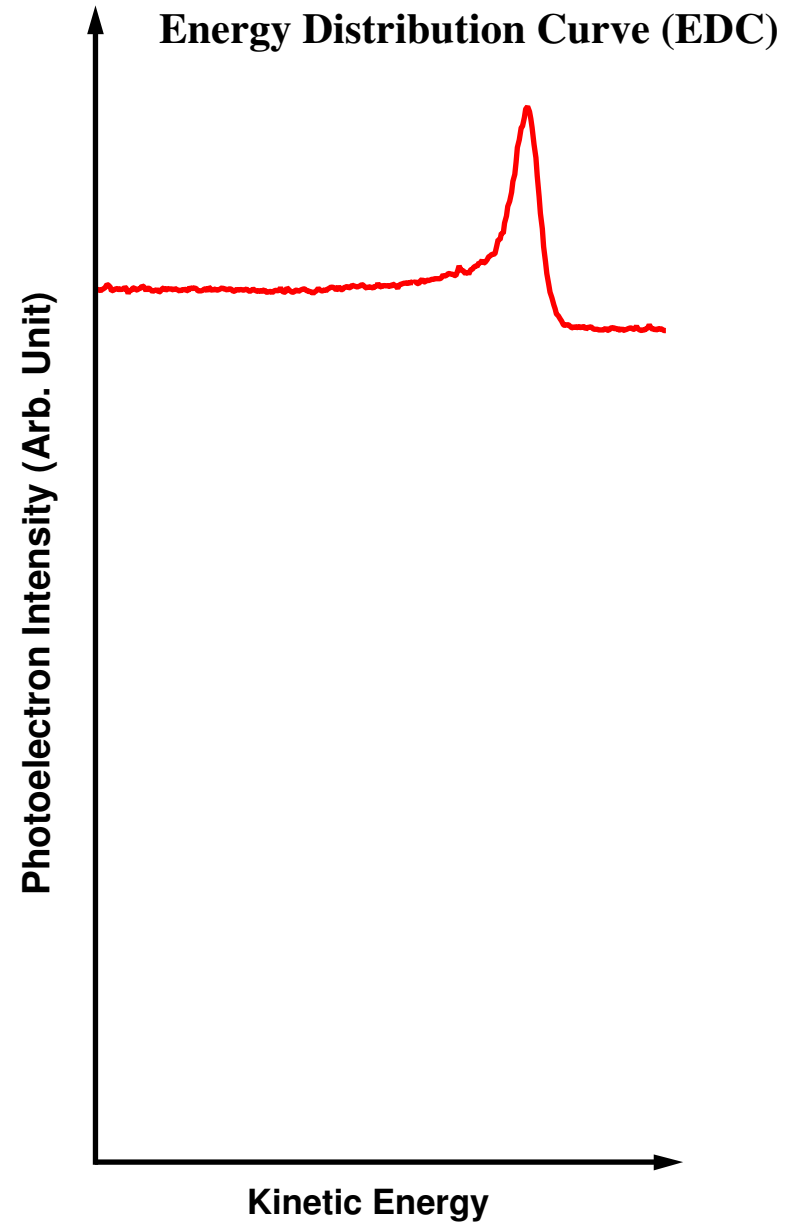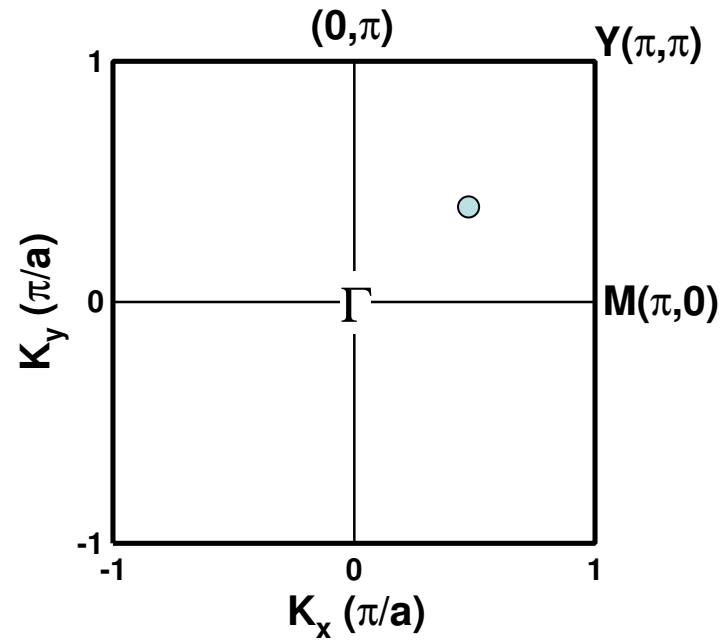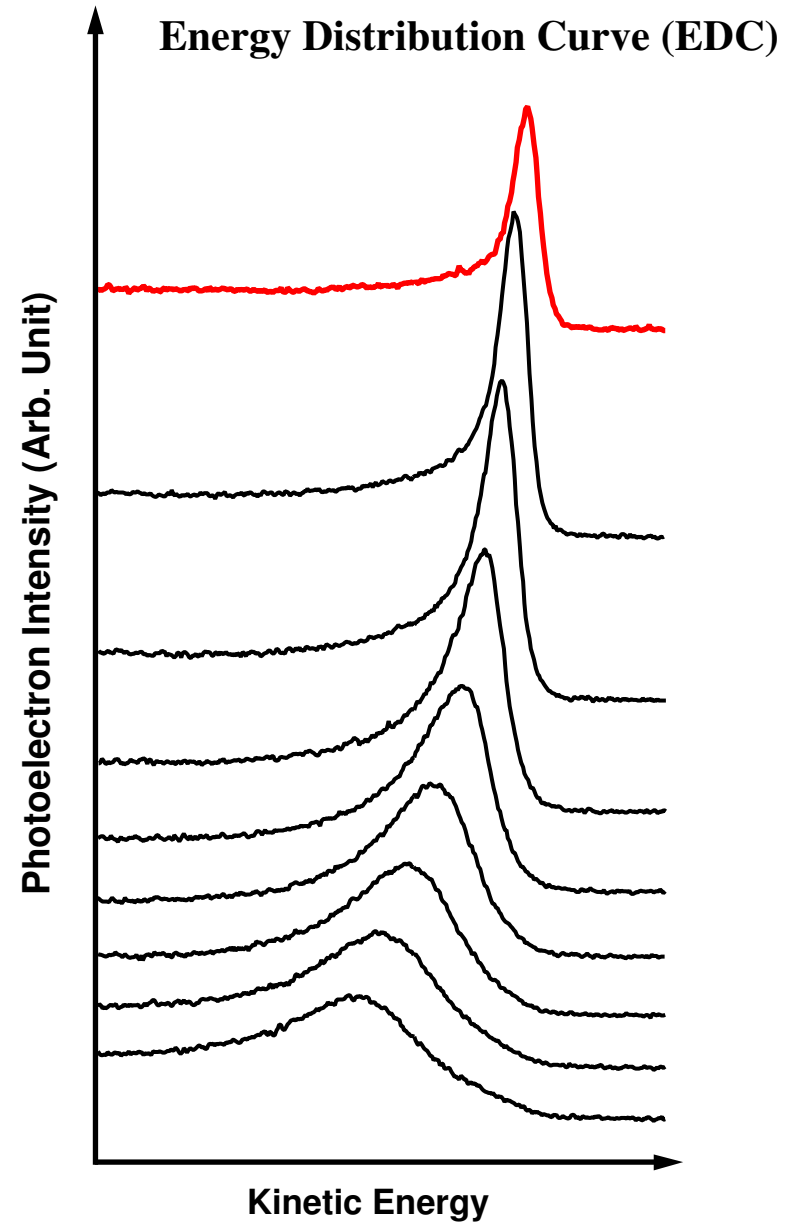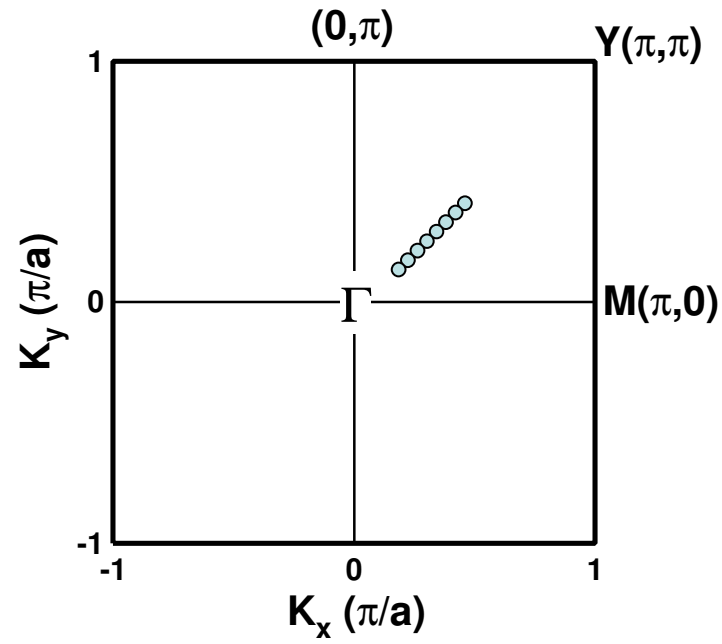
Energy Distribution Curve (EDC)

ARPES –Band Mapping and Fermi Surface

ARPES –Band Mapping and Fermi Surface

ARPES –Band Mapping and Fermi Surface

(0,π)   Y(π,π)

K_y (π/a)

Γ   M(π,0)

K_x (π/a)

E

E_F

k

k_F

Energy Distribution Curve (EDC)

Photoelectron Intensity (Arb. Unit)

Kinetic Energy
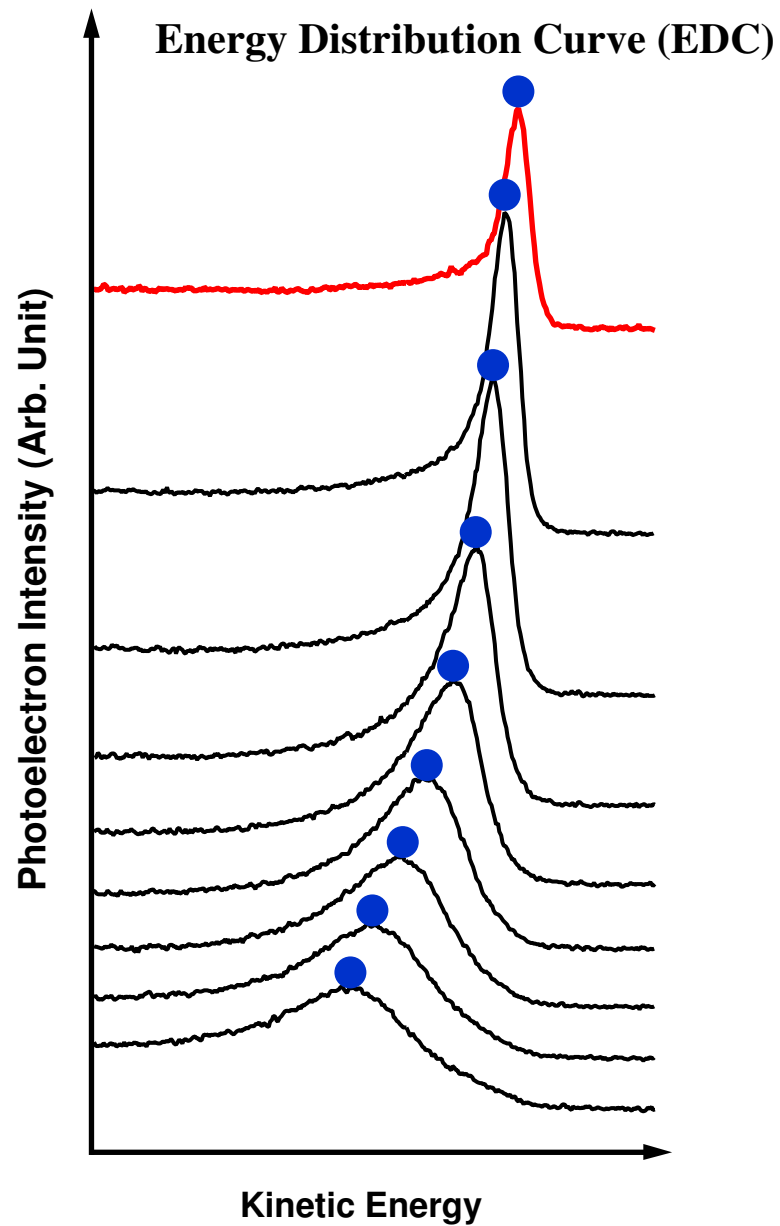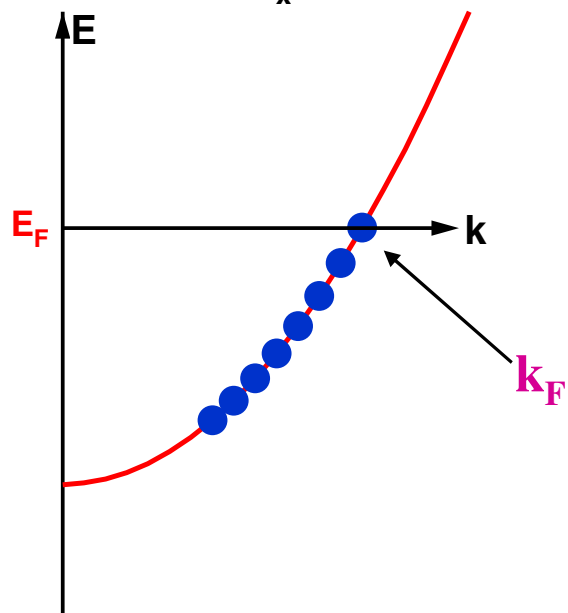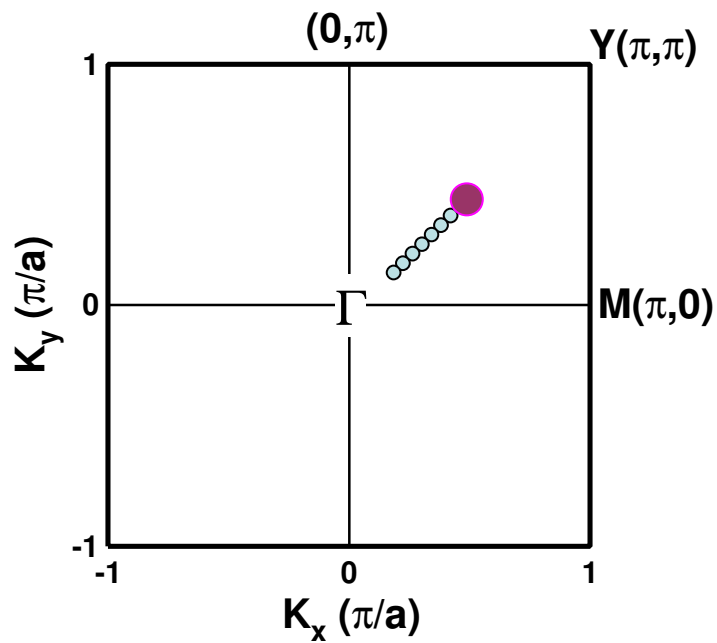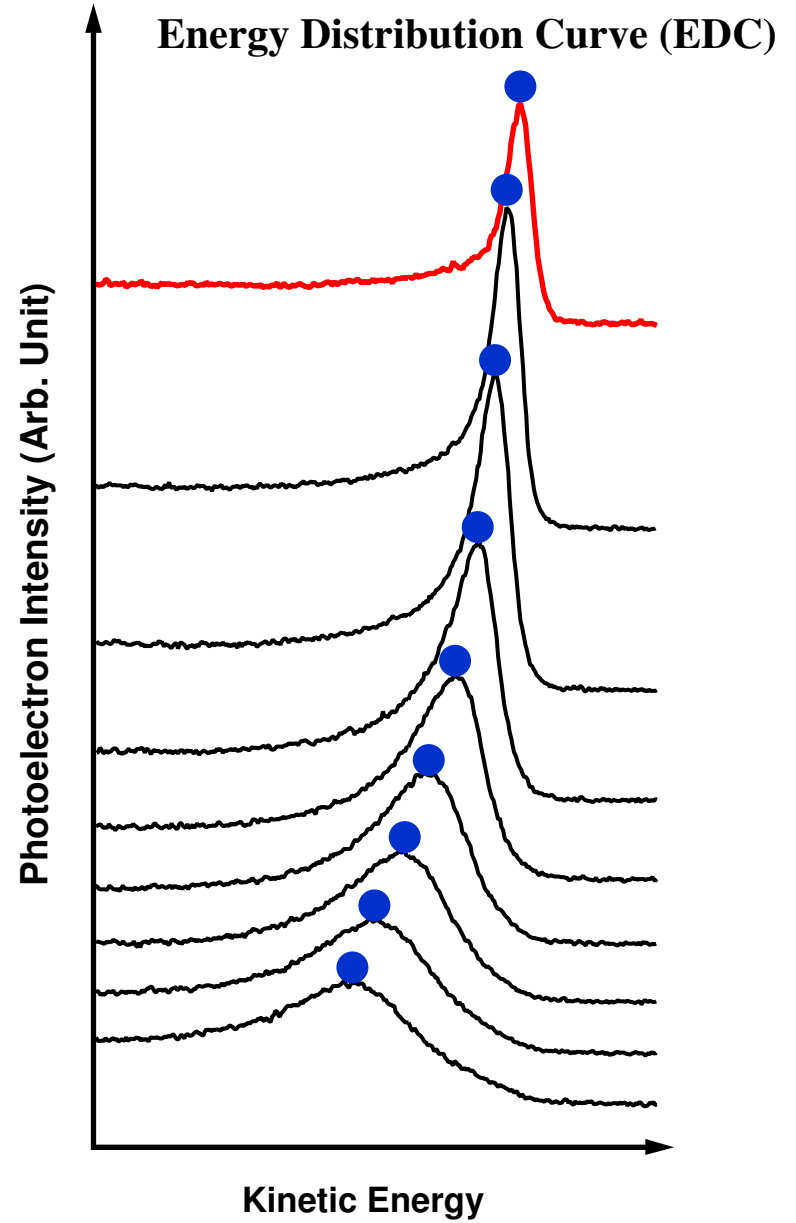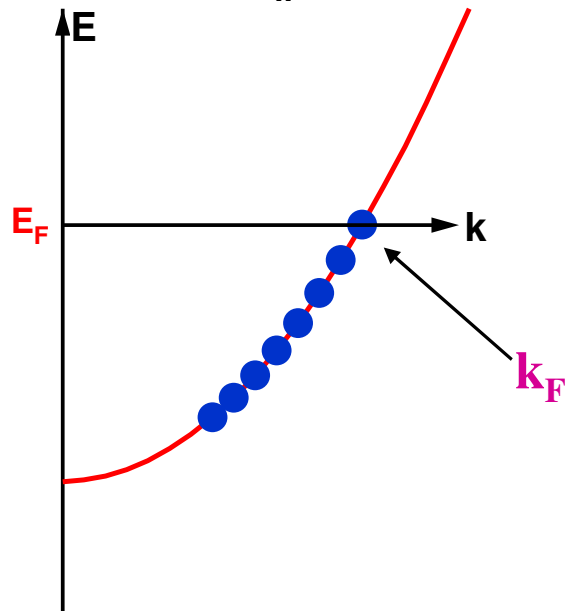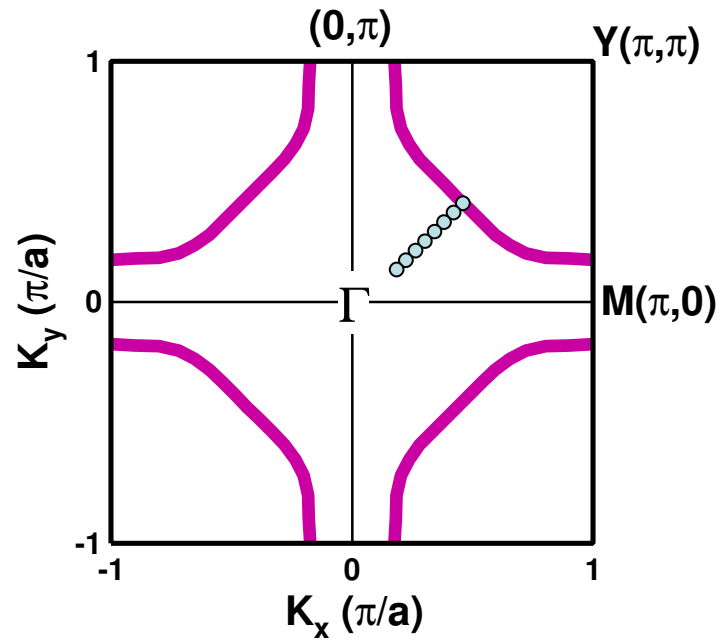
State-of-Art ARPES – Multiple Angle Collection

EDCs
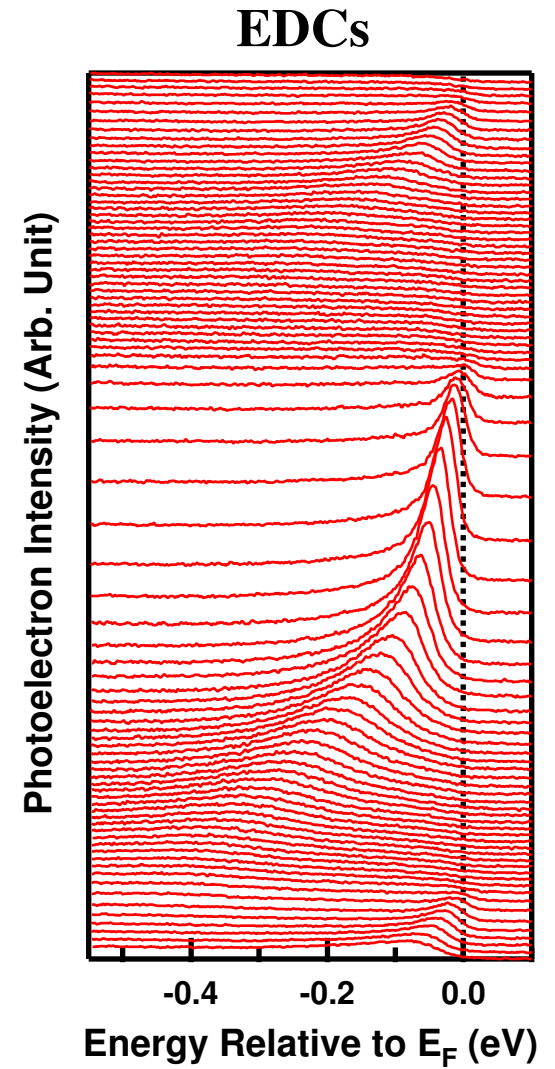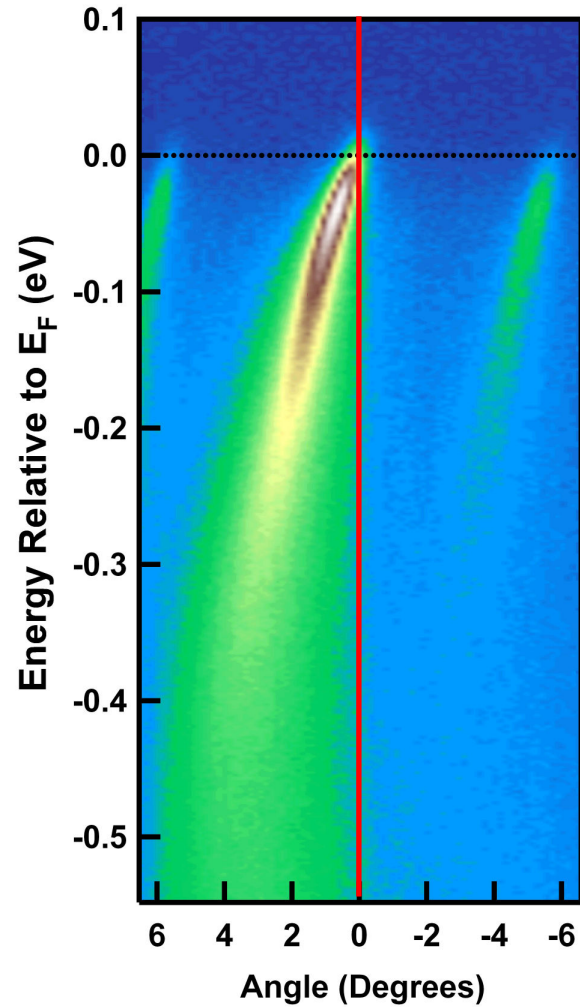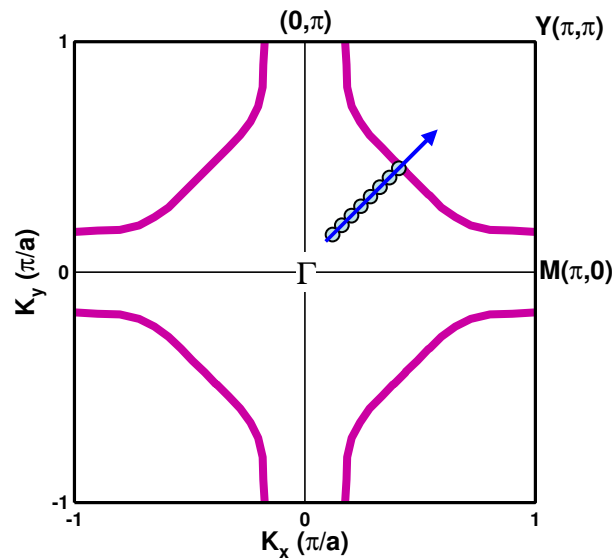
Direct Extraction of Electron Self-Energy: Momentum Distribution Curves

MDCs
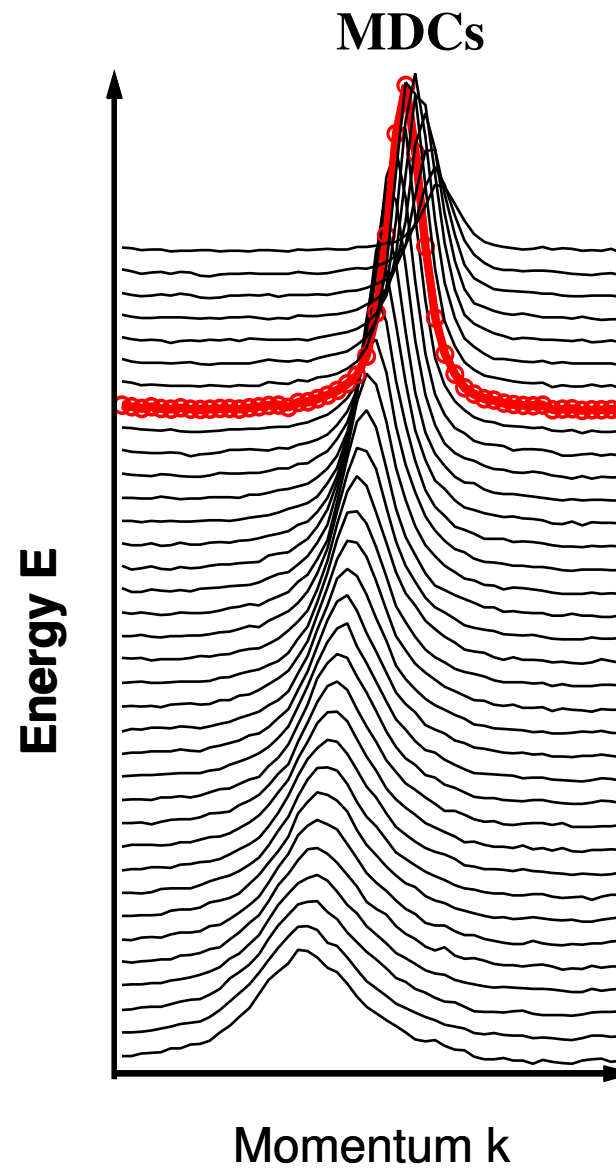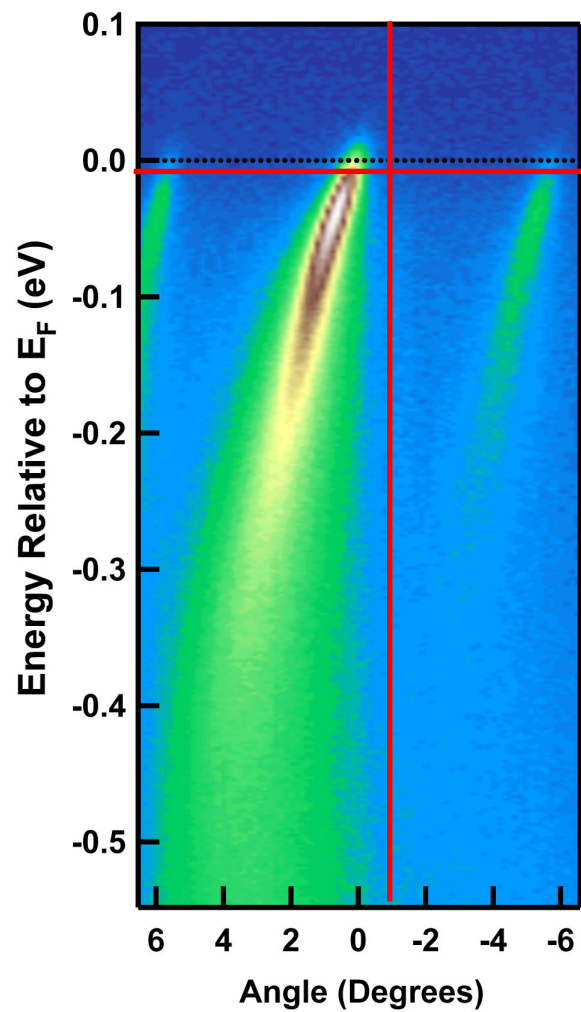
photoemission

Detected electrons $\propto N(\omega) \bullet \mathbf{f(\omega)}$

$$\because N(\omega) = \frac{1}{2\pi} \sum_k A(k,\omega)$$
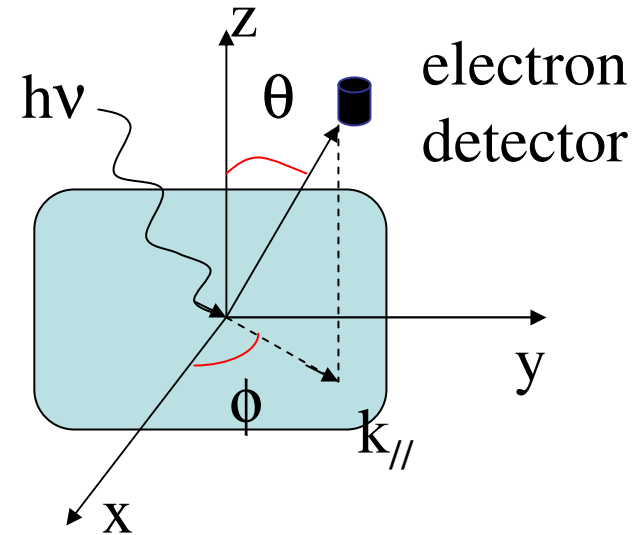
ARPES counting $\propto$ A(k, ω)$\bullet$f(ω)

$$\because A(k,\omega) = (-1/\pi)\,\mathrm{Im}\,G(k,\omega), \qquad G(k,\omega) = \frac{1}{\omega - \varepsilon(k) - \sum(k,\omega)}$$

$$\therefore A(k,\omega) = \frac{1}{\pi} \frac{\mathrm{Im}\sum(\omega,k)}{[\omega - \varepsilon_k - \mathrm{Re}\sum(\omega,k)]^2 + [\mathrm{Im}\sum(\omega,k)]^2}$$

PEAK POSITION: Dispersion (velocity; Effective mass; etc.)

PEAK WIDTH: ImΣ or 1/τ scattering rate

Manifestation of Many-Body Effects: Band Renormalization
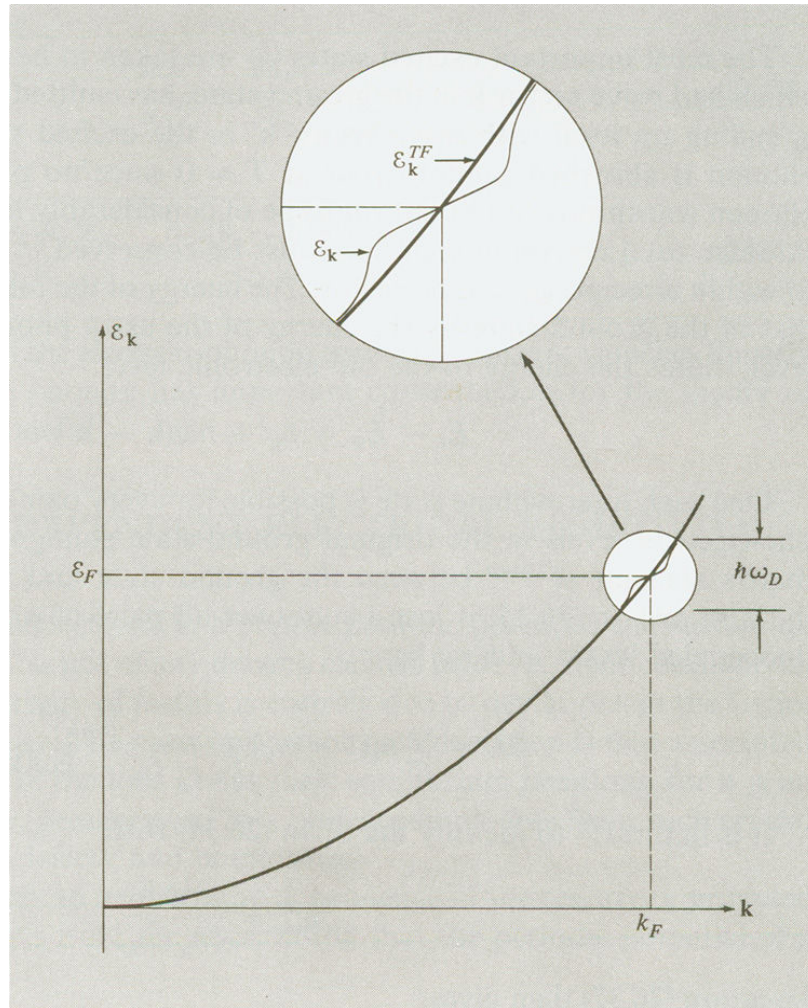
Ashcroft-Mermin, Solid State Phyics

Be(0001) Surface State
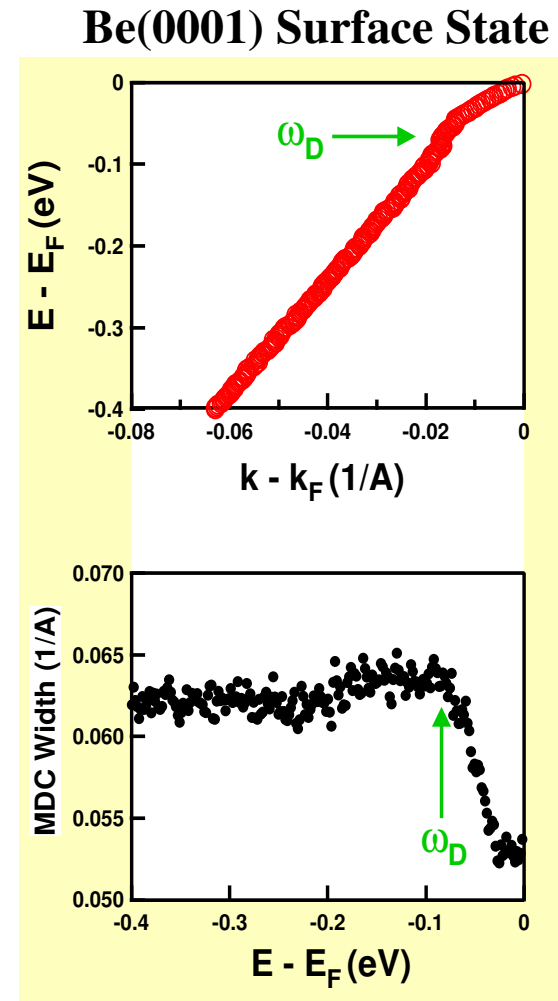
Hengsberger et al., PRL 83(1999)592.
S. Lashell et al., PRB 61(2000)2371.
S. J. Tang et al., Phys. Stat. Solidi.
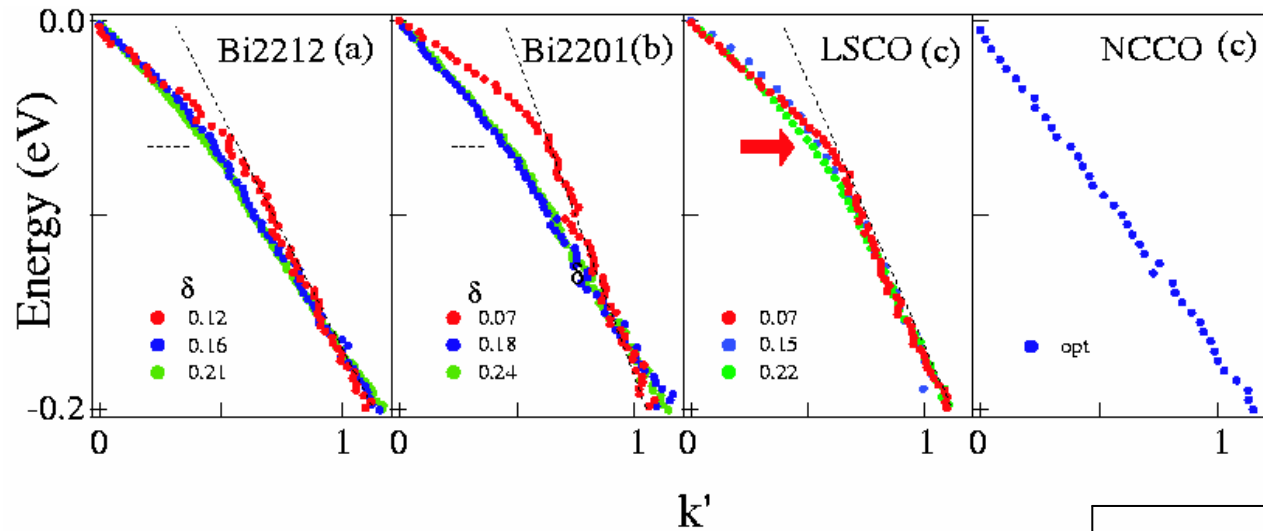
The kink is observed both below and above Tc in all hole-type cuprates

Drop in the ImΣ

UD-Bi2201   opt-Bi2212
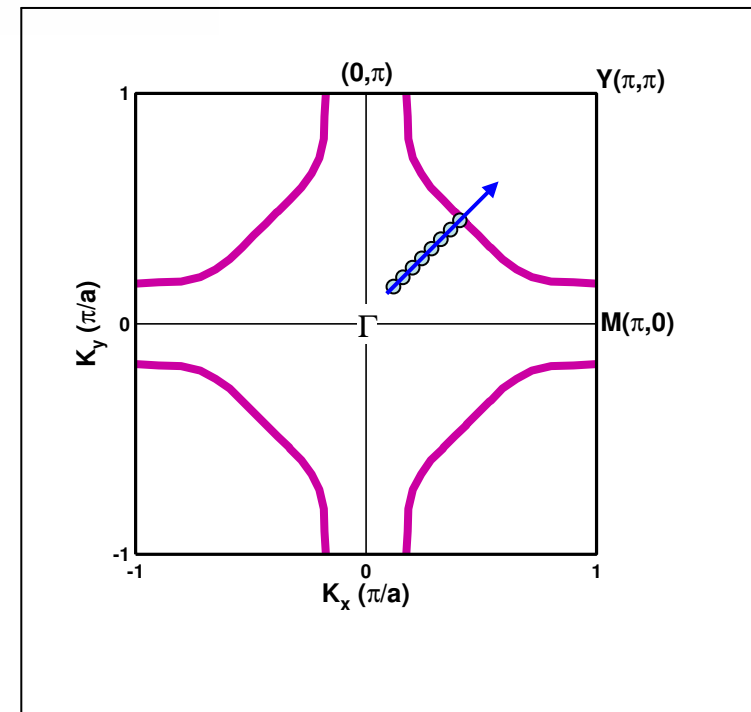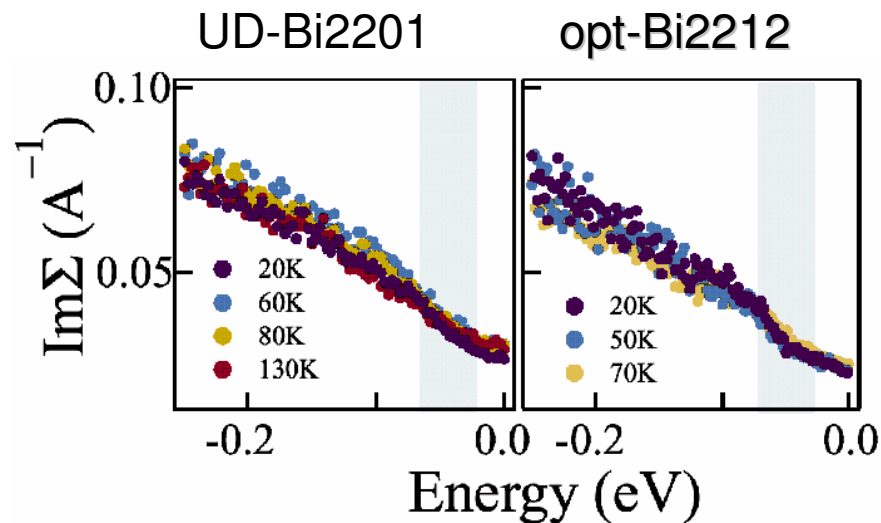
P. D. Johnson, et al., PRL 87, 177007 (2001)
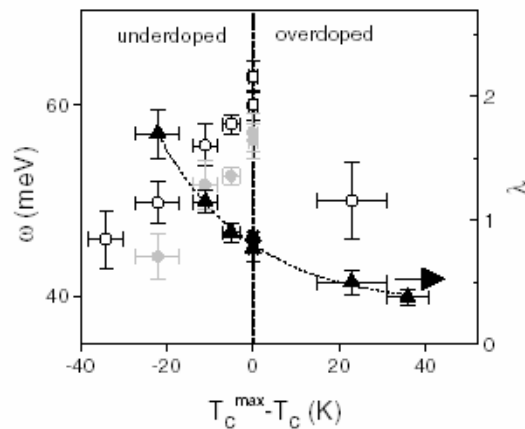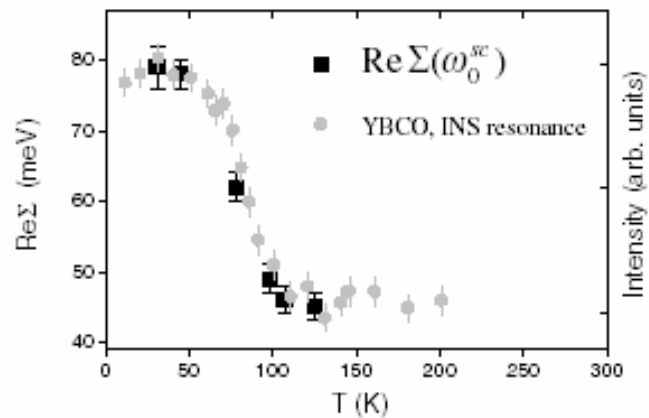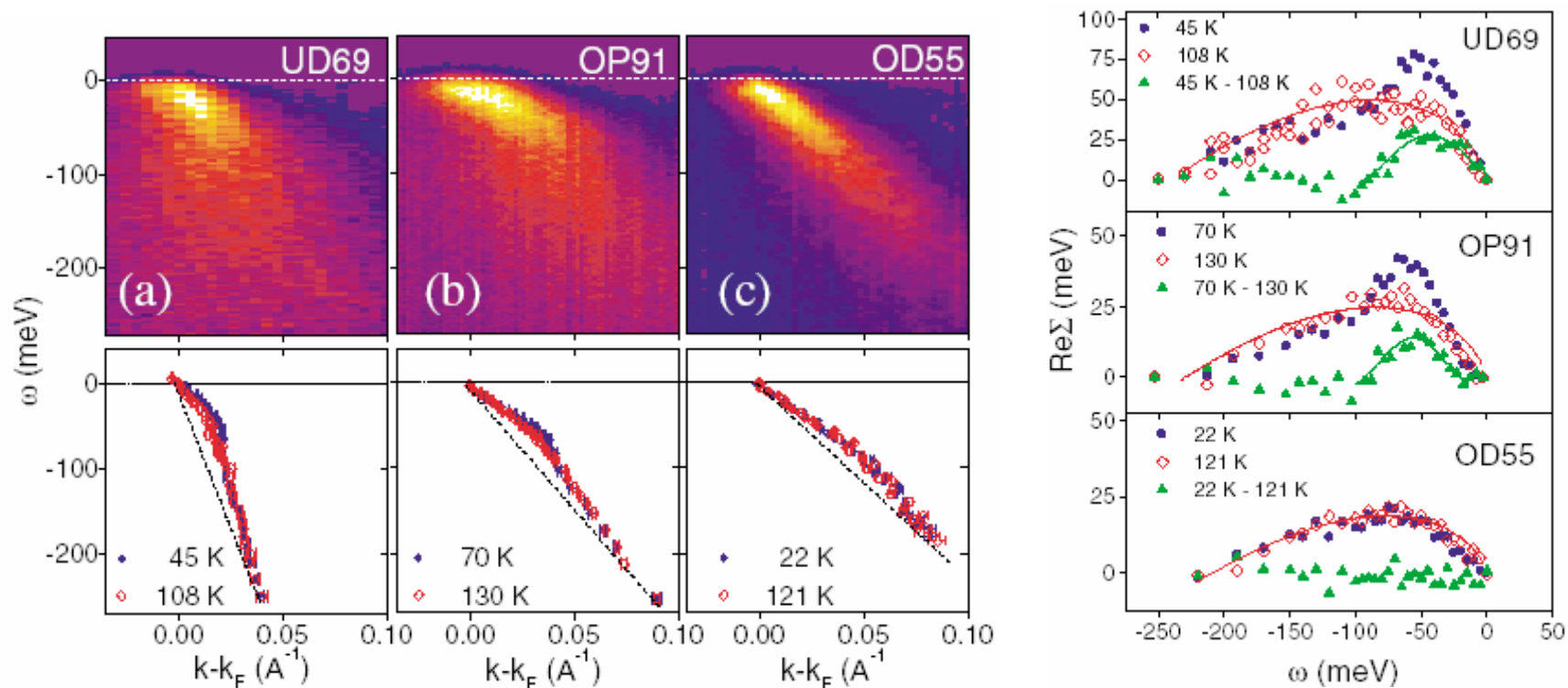
$$\lambda = -(\partial \mathrm{Re}\,\Sigma / \partial \omega)_{E_F}$$

Universal Nodal Fermi Velocity (v_F) in $(La_{2-x}Sr_x)CuO_4$
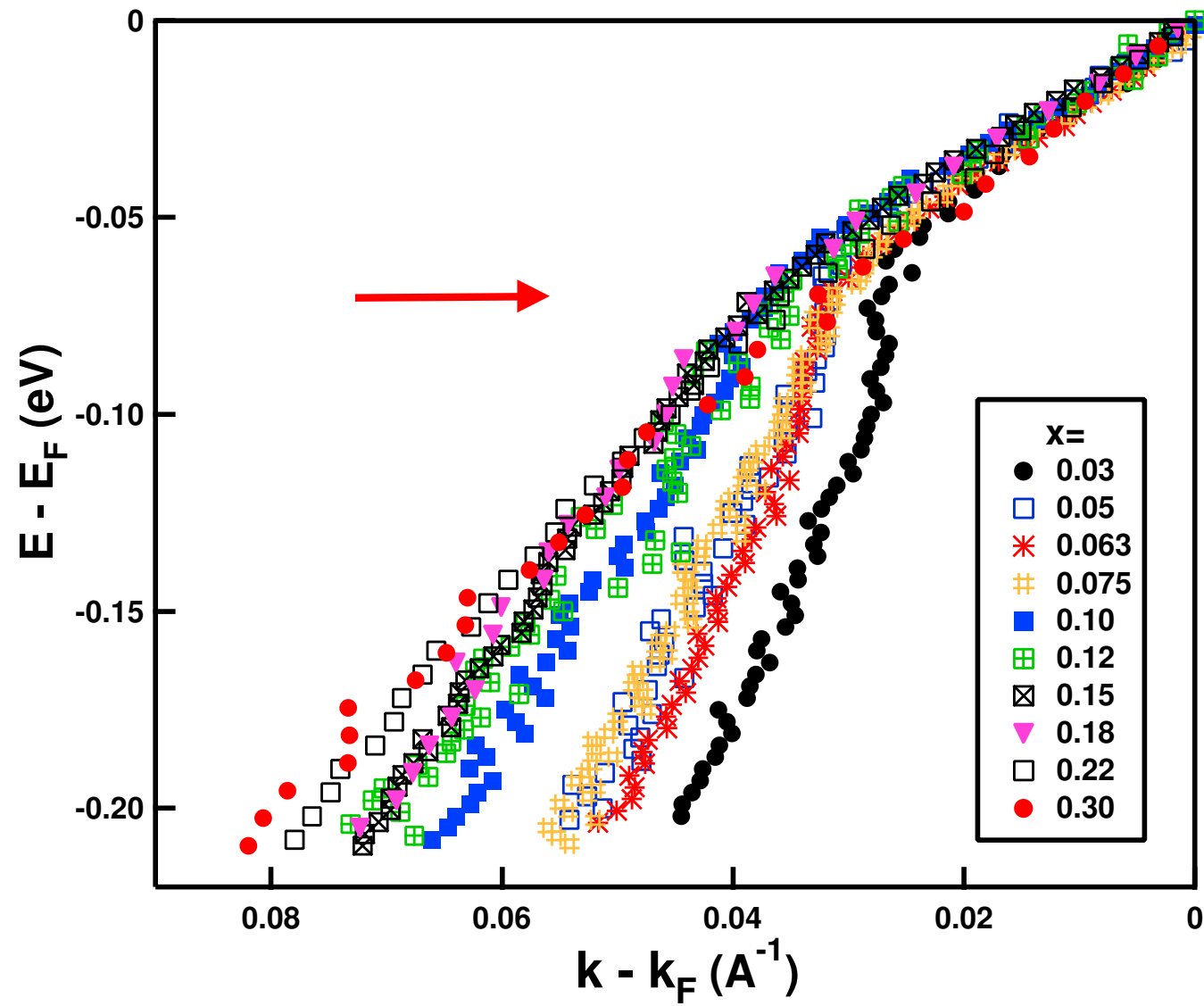
X. J. Zhou et al., Nature 423(2003)398.

Universal Nodal Fermi Velocity in Hole-Doped Cuprates
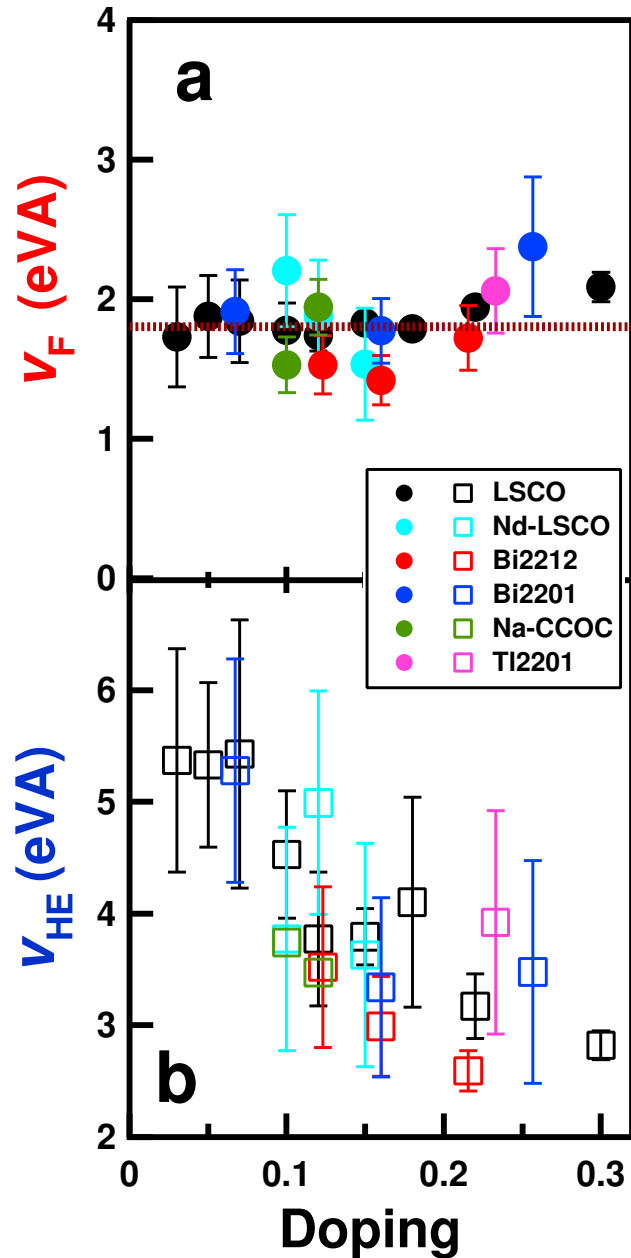
Observation of universal Fermi velocity
is unexpected.

Doping Dependence of High-Energy
Velocity is Anomalous
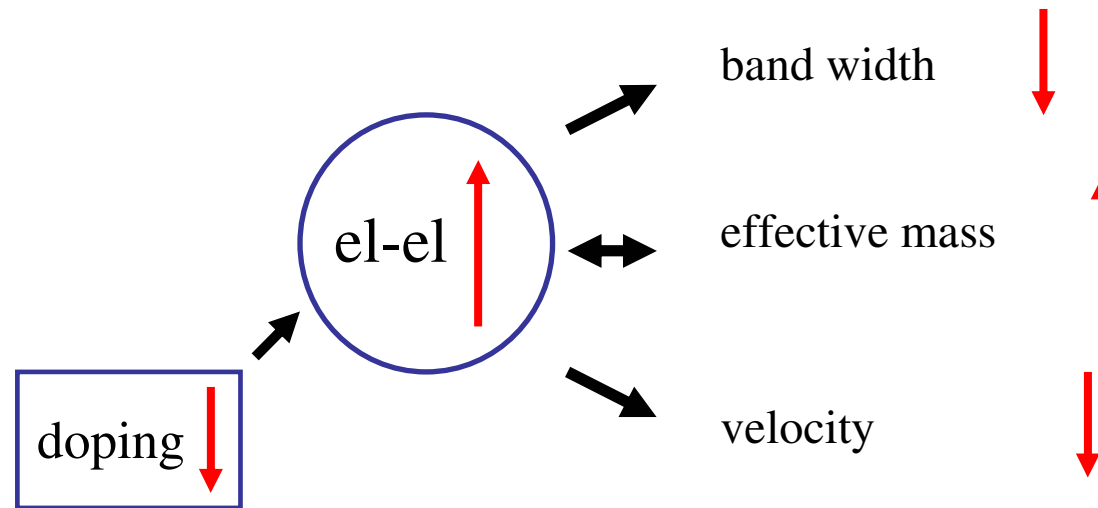
X. J. Zhou et al.,
Nature 423(2003)398.

Dispersion of LSCO along the (0,0)-(π,π) Nodal Direction

Finer structures

X. J. Zhou et al., PRL (05)
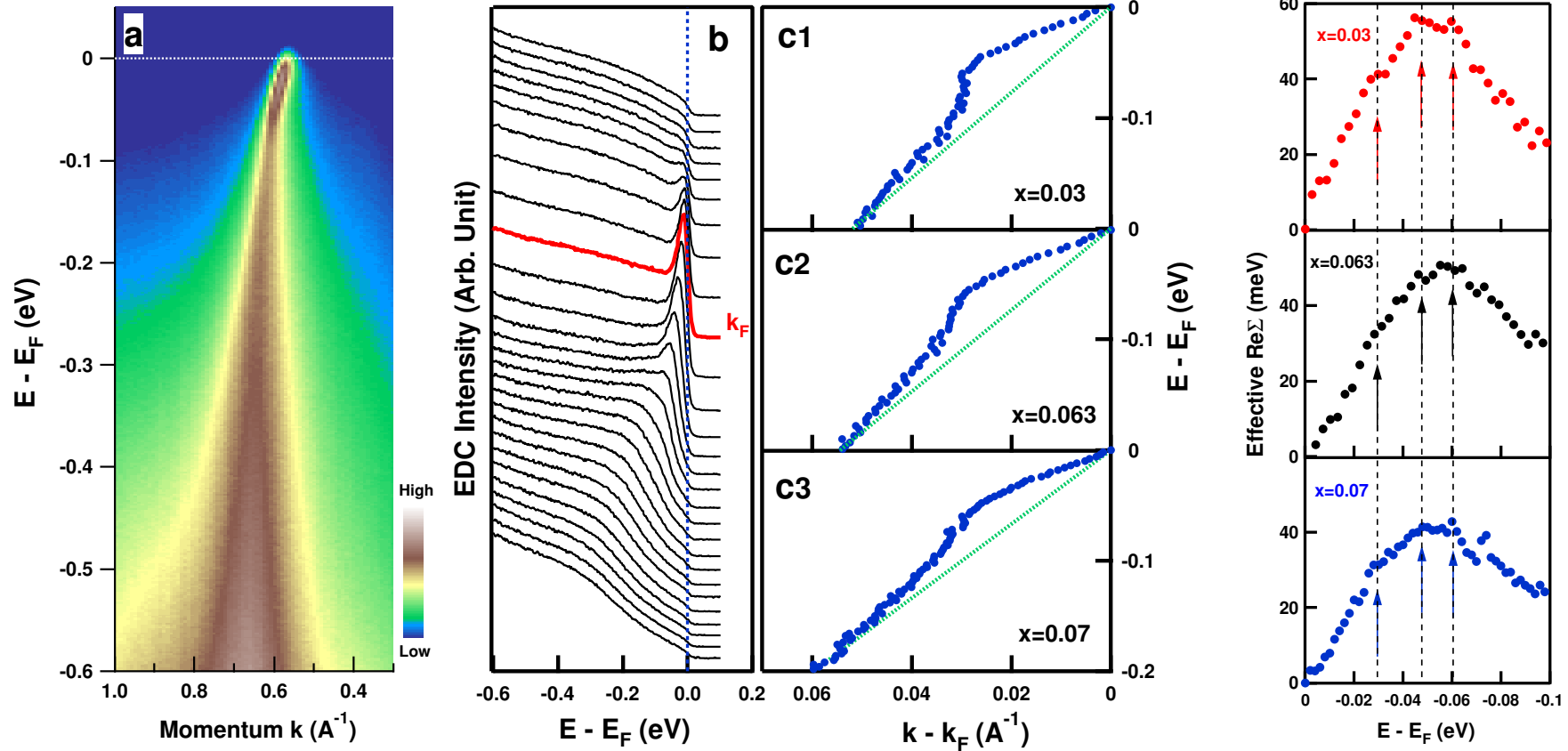
Extraction of Bosonic Spectral Function from ReΣ

In metals, the real part of self-energy is related to the bosonic spectral function by:

$$\mathrm{Re}\,\Sigma(k,\varepsilon,T) = \int_0^\infty d\omega\, \alpha^2 F(\omega;\varepsilon,k) K\left(\frac{\varepsilon}{kT},\frac{\omega}{kT}\right)$$

where

$$K(y,y') = \int_{-\infty}^\infty dx\, \frac{2y'}{x^2 - y'^2} f(x+y)$$

with f(x) being the Fermi-Dirac distribution Function

Maximum Entropy Method ⇒ α²F(ω)

Comparison of the Extracted Spectral Function with Known Structure
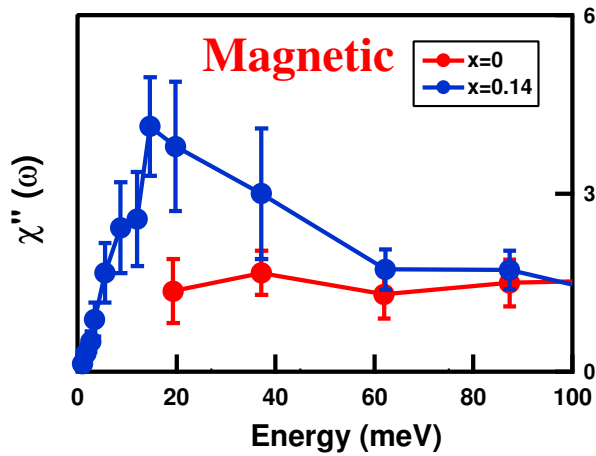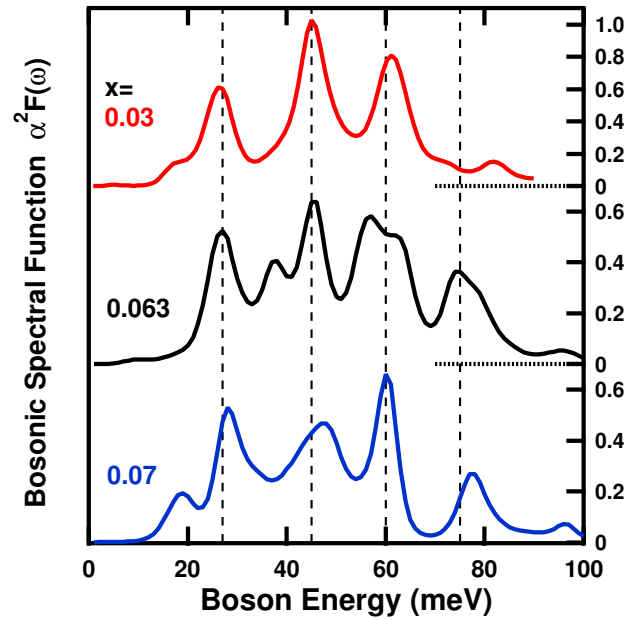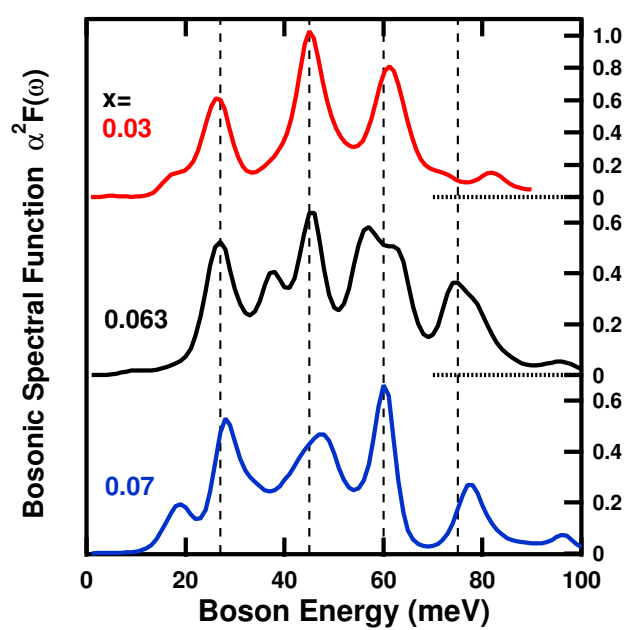
Hayden et al.,
PRL 76(1996) 1344.
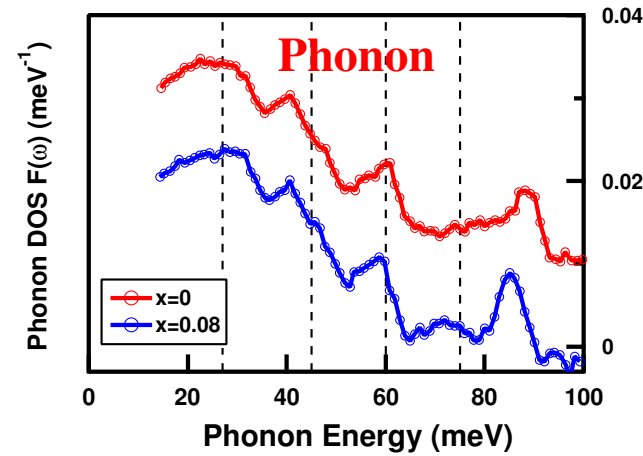
McQueeney et al.,
PRL 87(2001) 077001

(1). el-ph
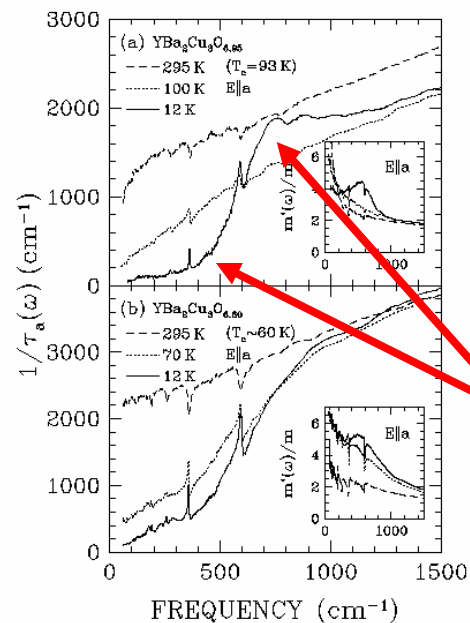(2). multiple
    phonons

Mode coupling in optical spectra

YBCO

C C Homes

D N Basov

T. Timusk

$R(\omega)$
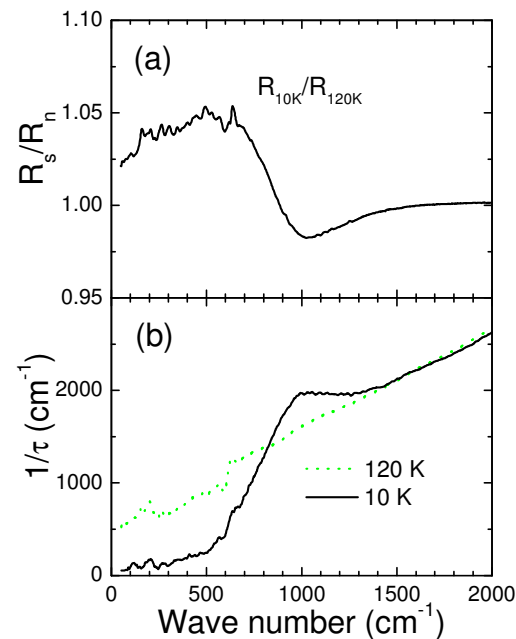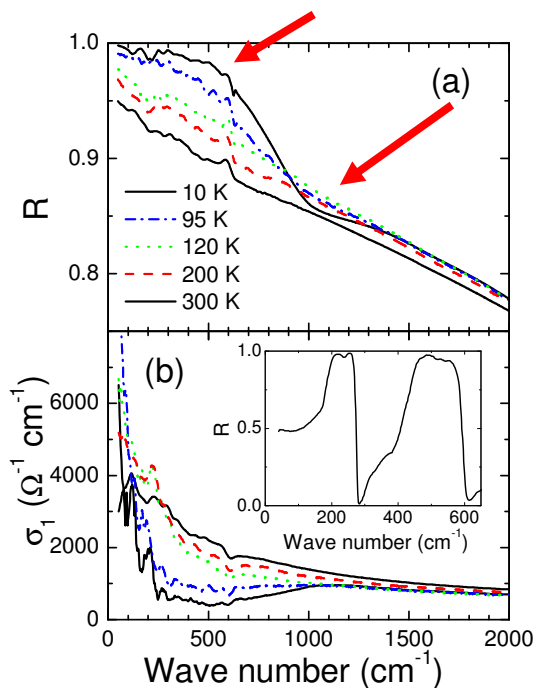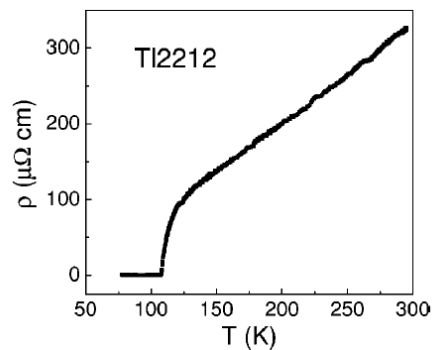
$\Rightarrow \sigma_1(\omega)$

$\Rightarrow 1/\tau(\omega)$

Due to mode coupling

Tl-2212 thin film T_c=108 K
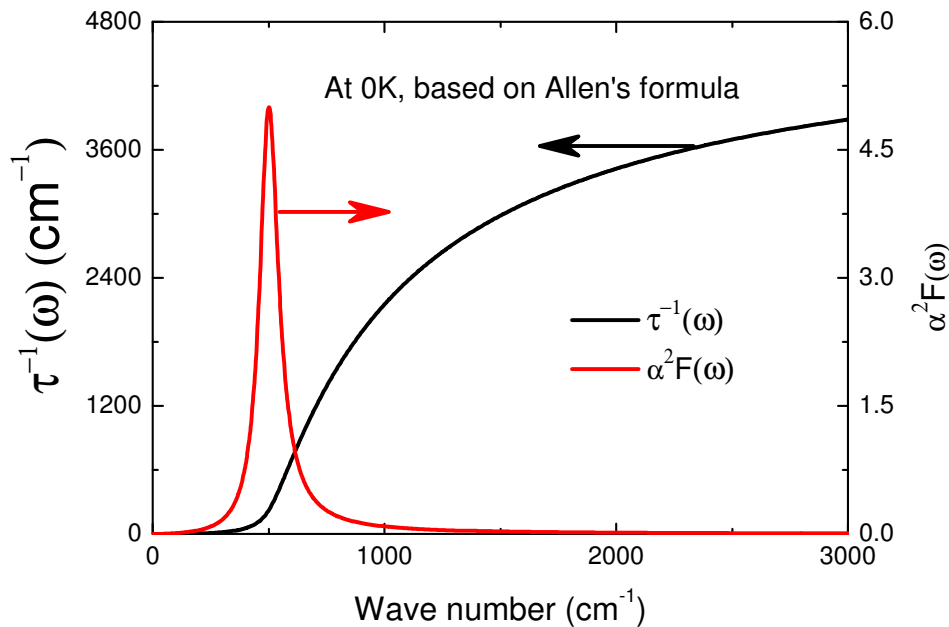
N. L. Wang et al., PRB03

The electron-boson (phonon) interaction

$$1/\tau(\omega) = \frac{2\pi}{\omega} \int\limits_{0}^{\infty} d\Omega (\omega - \Omega) \alpha_{tr}^2(\Omega) F(\Omega)$$

T=0 K

P.B.Allen 1971

$$\alpha^2 F(\omega) = \frac{\omega_p^2 \omega^2}{(\omega_0^2 - \omega^2)^2 + \gamma^2 \omega^2}$$

ω_0=500 cm-1

γ=100 cm-1

ω_p^2=50000 cm-2

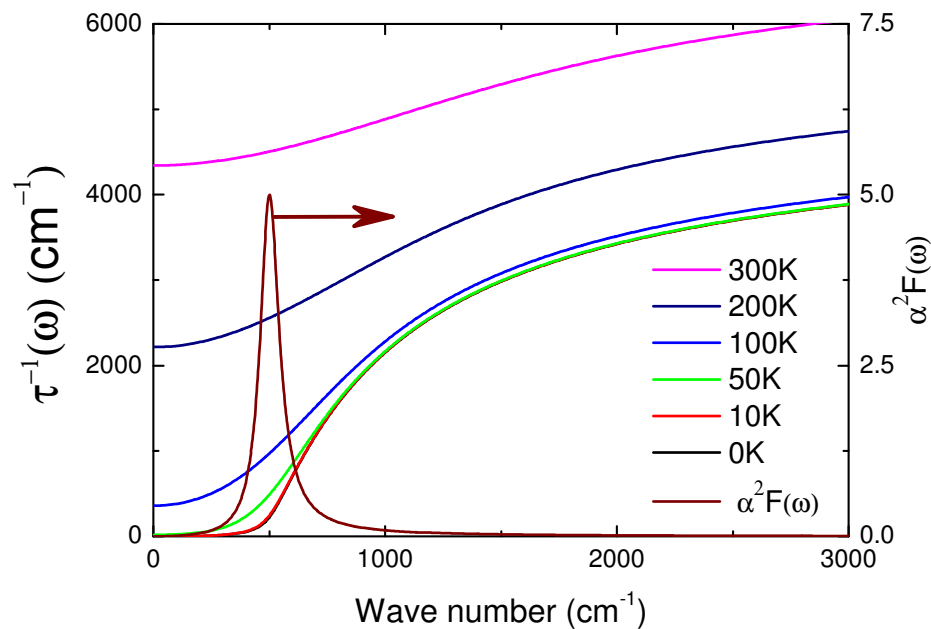At 0K, based on Allen's formula

$\tau^{-1}(\omega)$

$\alpha^2F(\omega)$

$\tau^{-1}(\omega)$ (cm^{-1})

$\alpha^2F(\omega)$

Wave number (cm^{-1})

Electron-phonon coupling at finite temperature

$$\frac{1}{\tau(\omega, T)} = \frac{\pi}{\omega} \int_0^\infty d\Omega \alpha^2 F(\Omega, T)[2\omega coth(\frac{\Omega}{2T}) -$$

$$(\omega + \Omega)coth(\frac{\omega + \Omega}{2T}) + (\omega - \Omega)coth(\frac{\omega - \Omega}{2T})]$$

Formula based on the Kubo formula for the conductivity

by Shulga 1991

Inversion of reflectance is a VERY ill-defined
problem, but the "image" of $\alpha^2 F(\Omega)$ is in the
data.

$T = 0$ Holstein Theory:

normal state !

$$\sigma(\nu) = \frac{\omega_P^2}{4\pi} \frac{i}{\nu} \int_0^\nu d\omega \frac{1}{\nu + \frac{i}{\tau} - \Sigma(\nu - \omega + i\delta) - \Sigma(\omega + i\delta)}$$

where

$$\Sigma(\omega + i\delta) = \int_0^\infty d\Omega\, \alpha^2 F(\Omega) \log|\frac{\Omega - \omega}{\Omega + \omega}| - i\pi \int_0^{|\omega|} d\Omega\, \alpha^2 F(\Omega)$$

Numerical inversion is possible but
requires high precision (Pb)
"Poor man's" inversion — use perturbation theory
Find:

$$\alpha^2 F(\nu) = \frac{\omega_P^2}{4\pi} \frac{1}{2\pi} \frac{d^2}{d\nu^2} \{\nu Re\,(\frac{1}{\sigma(\nu)})\} \quad \text{or} \quad W(\omega) = \frac{1}{2\pi} \frac{d^2}{d\omega^2}[\omega \frac{1}{\tau(\omega)}]$$

(A) $\alpha^2 F(\nu) = \dfrac{\omega_P^2}{4\pi}\dfrac{1}{2\pi}\dfrac{d^2}{d\nu^2}\{\nu Re\,(\dfrac{1}{\sigma(\nu)})\}$

Pb (actual, and numerically inverted --- these are indistinguishable

approximate (from (A))

K_3C_{60}

L. Pintschovius,
Rep. Prog. Phys.
57, 473 (1996)

$T_c = 19$ K

$\lambda = 0.8$

$\mu^* = 0.3$

very BCS-like

$G(\nu)$

$\alpha^2 F(\nu)$

$$\alpha^2 F(\nu) = \frac{\omega_P^2}{4\pi}\frac{1}{2\pi}\frac{d^2}{d\nu^2}\{\nu Re\left(\frac{1}{\sigma(\nu)}\right)\}$$

ν (meV)
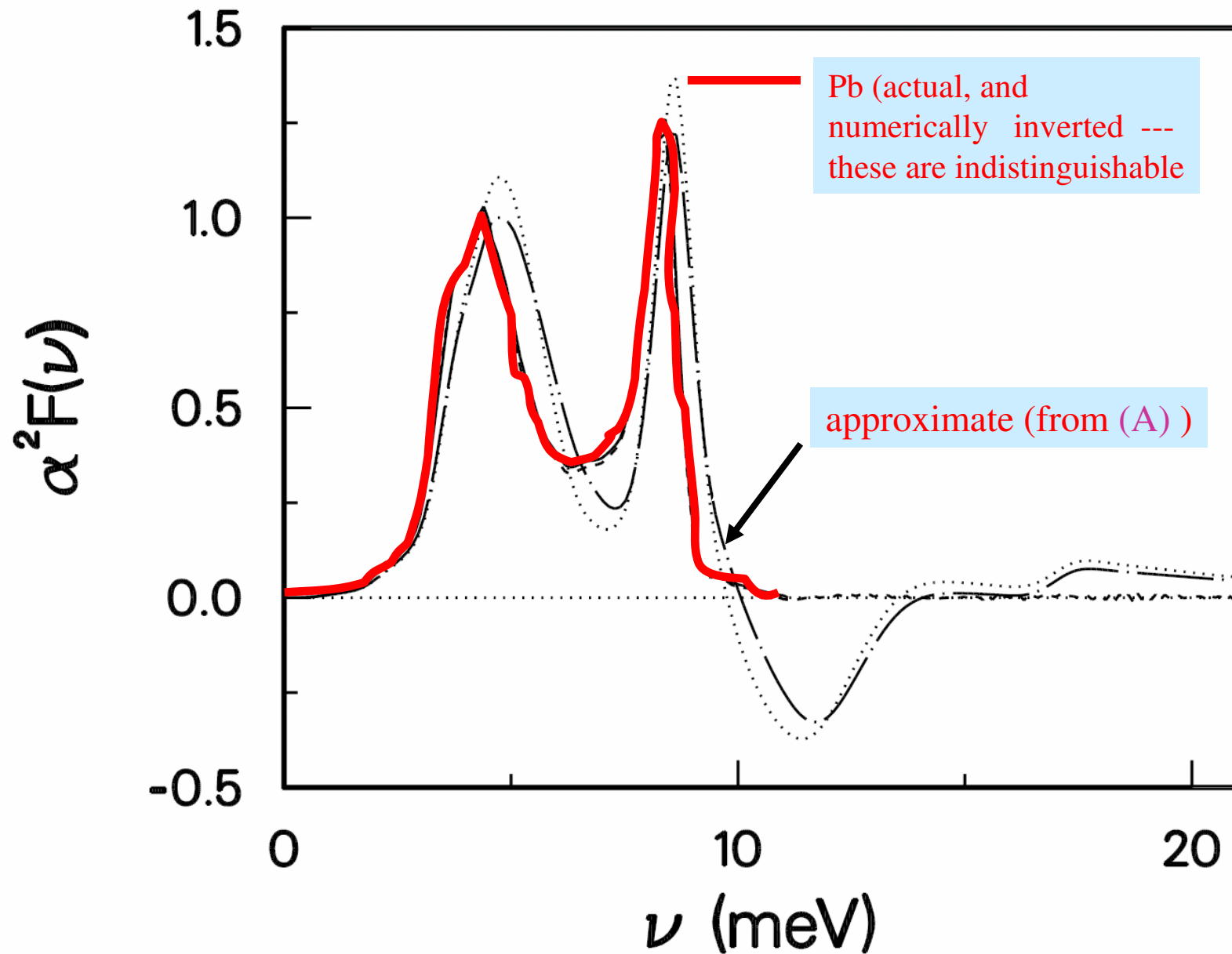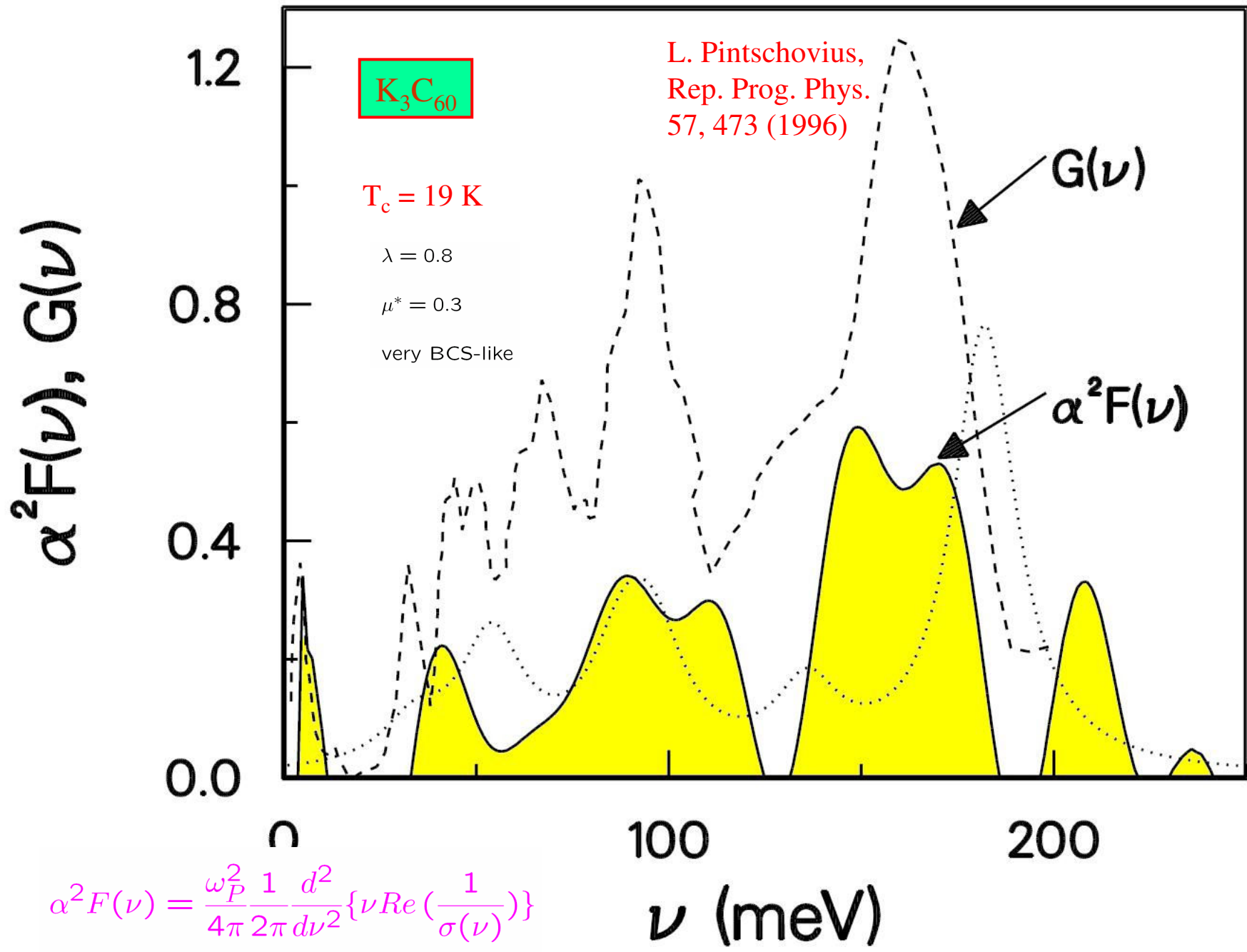
Coupling to 41 meV mode
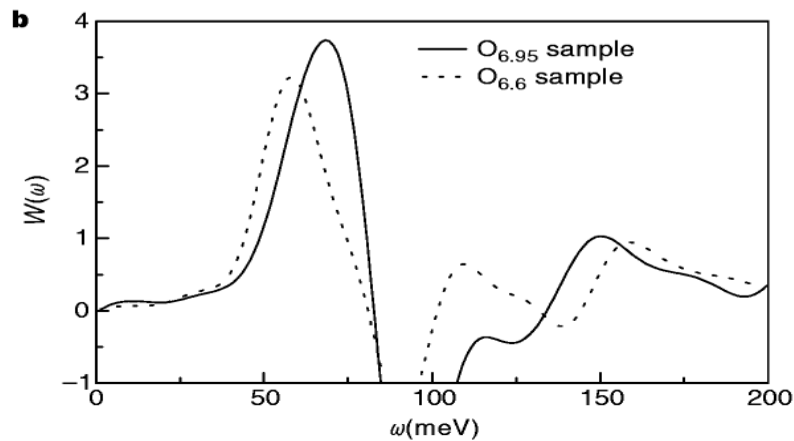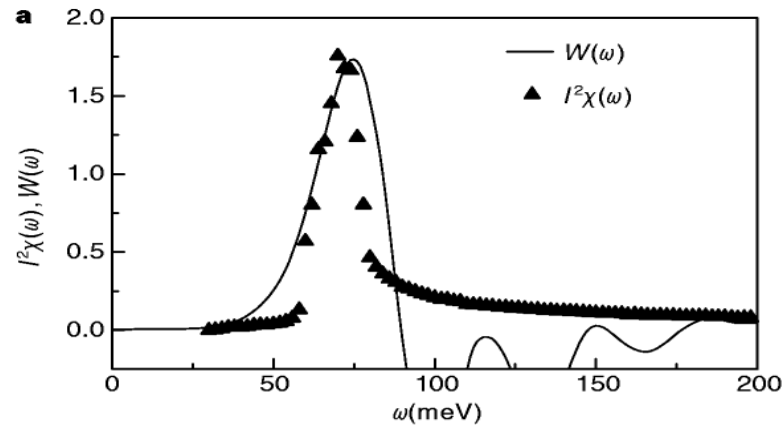
**J.P. Carbotte, E. Schachinger
and D.N. Basov, Nature 401,
354(1999)**

$$W(\omega) = \frac{1}{2\pi} \frac{d^2}{d\omega^2}[\omega \frac{1}{\tau(\omega)}]$$

The peak in W(ω): Δ + Ω

Because of d-wave pairing, the peak is shifted by Δ (not 2Δ!)

$$W(\omega) = \frac{1}{2\pi} \frac{d^2}{d\omega^2} \left[\omega \frac{1}{\tau(\omega)} \right]$$

2Δ + Ω
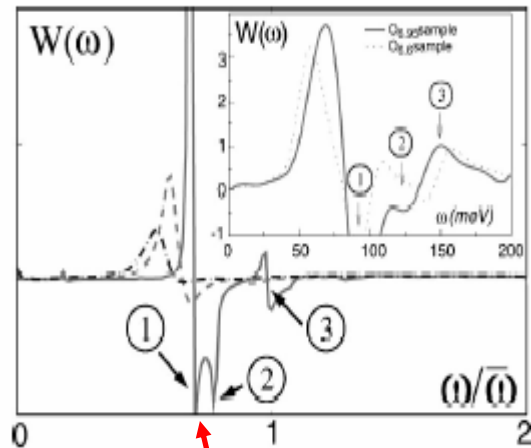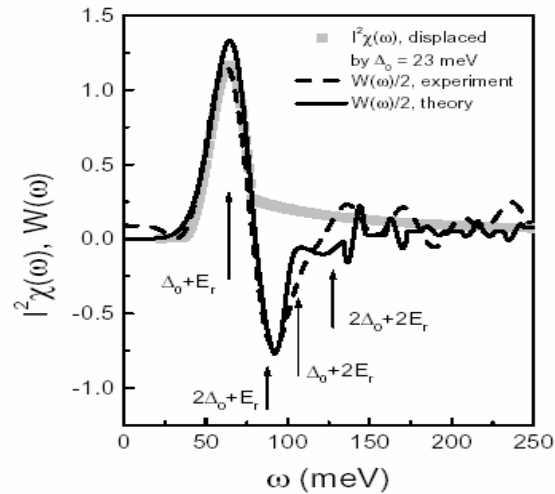
The peak in W(ω): Δ + Ω

**Because of d-wave pairing,
the peak is shifted by Δ (not
2Δ!)**

problem

the bosonic spectral function can not be negative. The negative values are linked with the overshoot in $1/\tau(\omega)$.

A mode is unable to cause a overshoot in $1/\tau$
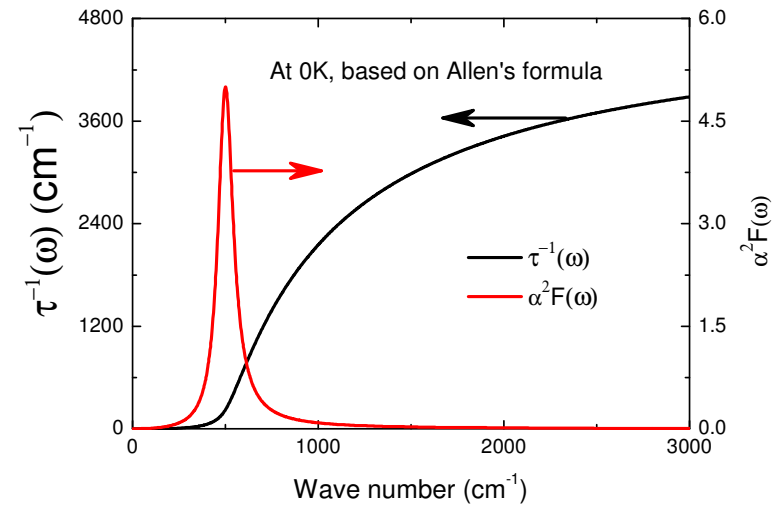
Allen's formula for the scattering rate in the superconducting state

$$1/\tau(\omega) = \frac{2\pi}{\omega} \int_0^{\omega - 2\Delta} d\Omega (\omega - \Omega) \alpha^2 F(\Omega) E\left[\sqrt{1 - \frac{4\Delta^2}{(\omega - \Omega)^2}}\right]$$
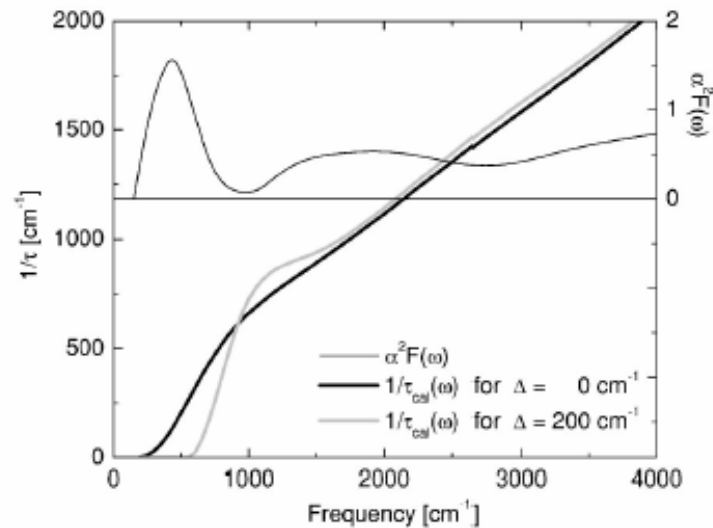
P.B.Allen 1971

E(x) is the second kind elliptic integral

FIG. 9. Model spectral function $\alpha^2 F(\omega)$ (thin line) is used to calculate the scattering rate $1/\tau_{cal}(\omega)$ from Eq. (13). For $\Delta = 0$ the calculated scattering rate resembles $1/\tau(\omega)$ of underdoped $YBa_2Cu_3O_{6.60}$ (Fig. 7). However, for finite values of the gap the calculated scattering rate resembles $1/\tau(\omega)$ of optimally doped $YBa_2Cu_3O_{6.95}$: there is an *overshoot* following the suppressed region (Fig. 7).

$$\frac{1}{\tau(\omega, T)} = \frac{\pi}{\omega} \int_{0}^{+\infty} d\Omega \alpha^2 F(\Omega) \int_{-\infty}^{+\infty} dz [N(z - \Omega) + N(-z + \Omega)]$$

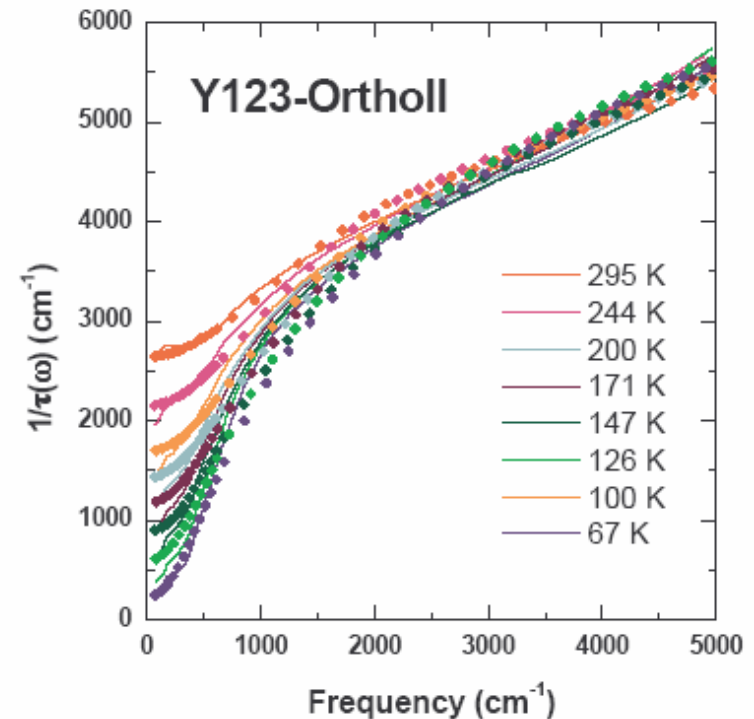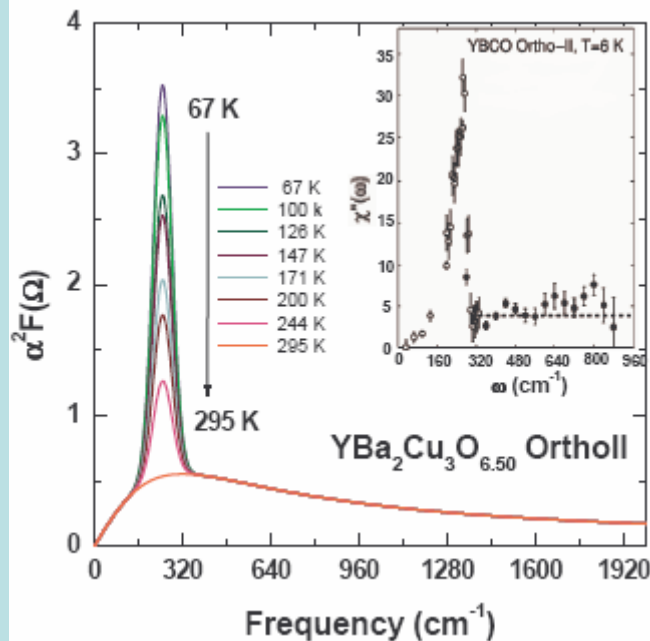$$[n_B(\Omega) + 1 - f(z - \Omega)][f(z - \omega) - f(z + \omega)]$$

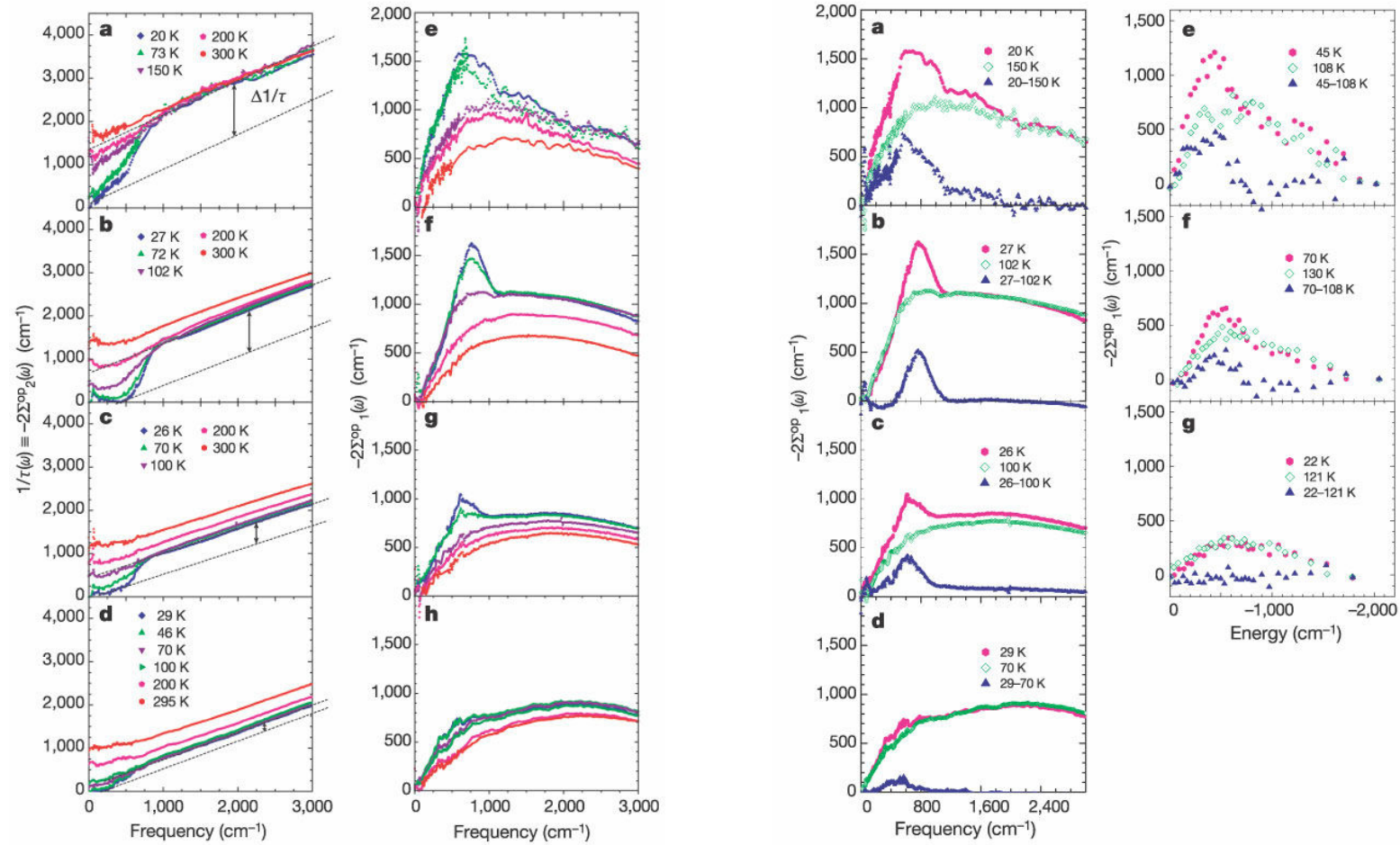$$N(z) = [N(0) + (1 - N(0)) \frac{z^2}{\Delta^2}] \theta(\Delta - |z|) + \theta(|z| - \Delta)$$

Gap Function
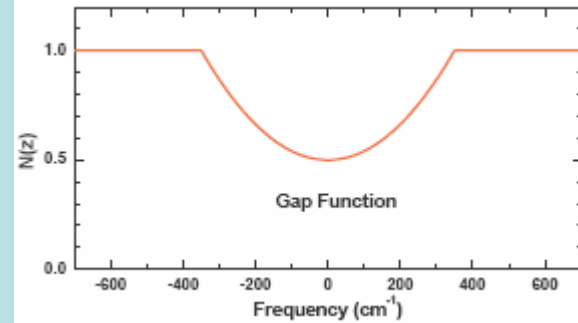
$$\alpha^2 F(\Omega) = PK(\Omega) + BG(\Omega)$$

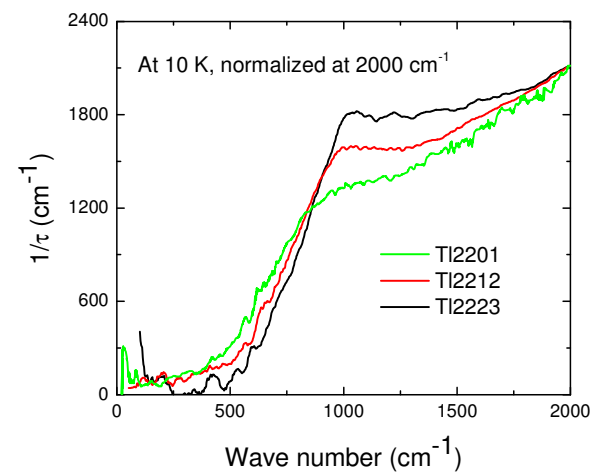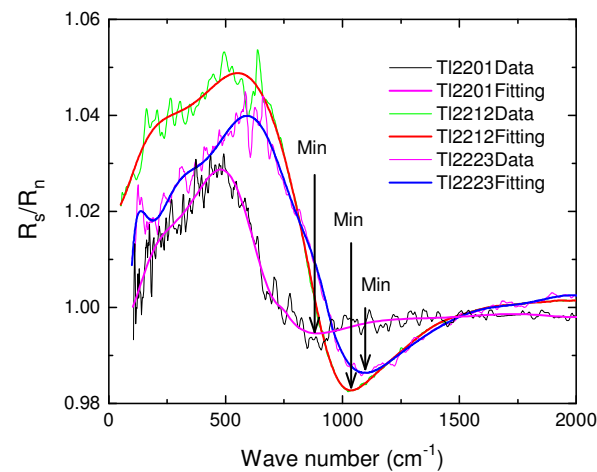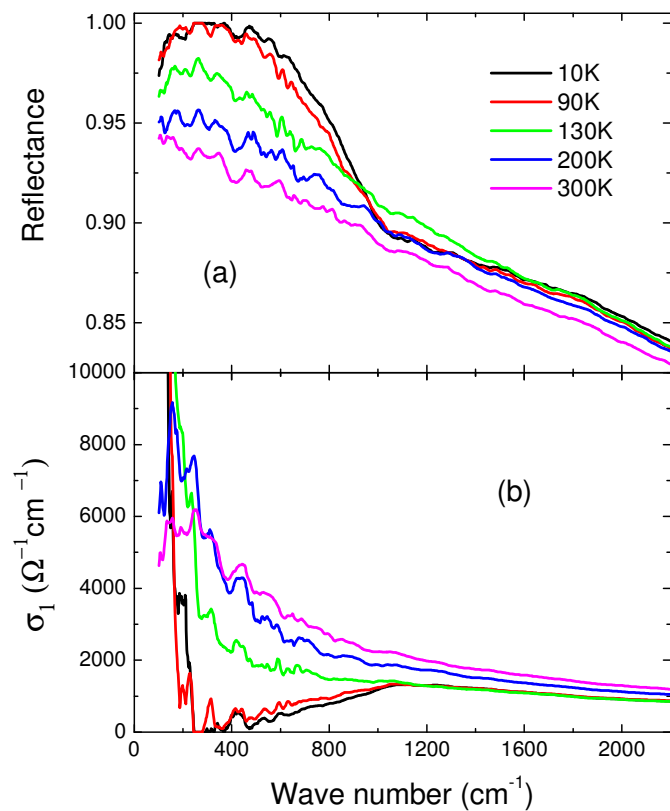$$PK(\Omega) = \frac{A}{\sqrt{2\pi}(d/2.35)} e^{-(\Omega - \Omega_{PK})^2 / [2(d/2.35)^2]}$$

$$BG(\Omega) = \frac{I_s \Omega}{\Omega_0^2 + \Omega^2}$$

Hwang, Timusk, Gu,
Nature 427, 714 (2004)

Optical data for Tl-2223 crystal

$$W(\omega) = \frac{1}{2\pi} \frac{d^2}{d\omega^2} [\omega \frac{1}{\tau(\omega)}]$$
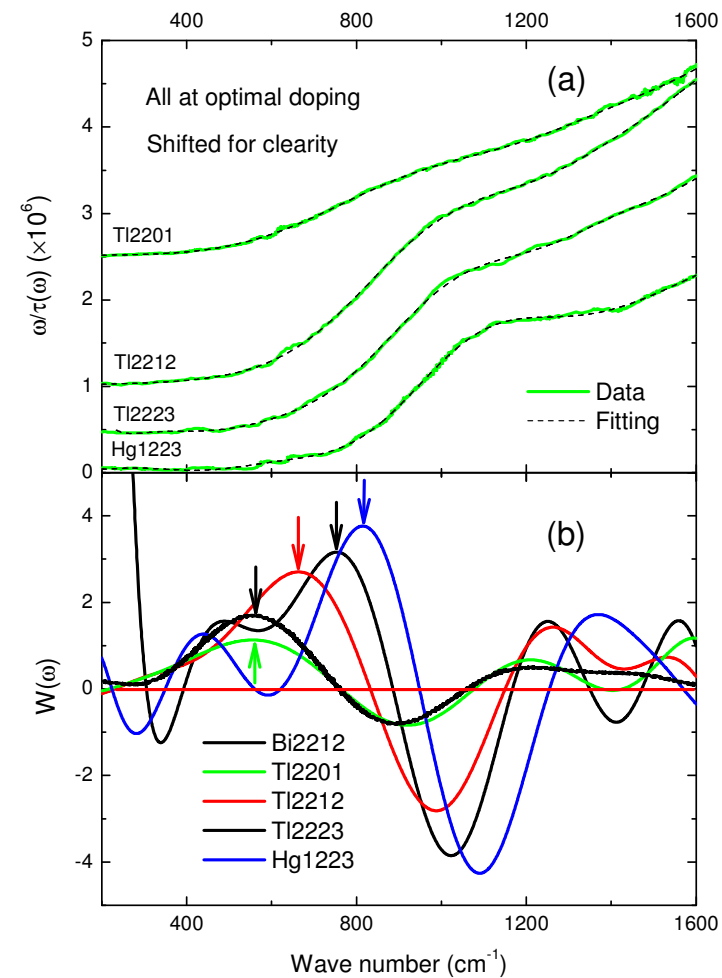
Carbotte et al. (Nature 1999):

Positive peak: $\Delta+\Omega$

Negative dip: $2\Delta+\Omega$

Abanov et al.(PRB 2001):

Negative dip: $2\Delta+\Omega$
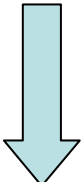
Positive peak: changes with temperature.

Data for Bi-2212: J. J. Tu, et al., PRB **66**, 144514 (2002).

Data for Hg-1223: J. J. McGuire, et al., PRB **62**, 8711 (2000).
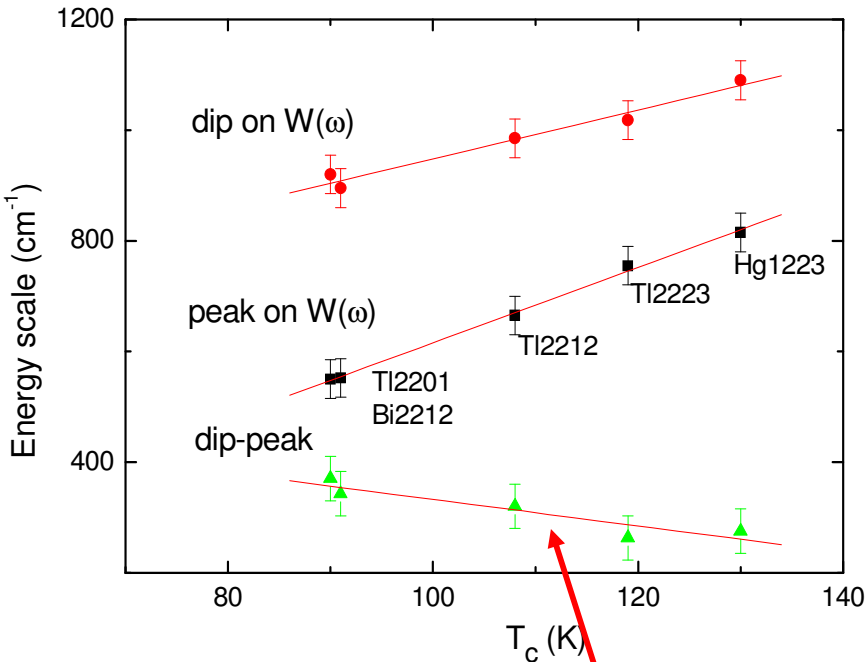
$$2\Delta+\Omega \propto T_c$$

$$\text{or } Tc=k(2\Delta+\Omega)$$

the scaling behavior means that not only the gap amplitude is proportional to Tc, but the boson mode energy is also proportional to Tc.

challenge phonon origin of bosonic mode

Y. C. Ma and N. L. Wang, PRB 72, 104518 (2005).
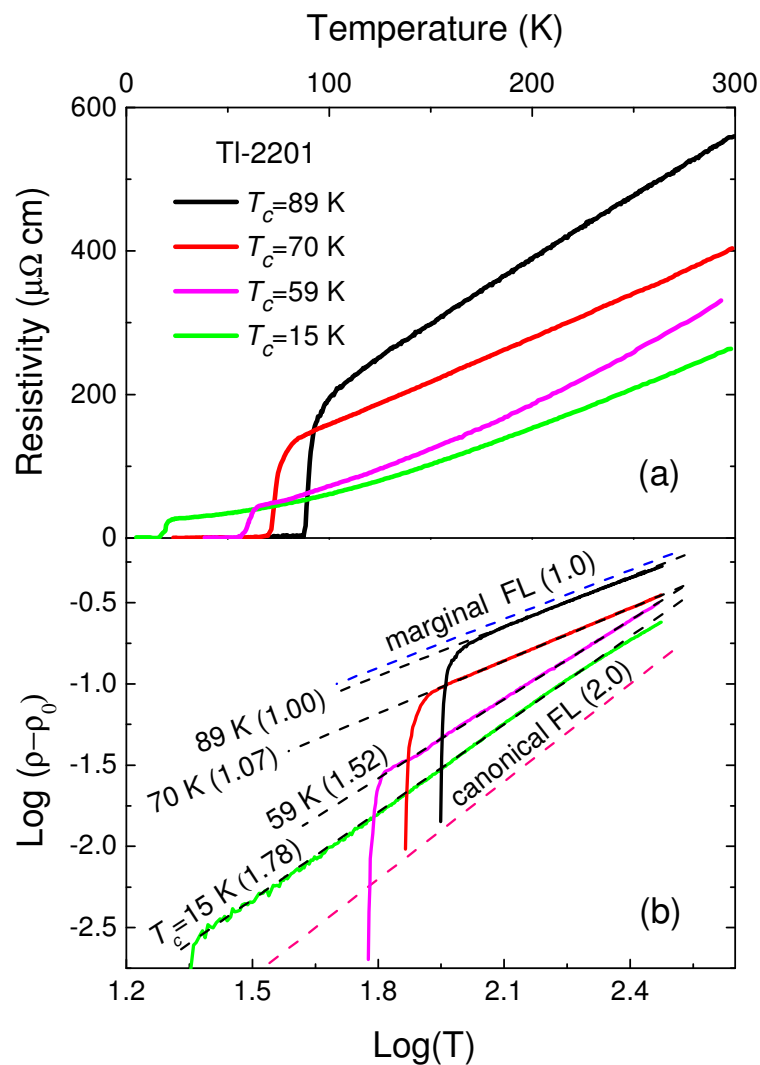
According to Carbotte et al., dip - peak=Δ

Not reasonable!

challenge the established model

Infrared scattering rate of overdoped Tl2Ba2CuO6+δ

Y. C. Ma and N. L. Wang, cond-mat/0511643, (PRB in-press)

Three crystals were selected for optical study:

Tc~89 K, nearly optimal doping

Tc~70 K, mediately overdoped
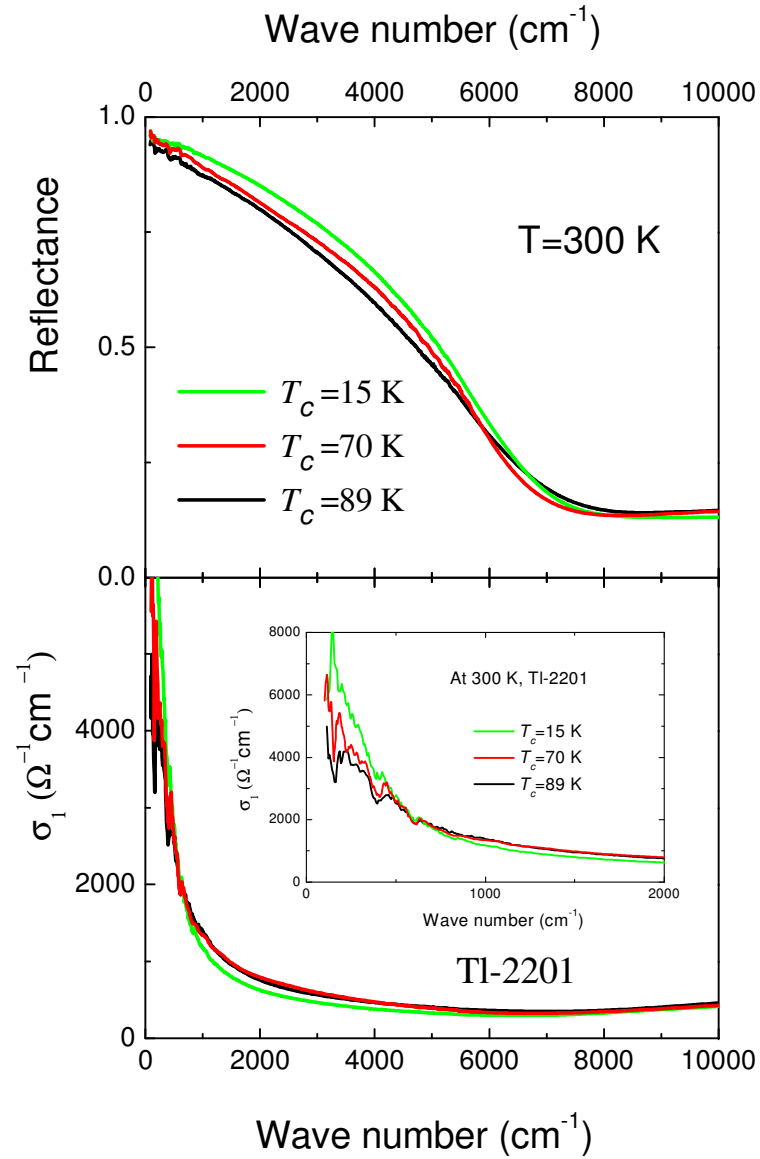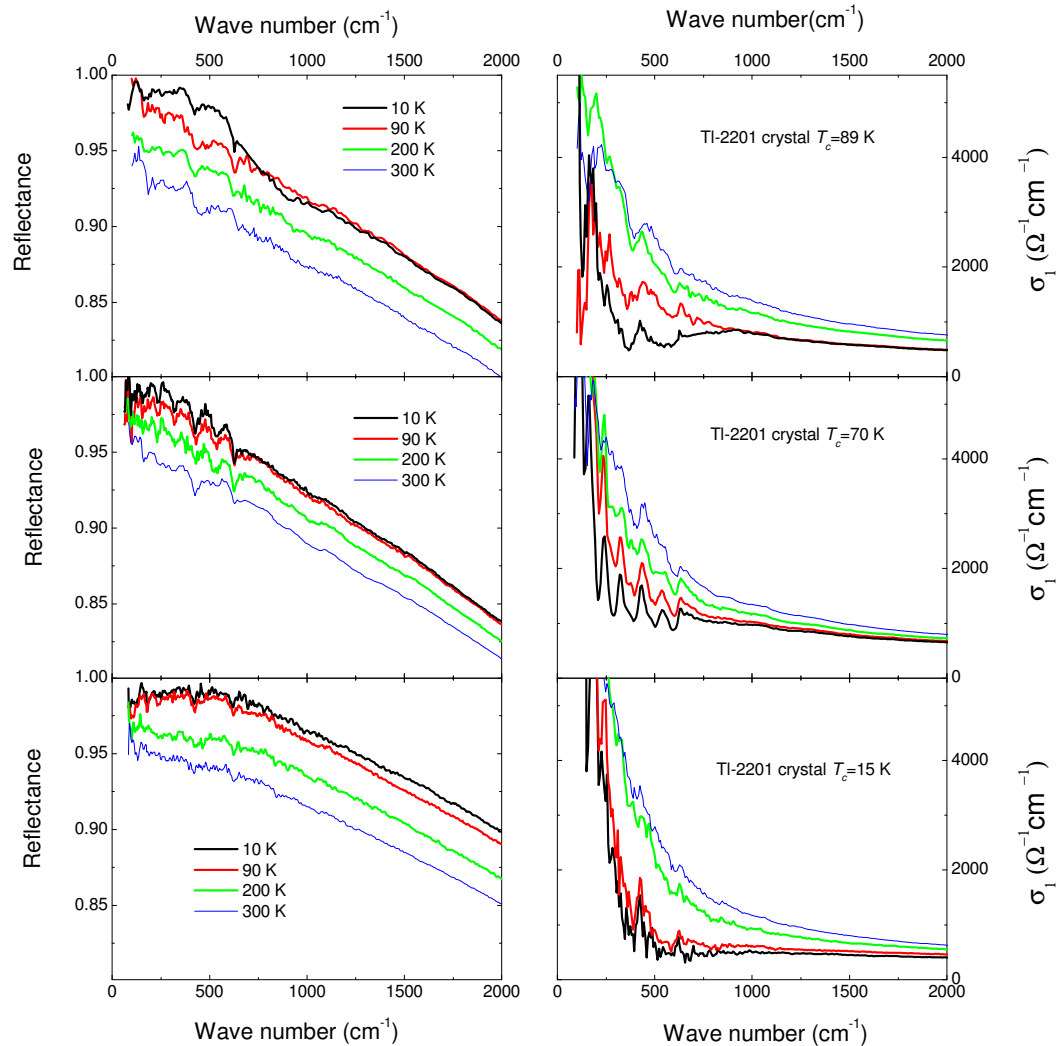
Tc~15 K, heavily overdoped

TABLE I: The spectral weight distribution calculated from Eq. (1) for three Tl-2201 crystals. All the data has been normalized to SW(8000) of the optimally doped sample.

Sample	T_c (K)	SW(600)	SW(8000)−SW(600)	SW(8000)
A	89	0.312	0.688	1.000
B	70	0.367	0.642	1.019
C	15	0.425	0.582	1.007

The effective carrier density does not increase further with doping in the overdoped region, the major change is the narrowing of low-ω Drude-like peak, originated from the reduction of the scattering rate.

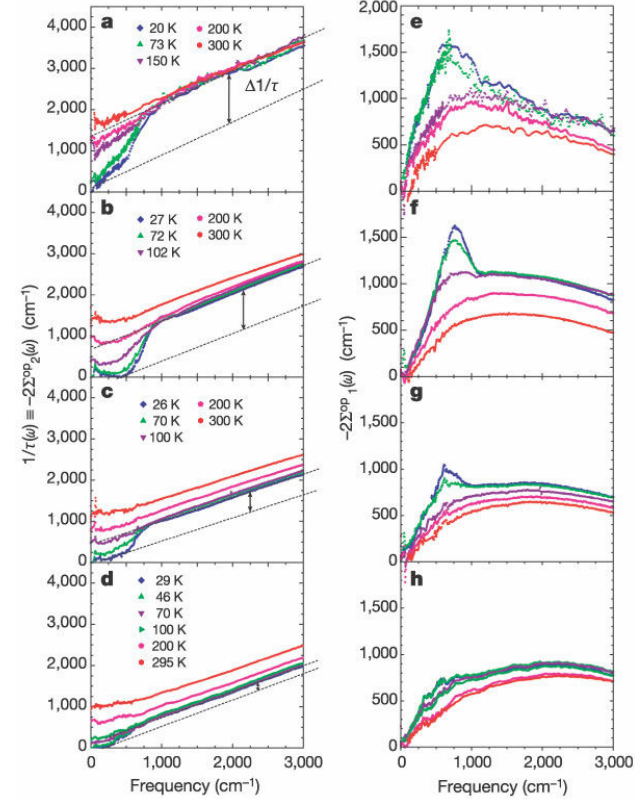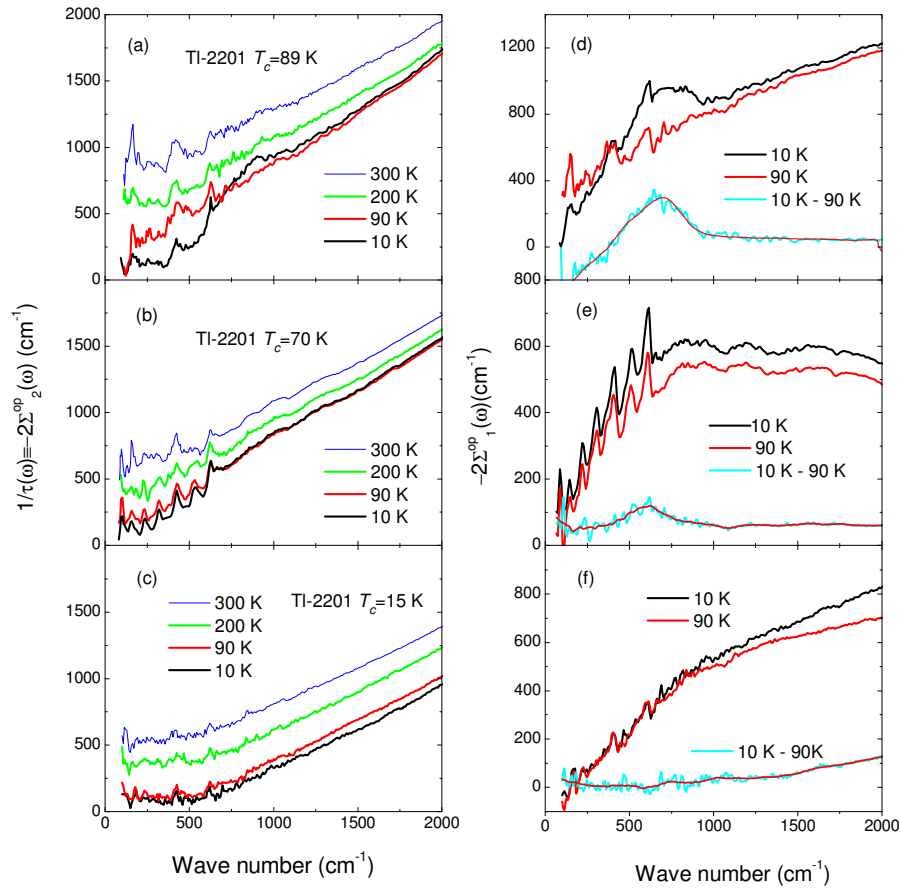# Low-ω R(ω) at low T changes significantly with overdoping

Mode-coupling feature becomes weak as the samples become overdoped, and disappears in the heavily overdoped Tc=15 K sample.
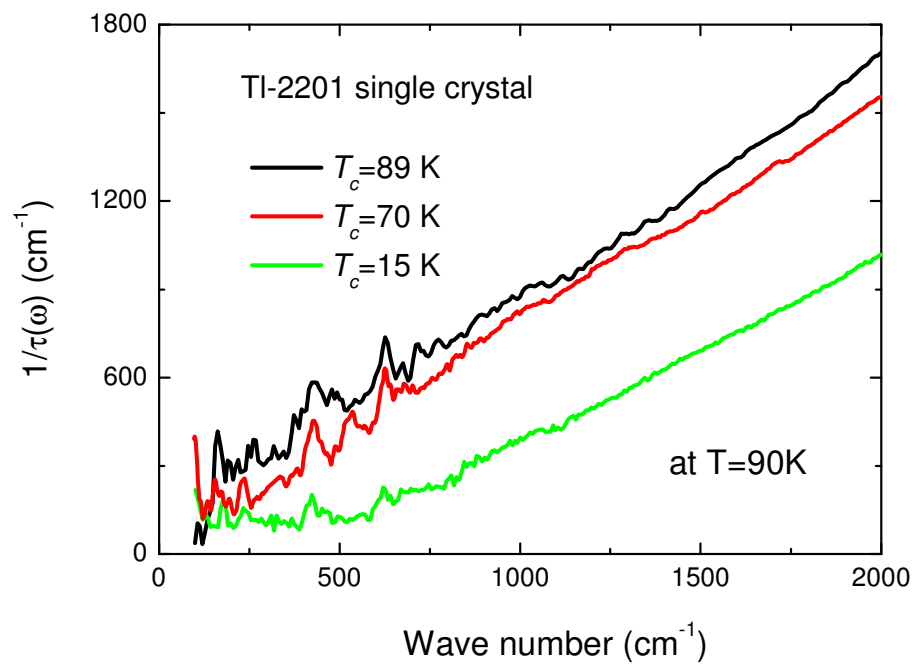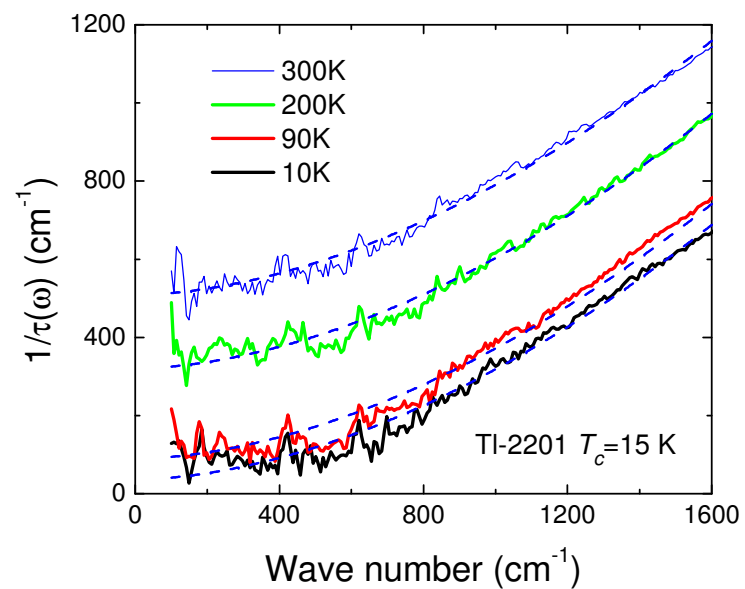
TI-2201 crystals

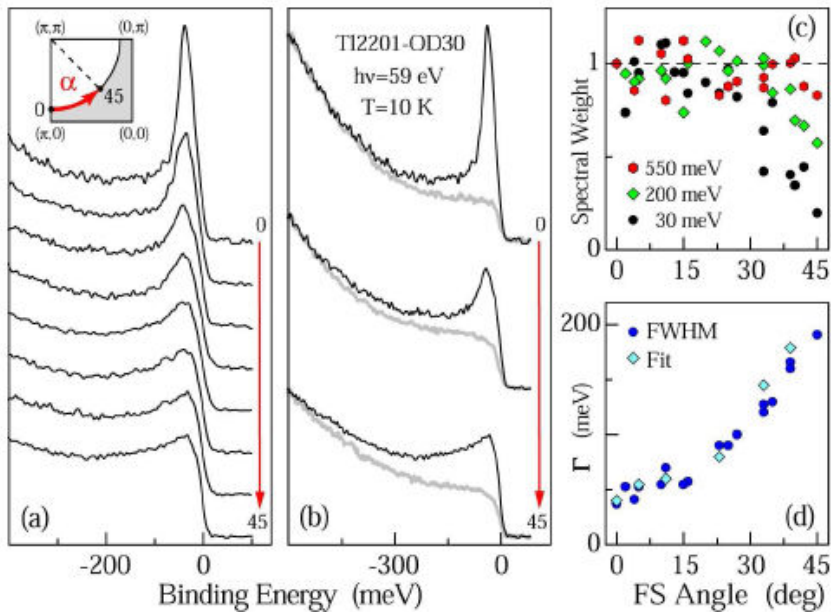$$\sigma(\omega) = \frac{i}{4\pi} \frac{\omega_p^2}{\omega - 2\Sigma^{op}(\omega)},$$

Confirm Hwang, Timusk and Gu's observation on overdoped Bi-2212

The spectral feature is not consistent with a coupling with a phonon, but could still be reconciled with a coupling to magnetic excitations.
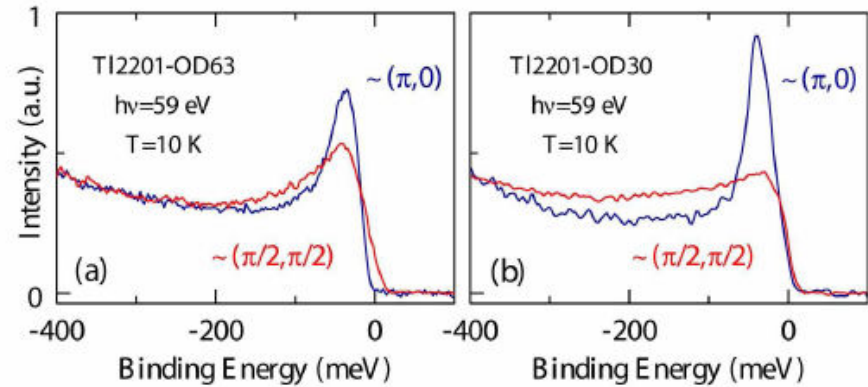
$$\frac{1}{\tau(\omega)} = \frac{\omega_p^2}{4\pi} \text{Re}\left(\frac{1}{\sigma(\omega)}\right)$$

M. Plate et al., PRL 95, 077001 (2005)

Antinodal quasiparticle lifetime strongly increase, and becomes longer than that near nodal region.

nodal quasiparticle peak becomes even broader in heavily overdoped sample than in intermediately overdoped sample

Naively, one can ascribe the reduction of the optical scattering rate to the increase of the lifetime of antinodal quasiparticles

However, the lifetime increase of the antinodal quasiparticles is not the sole reason.

$$\frac{1}{\tau(\omega)} = \frac{\omega_p^2}{4\pi} \mathrm{Re}\left(\frac{1}{\sigma(\omega)}\right)$$

v_k appears as a weighted factor in the integration. The larger the v_k and the smaller the τ^{-1}, the larger contribution it has to the transport.

$$\sigma(\omega) = -\frac{e^2}{4\pi^3\hbar}\int \frac{\vec{v}_k \vec{v}_k}{v_k} \frac{dS_F}{1/\tau - i\omega}$$

optimal doping

overdoping
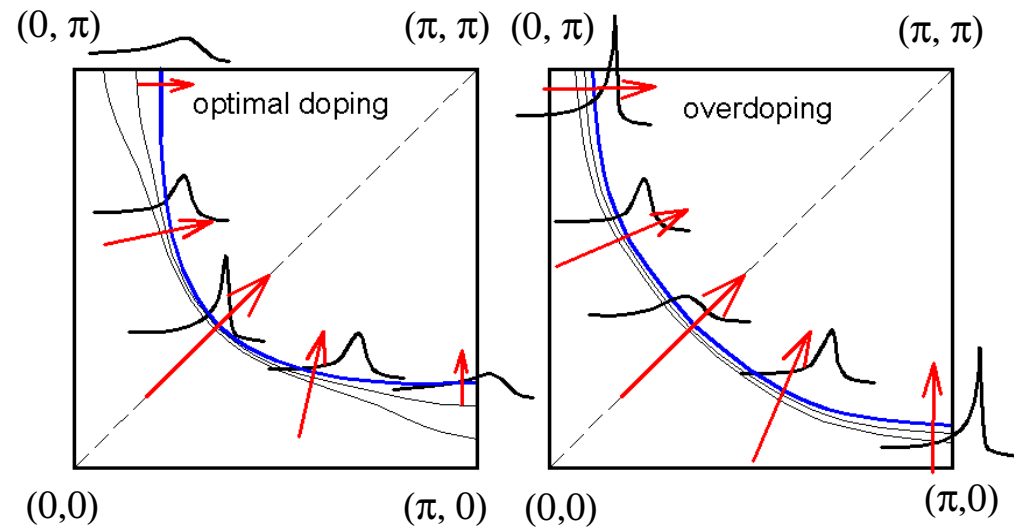
The change of the Fermi velocity arising from the shape change of Fermi surface with doping, especially near the antinodal region, also contribute to the transport.